LOCKHEED MARTIN ENERGY RESEARCH LIBRARIES
3 4456 0515739 9

CENTRAL RESEARCH LIBRARY
DOCUMENT COLLECTION

cy. 69

ORNL-4202
UC-80 – Reactor Technology

THE UNCLAD-METAL BREEDER REACTOR (UMBR) FOR DESALTING OR POWER

OAK RIDGE NATIONAL LABORATORY
CENTRAL RESEARCH LIBRARY
DOCUMENT COLLECTION
LIBRARY LOAN COPY
DO NOT TRANSFER TO ANOTHER PERSON
If you wish someone else to see this document, send in name with document and the library will arrange a loan.

OAK RIDGE NATIONAL LABORATORY
operated by
UNION CARBIDE CORPORATION
for the
U.S. ATOMIC ENERGY COMMISSION

Printed in the United States of America. Available from Clearinghouse for Federal Scientific and Technical Information, National Bureau of Standards, U.S. Department of Commerce, Springfield, Virginia 22151
Price: Printed Copy $3.00; Microfiche $0.65

LEGAL NOTICE

This report was prepared as an account of Government sponsored work. Neither the United States, nor the Commission, nor any person acting on behalf of the Commission:

A. Makes any warranty or representation, expressed or implied, with respect to the accuracy, completeness, or usefulness of the information contained in this report, or that the use of any information, apparatus, method, or process disclosed in this report may not infringe privately owned rights; or

B. Assumes any liabilities with respect to the use of, or for damages resulting from the use of any information, apparatus, method, or process disclosed in this report.

As used in the above, "person acting on behalf of the Commission" includes any employee or contractor of the Commission, or employee of such contractor, to the extent that such employee or contractor of the Commission, or employee of such contractor prepares, disseminates, or provides access to, any information pursuant to his employment or contract with the Commission, or his employment with such contractor.

ORNL-4202

Contract No. W-7405-eng-26

NUCLEAR DESALINATION PROGRAM

THE UNCLAD-METAL BREEDER REACTOR (UMBR) FOR DESALTING OR POWER

R. P. Hammond
C. C. Burwell
R. S. Carlsmith
J. G. Delene
L. C. Fuller
A. E. Goldman
D. B. Lloyd
J. T. Roberts
J. E. Savolainen
R. P. Wichner

JANUARY 1969

OAK RIDGE NATIONAL LABORATORY
Oak Ridge, Tennessee
operated by
UNION CARBIDE CORPORATION
for the
U.S. ATOMIC ENERGY COMMISSION

LOCKHEED MARTIN ENERGY RESEARCH LIBRARIES
3 4456 0515739 9

ACKNOWLEDGMENTS

Particularly valuable contributions were made by the following individuals in the areas indicated:

T. D. Anderson, ORNL — Reactor Data
E. L. Compere, ORNL — Reactor Chemistry
T. Denton, ORGDP — Cost Analysis
J. M. Googin, Y-12 — Fuel Fabrication
J. A. Lane, ORNL — Evaluation
R. Salmon, ORNL — Shipping
A. B. Townsend, Y-12 — Fuel Fabrication
G. Young, ORNL — Evaluation

We are most grateful for their assistance.

CONTENTS

Page

ABSTRACT ix
1. INTRODUCTION 1
2. SUMMARY AND CONCLUSIONS 2
2.1 Overall Characteristics 2
2.2 Technical Feasibility 3
2.2.1 Fuel Irradiation Stability 3
2.2.2 Fuel-Coolant Compatibility 5
2.2.3 Fission-Product Release 5
2.2.4 Maintenance 6
2.2.5 Fuel Fabrication 6
2.3 Economics 7
2.4 Safety 8
2.5 Conclusions 8
2.6 Areas for Future Work 9
2.6.1 Experimental Work 10
2.6.2 Study and Planning Activities 10
3. DESCRIPTION OF CONCEPT 11
3.1 Core and Blanket 11
3.2 Fueling Concept 15
3.3 Steam Generation System 16
3.4 Fission-Product Removal and Maintenance Concepts 19
References 19
4. PHYSICS 20
4.1 Calculational Methods 20
4.2 Equilibrium Fuel Cycle 20
4.3 Reactivity Coefficients 29
4.4 Sodium Voiding Effects 31
4.5 Startup on ^{235}U 34
5. CORE AND BLANKET FUEL PERFORMANCE UNDER IRRADIATION 35
5.1 Core Fuel 35
5.1.1 Selection of Thorium-Based Alloy 35

5.1.2 Irradiation Characteristics of Thorium-Uranium Binary Alloys 36

5.1.3 The Thorium-Uranium-Plutonium Ternary System 39

5.2 Blanket Fuel 40

5.3 Summary of Fuel Compositions and Design Conditions 42

References 43

6. THERMAL AND HYDRAULIC ANALYSES 45

6.1 Assumptions and Method of Calculating Temperature Distributions 45

6.2 Pressure Drop Estimates 48

6.3 Engineering Peaking Factors 48

6.4 Computation of Coolant Hole Size 49

6.5 Results of the Thermal and Hydraulic Calculations 49

6.6 Effect of Fuel Growth on Maximum Fuel Temperature 52

6.7 Effect of a Plugged Coolant Hole 53

6.8 Effect of Loss of Coolant Pumping Power 56

6.9 Effect of Surface Film 59

References 59

7. REACTOR CHEMISTRY 60

7.1 Corrosion 60

7.1.1 Thorium 61

7.1.2 Uranium 62

7.2 Compatibility Data from Dounreay Reactor Experiment 64

7.3 Corrosion Control 65

7.4 Fission-Product Transport 67

7.5 Fission-Product Behavior 69

7.6 Sodium Activation 70

7.7 Coolant Impurities 71

7.8 Materials of Construction of Coolant Loops 73

References 74

8. FABRICATION AND REPROCESSING 77

8.1 Core Element Fabrication Cycle 77

8.2 Core Element Fabrication Methods 79

8.3 Blanket Element Refabrication 81

8.4 Reprocessing 82

References 83

9. ECONOMICS 84

9.1 Economic Factors 84

9.2 Plant Availability 85

9.3 Fuel-Cycle Costs 85

9.4 Capital Costs 87

9.5 Operating and Maintenance Costs 89

9.6 Nuclear Insurance 89

9.7 Heat and Power Costs 89

9.8 Effect of Scaleup to 10,000-Mw(th) Single-Core Ratings 92

References 92

APPENDIX A. DESCRIPTION OF ALTERNATE CONCEPTS OF THE UNCLAD-METAL-FUELED FBR — THE U-Pu-Fs AND Th-^{233}U FUELED REACTORS 97

APPENDIX B. FUEL ELEMENT REFABRICATION COST STUDY 115

APPENDIX C. PRELIMINARY ESTIMATES OF FUEL PREPARATION AND REPROCESSING COSTS FOR EVALUATION OF Th-U-Pu METAL-FUELED FAST BREEDER REACTOR 129

APPENDIX D. REFUELING TIME STUDY 133

APPENDIX E. SUMMARY REACTOR DESIGN SPECIFICATIONS AND CAPITAL COST ESTIMATES 136

ABSTRACT

Reactor concept studies are being conducted under the Nuclear Desalination Program at ORNL to investigate the possibilities of producing low-cost low-temperature heat suitable for seawater distillation. This report presents the findings of preliminary investigations of sodium-cooled fast breeder reactors fueled with unclad metal. Three fuel materials are considered — (1) thorium-based thorium-uranium binary alloys, (2) thorium-based thorium-uranium-plutonium ternary alloys, and (3) uranium-based alloys. Together with the two unclad-metal blanket materials — thorium and uranium — used singly or jointly, a number of reactor core combinations is possible.

Use of unclad metals as core and blanket materials appears to be technically feasible, based on the incomplete available data. Good breeding gains and doubling times were calculated for all systems considered because of the absence of cladding and other diluents. The characteristics of two reactors fueled with the thorium-based thorium-uranium-plutonium ternary alloy combined with uranium blanket material are presented in the body of the report, while the less desirable low-temperature all-uranium-based fuel system and the nearer term high-temperature all-thorium based fuel system are discussed briefly in the appendices. The two reactors considered are one designed primarily for low-temperature steam production for desalting and one designed primarily for power production.

1. INTRODUCTION

This report presents part of the results of a systematic search for sources of low-cost energy, which has been a major objective of the AEC Nuclear Desalination Program. In the course of this search, detailed economic and technical analyses were made of various reactor types that use different coolants and types of fuel considered to be within the reach of present-day technology. For all the solid-fuel reactors examined, metal fuel showed a high potential for low-cost energy if its traditional vulnerability to irradiation damage could be mitigated or the cost of recycling could be lowered.

A reactor concept is described that was obtained by lowering the temperature of the sodium-cooled fast breeder reactor to where the ceramic fuel elements would be replaced with metal elements and the cladding eliminated. These steps reduced markedly the amount of inert diluent material in the reactor, hardened the neutron spectrum, and substantially improved the neutron economy and nuclear performance. The reactor differs from other liquid-metal-cooled fast breeders primarily in the fuel. Other system components are similar to those in a ceramic-fueled LMFBR.

The specific objectives of this preliminary study were to explore the economic potential and preliminary technical feasibility of a reactor system with unclad fuel in a low-temperature concept for process-heat production and in a power-production concept. The report discusses the critical research and development problems and outlines a program of investigation.

2. SUMMARY AND CONCLUSIONS

A preliminary review was made of a fast breeder reactor concept based on unclad metallic fuel. The fuel is formed into massive slugs containing hexagonal sodium coolant holes to minimize structural material. The absence of large amounts of structural material and other diluents and a favorable design for heat transfer and fluid flow result in high fuel density in the core and blanket and produce high breeding gains and short doubling times.

Three fuel materials were considered: (1) thorium-based thorium-uranium binary alloys, (2) thorium-based thorium-uranium-plutonium ternary alloys, and (3) uranium-based alloys. Together with the two unclad-metal blanket materials (thorium and uranium) used singly or jointly, a considerable number of reactor fuel combinations is possible.

A thorium-based ternary fuel alloy combined with all-uranium blankets is the reference system used for the reactor concepts presented in the main body of this report, while Appendix A gives brief summary descriptions of a low-temperature concept fueled with the metallurgically less desirable all-uranium alloy system and a high-temperature concept fueled with the nearer term all-thorium alloy system. With the reference combination of materials the important properties of thorium — high melting point, high thermal conductivity, and irradiation stability — are fully utilized in the core, and the neutronic advantage of uranium as a fertile material is partially retained by its use in the blankets, where its poor irradiation stability is not limiting.

Overall characteristics, status of feasibility information, safety considerations, and economic aspects are summarized below and presented in more detail in the succeeding chapters. Conclusions and an outline of areas for future work are given in Sections 2.5 and 2.6, respectively.

2.1 Overall Characteristics

The salient characteristics of two versions of a 3500-Mw(th) reactor — one designed primarily for the production of low-temperature steam for single-purpose water desalination plants and the other designed

primarily for the production of power — are given in Table 2.1. The primary sodium outlet temperatures (350 and 525°C), as well as many other design characteristics for the two versions, were chosen arbitrarily and may be improved upon later. The two concepts are believed to represent reasonable choices that illustrate the effect of coolant temperature. In both versions the maximum internal fuel temperature is set at 650°C (1200°F). The main difference between them is, therefore, the higher allowable specific power for the low-temperature reactor because of the higher average temperature drop between fuel and coolant.

In a similar fashion the intermediate heat exchanger and steam-generator operating conditions given in Table 3.1 (see Chapt. 3) were selected as reasonable choices for the primary purposes intended; that is, brine heating at 120°C (250°F) for the low-temperature reactor* and power generation for the high-temperature reactor.

2.2 Technical Feasibility

A key question regarding technical feasibility of the concept concerns the use of unclad fuel. There are several separate aspects to this question that are briefly described below and are discussed in more detail in the main body of the report. In summary, while proof of feasibility cannot be claimed, there is evidence supporting feasibility in all areas.

2.2.1 Fuel Irradiation Stability

Thorium-based thorium-uranium alloys are essentially dispersions of uranium in thorium and, based on reported experimental data, possess the excellent radiation stability of pure thorium with compositions up to 20 wt % uranium. These fuels do not exhibit breakaway swelling even under the most drastic conditions tested — 1000°C, 100 Mwd/kg burnup, and 30 wt % uranium. Instead, there occurs predictable, temperature-dependent growth caused by the accumulation of fission products. Irradiation data indicate that the selected design conditions of 650°C maximum fuel temperature and 10 vol % growth allow an average burnup of 33 Mwd/kg.

---

*The coolant temperature chosen for the low-temperature reactor is also sufficient for brine temperatures higher than 120°C.

Table 2.1. Summary of Reactor Characteristics

	Process-Heat-Production Reactor	Power-Production Reactor
Gross reactor thermal power, Mw	3500	3500
Core sodium inlet temperature, °C	170	345
Core sodium outlet temperature, °C	350	525
Maximum core fuel temperature, °C	650	650
Type of fuel in core	Th-U-Pu metal	Th-U-Pu metal
Type of fuel in blanket	Depleted U metal	Depleted U metal
Average specific power, kw/kg	290	220
Average power density, kw/liter	1690	1284
Fissile enrichment, %	12.85	12.54
Reactor fissile inventory, kg	2323	2770
Total system fissile inventory, kg	2951	3376
Reactor breeding ratio	1.64	1.64
Fissile material exponential doubling time, years	3	3.4
Annual net Pu production, kg	685	680
Maximum fuel exposures, Mwd/kg		
Core	40	40
Blanket	3	3
Core residence times, days at 0.90 plant factor	127	167
Number of core elements	249	376
Number of radial blanket elements	163	206
Prime steam conditions		
Temperature, °C		365
Pressure, psia		1450
Net thermal efficiency, %	7.4[a]	36.6
Power cost estimate, mills/kwhr		2.3[b]

[a]Turbine exhaust at 127°C (260°F).

[b]Based on capital costs at $135/kw(e), 12% annual charge rate for plant investment, 10% annual charge rate for fuel inventory, and a plutonium value of $9.30/g.

Irradiation testing of the mixed-cycle fuel, nominally, Th–15 wt % U–7 wt % Pu alloy, is lacking; however, phase equilibrium studies indicate that the plutonium resides primarily in the uranium phase. Hence, prospects for radiation stability of the ternary alloy are good, since the ternary alloy would be expected to exhibit the properties of thorium.

The design specifies depleted uranium for the blankets and presumes a maximum irradiation lifetime of 3 Mwd/kg at a maximum irradiation temperature of 600°C. This selection is based on United Kingdom tests of their "adjusted" uranium composition carried out on unclad specimens in a sodium environment. Irradiation tests on similar alloys are in progress in the U.S. at Savannah River and Pacific Northwest Laboratories but have not yet covered the temperature and burnup range of present interest.

2.2.2 Fuel-Coolant Compatibility

While the basic compatibility of thorium and uranium with sodium is not in question, oxygen in the sodium would react with either metal, and an experimental program would be necessary to define acceptable operating conditions for the system. Applicable experience on uranium-NaK compatibility is being accumulated in the Dounreay reactor, where the primary NaK coolant at a velocity of about 10 fps is in direct contact with uranium-molybdenum metal fuel with a surface temperature of 600°C. United Kingdom personnel report the presence of an adherent oxide film on the uranium fuel and estimate a low uranium concentration (1 ppb) in the primary circuit. Experience with thorium-sodium compatibility is also reported, in which because of the formation of an adherent oxide film, thorium was found to act slowly in removing oxygen from the system after formation of the initial oxide film.

2.2.3 Fission-Product Release

Calculations show that less than 0.07%* of the fission products would escape by recoil from the unclad fuel. The magnitude of the effect of

---

*Approximately equivalent to the release to the coolant of all fission products from a 2.5-Mw(th) system.

fission-product release on the reactor chemistry is indicated by the fact that at this rate approximately 0.5 ppm of fission products would reach the sodium coolant each year. Cold traps have been found to be effective in removing most solid fission products from sodium. The gaseous products, xenon and krypton, mix with the helium cover gas and can be removed by passing the cover gas through charcoal beds at reduced temperatures. One of the uncertainties associated with fission-fragment recoil is the amount of heavy metal lost with the recoiling fission fragments. Experiments with a UO_2 surface in a vacuum indicate that approximately nine atoms of uranium are torn away with each recoiling fission fragment that leaves the surface. It is not known how valid this result is for the system under consideration, but applying the result to a system fueled with uranium gives a loss from the core and blankets of 22 g per day, which appears acceptable from the standpoint of fuel loss.

2.2.4 Maintenance

The use of unclad fuel could result in more severe maintenance problems with this concept than with other fast breeder reactor designs. Even for a highly contaminated system, however, the maintenance question is likely to be one of economics rather than technical feasibility. The feasibility of maintaining contaminated systems has been demonstrated by work at ORNL on fluid-fueled reactor systems.

2.2.5 Fuel Fabrication

The fuel and blanket element fabrication method assumed for the concept consists of extrusion of a mixed metal powder compact followed by high-temperature sintering and sizing to final dimensions and density. The refabrication technique requires hydriding, dehydriding, and grinding steps prior to the extrusion and sintering operations. While no development work has been undertaken on the complete process with the fuel composition and shape considered, successful experience does exist for the separate steps of the process on similar materials. Alternate fabrication methods have been used and could be considered.

2.3 Economics

If operating a reactor with unclad metallic nuclear fuel is feasible, the economic advantages are evident and substantial. The high neutron efficiency produces a large bred fuel credit that more than offsets other fuel-cycle costs. An unclad fuel can be shaped into forms impossible or very costly for a clad fuel. Even with the lower burnup obtainable with unclad metal fuel, the fuel fabrication cost per unit of energy released appears to be lower than that obtainable with clad metal or ceramic fuels. In Chapter 9, details are given of the presently available information pertinent to the cost of energy from this type of reactor. The information was assessed by members of the Oak Ridge Reactor Evaluations Group in a manner consistent with that used for their evaluations of other reactors, and their results are summarized in Table 2.2, which gives the

Table 2.2. Summary of Projected Product Costs

	Process-Heat-Production Reactor	Power-Production Reactor
Gross reactor thermal power, Mw	3500	3500
Net annual electrical power production		
kwhr	2.04×10^9	10.1×10^9
Mw	258	1280
Annual production of 127°C (260°F) steam, MBtu	86.4×10^6	
Assumed plant factor	0.9	0.9
Annual charge rate for depreciable capital, %		
Public ownership	7	7
Private ownership	12	12
Cost of 127°C (260°F) steam, ¢/MBtu		
Public ownership	6.45	
Private ownership	13.8	
Power cost, mills/kwhr		
Public ownership		1.2
Private ownership		2.2

projected costs of heat energy and power for the two designs. The assessment shows that a strong economic incentive exists to seek out the remaining proof of feasibility.

2.4 Safety

While a full safety analysis based on the unclad-metal fuel concept is premature and beyond the scope of this report, certain safety aspects were investigated and appear favorable. There is a significant fast negative power coefficient produced by fuel expansion and by the Doppler effect. For slower effects, such as loss of coolant flow and sodium voiding, the short core and the properties of thorium provide responses comparable to those of reactors with clad ceramic fuel. For example, the sodium voiding reactivity coefficient is more than $1.00 negative for complete voiding of the cylindrical core and about $1.50 positive, at most, for voiding of the center of the core only. These values appear to be in a desirable range. The voiding coefficient can be made either more negative or more positive by varying the core geometry, and calculations of such variations have shown that the effect on reactor economics is minor. Neutronic safety aspects are covered in more detail in Chapter 4, while some thermal and hydraulic safety considerations unique to this concept are discussed in Chapter 6.

2.5 Conclusions

This preliminary review of the unclad-metal-fueled breeder reactor concept supports the following conclusions:

1. If technical feasibility can be demonstrated, the concept offers very attractive heat and power costs over a wide range of coolant temperatures. In fact, the similarity of the two core versions suggests that the system could be designed to operate initially as a low-temperature process-heat source and later be upgraded to produce substantial quantities of power. Such a design possibility is not unique to the unclad metal concept but may be particularly desirable for future agricultural water desalting projects. It should be explored further, with primary attention given to the steam-generation and brine-heating systems.

2. The fuel doubling rates are more than adequate for any projected estimates of the needs of the nuclear power industry.

3. The mixed-fuel concept derives important advantages from the metallurgical and thermal properties of thorium and produces about half of its energy from ^{233}U fission. The combination of breeding gain, burnup, and specific power makes the overall performance of the concept outstanding.

4. The use of thorium and the shape of the core provide coolant-void parameters in a desirable range.

5. Although the feasibility of operating large masses of fuel and blanket metal in direct contact with sodium has not been demonstrated in this country, the available experience indicates that problems similar in kind, though lesser in degree, are being solved. The most pertinent experience is that of the Dounreay Fast Reactor. It appears that this question can be resolved by adequate design verified by experimental tests.

6. While there is not yet sufficient proof that the particular fuel composition selected can be irradiated to the proposed levels without affecting its thermal and structural properties, the available information gives positive support for the levels assumed. The relatively short irradiation times and low temperatures required to demonstrate fuel irradiation properties would enable testing to be achieved in a relatively short period at reasonable cost.

7. The initial breeding ratios of the reference concepts fueled with ^{235}U are about 1.2. As ^{233}U and plutonium breed in, the breeding ratios rise and rapidly approach the equilibrium values.

8. Although detailed studies have not been made of the various fueling alternatives, the concept appears to be versatile in a developing breeder system in that it may be arranged to accept either uranium or plutonium fuel and can produce either in its blanket.

2.6 Areas for Future Work

It is recognized that additional study and experimental work will be necessary to produce the information needed to prepare detailed reactor

conceptual designs based on the unclad-metal-fueled system. The major initial activities indicated are the following.

2.6.1 Experimental Work

1. Core materials compatibility testing is needed to identify the effects of temperature, flow rate, sodium purity, and fuel composition on mass transport.

2. An investigation of fuel fabrication methods is needed to determine dimensional tolerances, alloy quality, and critical physical properties of the fuel and blanket elements that may be expected from a given fabrication method as influenced by fuel element shape and composition.

2.6.2 Study and Planning Activities

1. An investigation of alternative fuel element shapes is needed.

2. Fuel irradiation test planning is required.

3. An investigation of alternative fuel element fabrication and chemical processing methods and costs should be made.

4. An investigation is needed of the response of the reference design to various operational transients and accident conditions.

5. Thermal stress analyses should be made of fuel element and coolant hole shapes.

6. Investigations should be made in more detail of the fuel and blanket element handling techniques and of a remote maintenance concept.

3. DESCRIPTION OF CONCEPT

Two versions of the unclad-metal-fueled breeder reactor concept with thermal ratings of 3500 Mw were considered. One version is designed primarily for the production of low-temperature process steam for desalination of seawater, but it includes power-conversion equipment adequate for the needs of an evaporation complex. The other version is designed primarily for power production and includes power-conversion equipment typical of a central power station.

3.1 Core and Blanket

The reference reactor is sodium cooled and has unclad metal fuel in both core and blanket regions. The equilibrium core fuel is a thorium-based alloy with a nominal composition of Th–15 wt % U–7 wt % Pu. The blanket is depleted uranium of a "low-alloy" composition, such as the British "adjusted" uranium (400 to 1200 ppm aluminum, 600 ppm carbon, 300 ppm iron, balance uranium).

The core region is cylindrical and 1.5 ft high. The power-production core is 8.2 ft in diameter and the process-heat-production core is 7 ft in diameter. Lower coolant temperatures in the latter core give rise to a higher average thermal driving force and thereby allow a higher power density. Hence, the core volume is smaller.

Plant characteristics are summarized in Table 3.1, and conceptual arrangements of the core and reactor vessel are shown in Figs. 3.1 and 3.2.

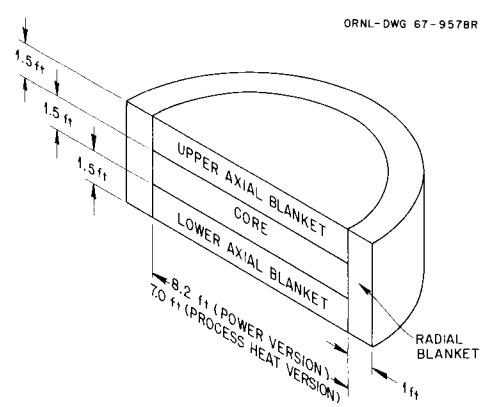

Fig. 3.1. Conceptual Core Arrangement.

Table 3.1. Characteristics of Reference Design

	Process-Heat-Production Concept	Power-Production Concept
Power		
Reactor thermal power, Mw	3500	3500
Fraction of power produced in core	0.79	0.82
Fraction of power produced in axial blanket	0.16	0.14
Fraction of power produced in radial blanket	0.05	0.04
Specific power		
Core metal, kw/kg	290	220
Core fissile, kw/kg	2,250	1,750
Core power density, kw/liter		
Average	1,690	1,284
Peak	2,300	1,740
Core peak-to-average power ratio	1.36	1.35
Breeding characteristics		
Total breeding ratio	1.64	1.64
Core conversion ratio	0.74	0.75
Fuel yield, % per year	23	20
System exponential doubling time, calendar years	3.0	3.4
Annual fissile Pu production, kg	685	680
Equilibrium inventories, including fission products		
Core metal, kg	9,500	13,000
Blanket metal, kg	78,800	96,500
Fissile, kg		
Core	1,231	1,645
Blanket	1,092	1,125
Processing	249	250
Fabrication	379	356
Total for system	2,951	3,376
Fuel and core data		
Core material	(Th-U-Pu) metal	(Th-U-Pu) metal
Blanket material	U metal	U metal
Equilibrium fissile enrichment (wt % heavy metal + F.P.)	12.85	12.54
Dimension across flats of hexagonal coolant holes in core fuel block, in.	0.295	0.244
Thickness of web between coolant holes, in.	0.131	0.108
Length of fuel block, in.	18	18
Total core elements	249	376
Total radial blanket elements	163	206
Core geometry	Cylinder	Cylinder
Core equivalent dimensions, ft		
Diameter	7.0	8.2
Active height	1.5	1.5
Core volume, liters	1,640	2,240
Core volume fractions		
Fuel	0.47	0.47
Sodium	0.50	0.50
Structure	0.03	0.03
Number of control rods	70	80
Control rod material	B_4C	B_4C
Reactor physics data		
Medium fission energy, kev	294	300
"Fuel depletion" reactivity change, δk/day	1.17×10^{-3}	8.6×10^{-4}
Reactivity change on sodium loss from core and axial blanket, δk	−0.0041	−0.0042

Table 3.1 (continued)

	Process-Heat-Production Concept	Power-Production Concept
Reactor physics data (continued)		
Maximum reactivity change on sodium loss from one core assembly, δk	+0.00008	+0.00003
Maximum reactivity change upon removing one core fuel assembly, δk	0.0021	0.0015
Worth of all control rods, δk	0.0658	0.0563
Thermal and hydraulic data		
Reactor inlet temperature, °C	170	345
Reactor outlet temperature, °C	350	525
Primary sodium system		
Number of loops	3	3
Sodium flow per loop, lb/hr	39×10^6	40.3×10^6
Sodium temperature rise, °C	162	162
Number of pumps per loop	1	1
Design total head, ft	260	264
Nominal pump motor power, hp	5,200	5,400
Intermediate heat exchangers		
Number	3	3
Area per exchanger, ft^2	46,000	46,000
Primary inlet temperature, °C	350	525
Primary outlet temperature, °C	170	345
Secondary inlet temperature, °C	149	324
Secondary outlet temperature, °C	298	476
Secondary sodium system		
Number of loops	3	3
Sodium flow per loop, lb/hr	46.7×10^6	48.7×10^6
Sodium temperature rise, °C	128	128
Number of pumps per loop	1	1
Design total head, ft	95	96
Nominal pump motor power, hp	2,300	2,400
High-pressure steam generator		
Total number per reactor	3	3
Area per exchanger, ft^2	70,000	46,000
Steam per flow exchanger, lb/hr	2.87×10^6	4.53×10^6
Feedwater temperature, °C	120	220
Steam outlet temperature, °C	243	366
Steam outlet pressure, psia	173	1,450
Low-pressure steam generator		
Total number per reactor	3	
Area per exchanger, ft^2	26,000	
Steam per flow exchanger, lb/hr	1.07×10^6	
Feedwater temperature, °C	120	
Steam outlet temperature, °C	127	
Steam outlet pressure, psia	38	
System operating data at 0.9 plant factor		
Thermal efficiency, %		
Gross	8.1[a]	38.2
Net	7.4[a]	36.6
Annual prime heat production, MBtu	94.2×10^6	94.2×10^6
Annual 227°C (260°F) heat production, MBtu	86.4×10^6	
Annual gross electrical power production		
kwhr	2.24×10^9	10.5×10^9
Mw	284	1,332

[a]With turbine exhaust at 127°C (260°F). Net power production is assumed to be primarily used for desalting-evaporator operation and product-water pumping.

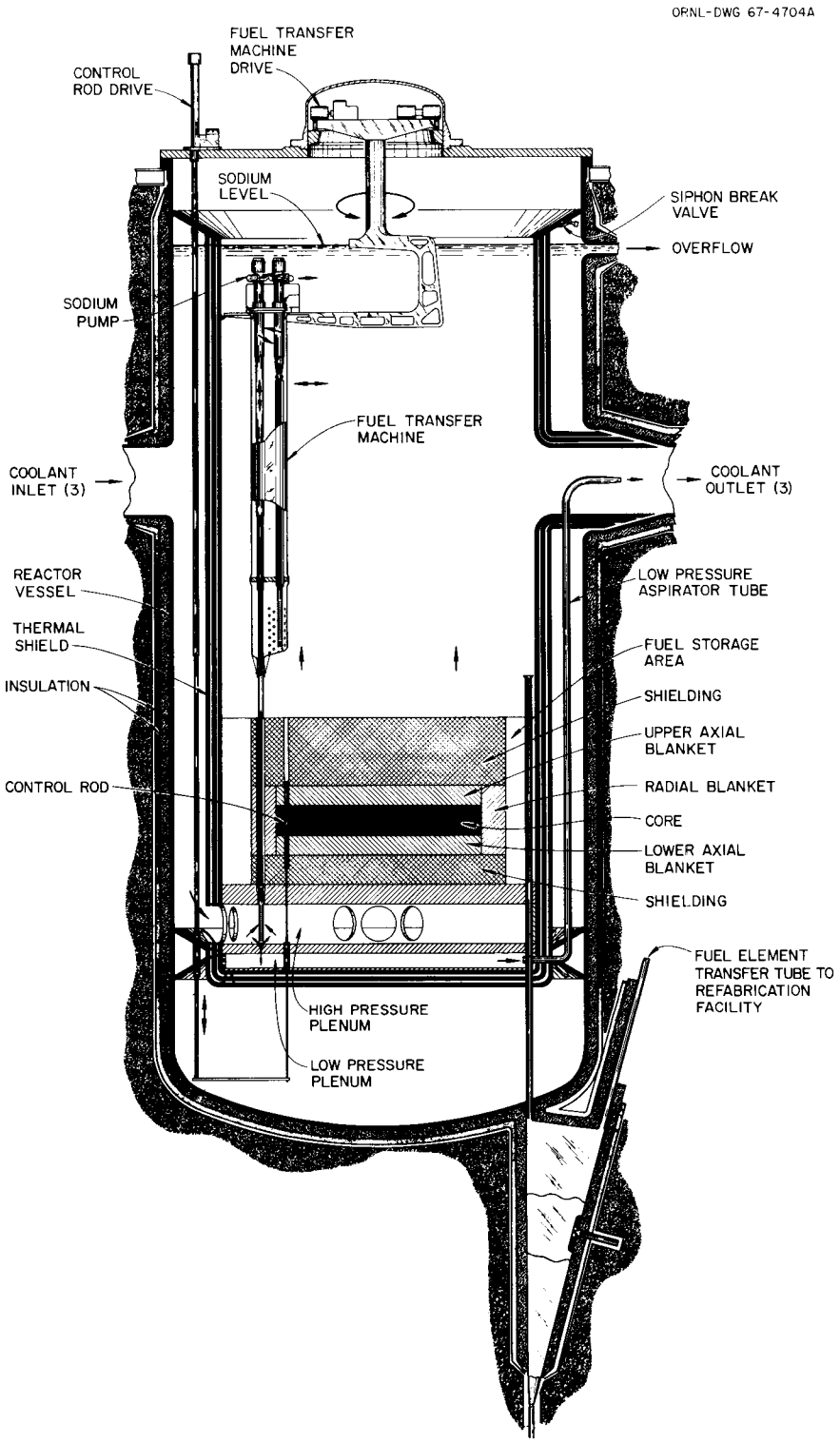

Fig. 3.2. Reactor Vessel and Internals.

3.2 Fueling Concept

The basic fuel element, shown in Fig. 3.3, is a hexagonal prism with hexagonal coolant passages parallel to the axis. The dimensions of the coolant holes and the thickness of the web are determined by the specific power of the system. Table 3.1 gives these dimensions for both the power- and the process-heat-production cores.

The core fuel element assembly, shown in Fig. 3.4, is a hexagonal container that holds the core fuel element and similarly shaped axial blanket and shielding blocks. The radial blanket elements are similar except that they contain only depleted uranium elements and shielding blocks.

ORNL-DWG 67-10461

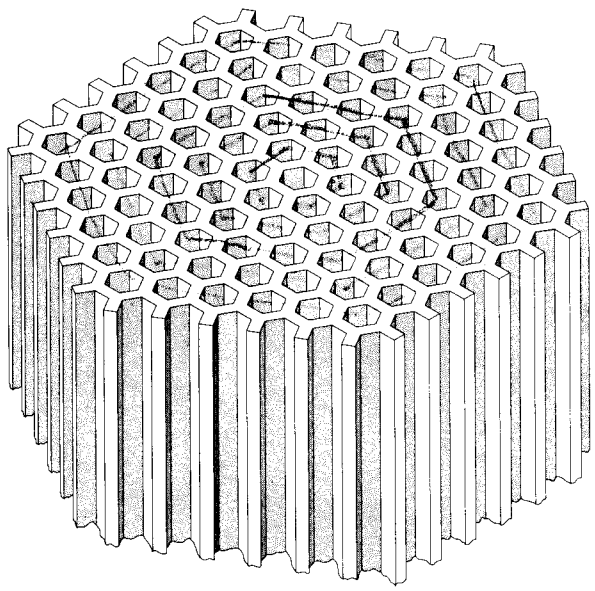

Fig. 3.3. Basic Fuel Element.

ORNL-DWG 67-4705AR

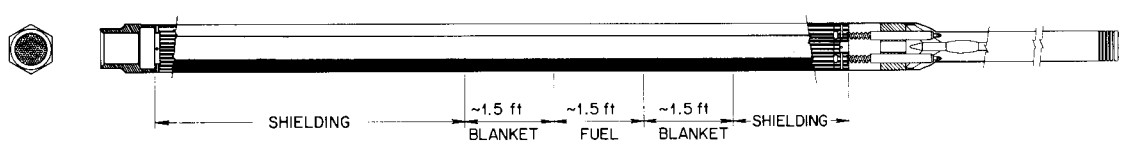

Fig. 3.4. Fuel Element Assembly.

The hexagonal fuel element container serves as the basic handling unit and maintains alignment of the individual parts in the core, blanket, and shielding sections of the assembly. It is constructed of a suitable material, such as V–20% Ti, and has contact surfaces clad with Stellite to reduce galling. Since the fuel element containers in the radial blanket receive less irradiation than those in the core and axial blanket, they are assumed to be reused for ten fuel-irradiation cycles before replacement.

Off-stream fuel loading and unloading is accomplished by means of a fuel-handling machine located inside the reactor vessel. The spent fuel is allowed to cool several days inside the reactor vessel and is then transferred through a sodium filled transfer tube to the refabrication facility.

3.3 Steam Generation System

The primary and secondary sodium heat transport systems are similar to those proposed for other large sodium-cooled fast breeder reactors. Figures 3.5 through 3.8 show the arrangement of these systems for the power- and process-heat-production reactors. Table 3.1 summarizes the salient features of each system.

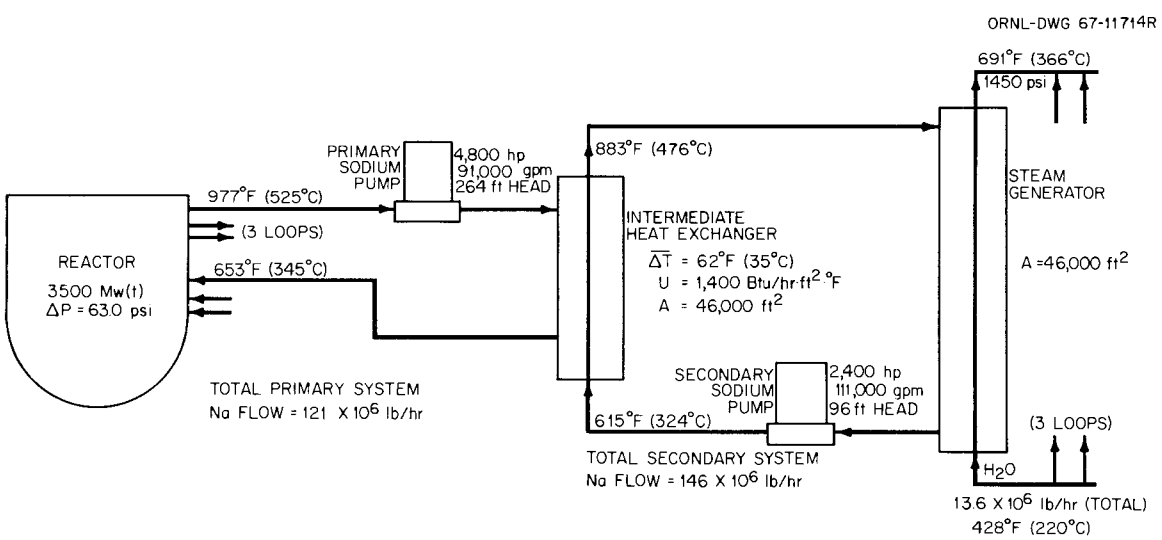

Fig. 3.5. Sodium Heat Exchangers for Mixed-Fuel Power-Production Concept.

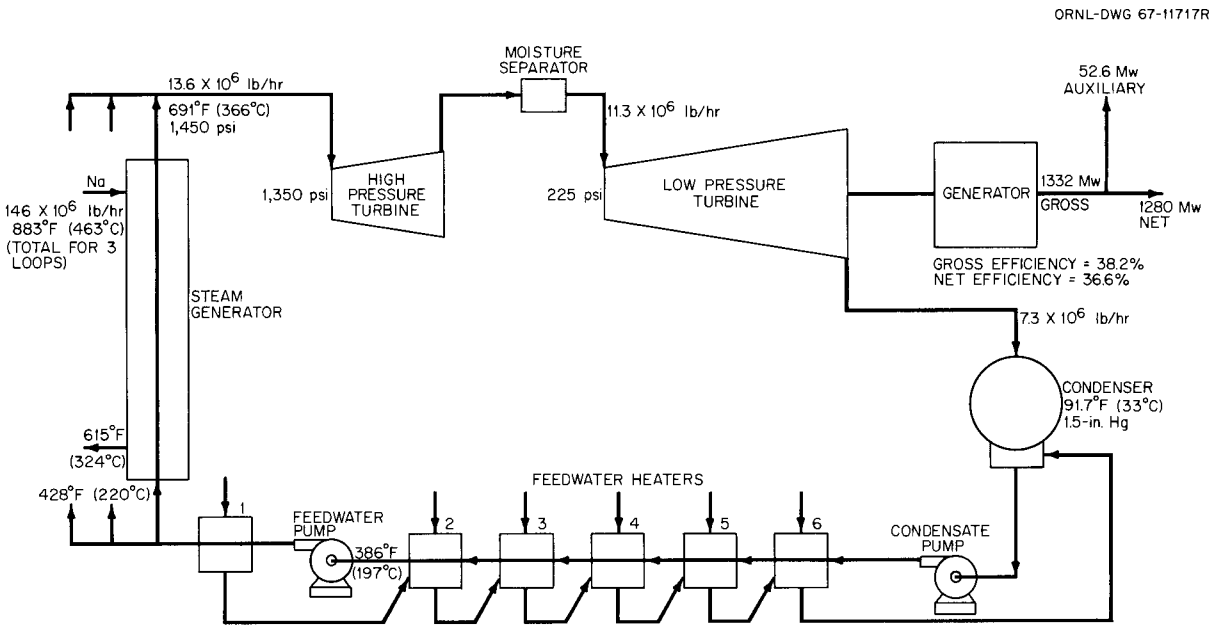

Fig. 3.6. Steam Cycle for Mixed-Fuel Power-Production Concept.

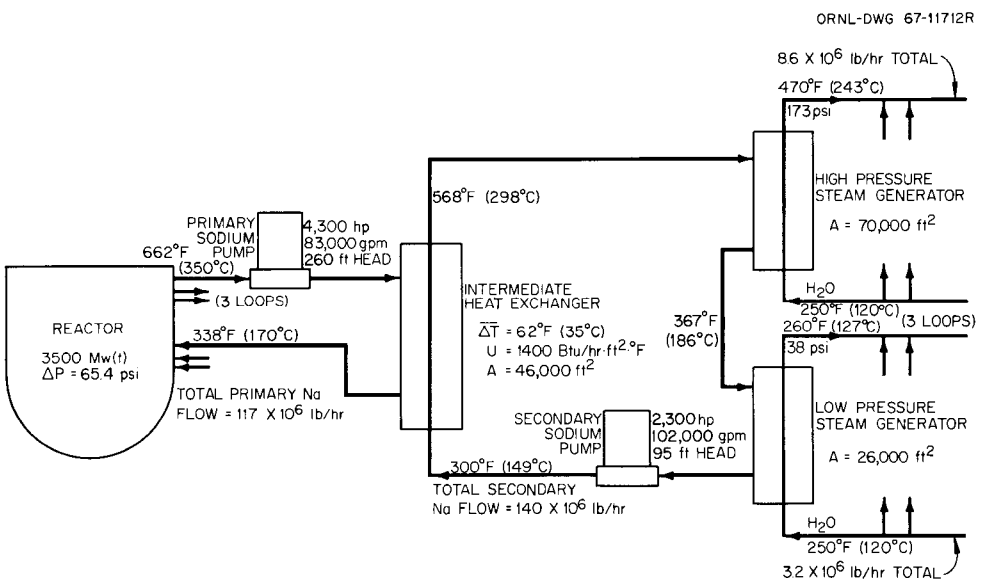

Fig. 3.7. Sodium Heat Exchangers for Mixed-Fuel Process-Heat-Production Concept.

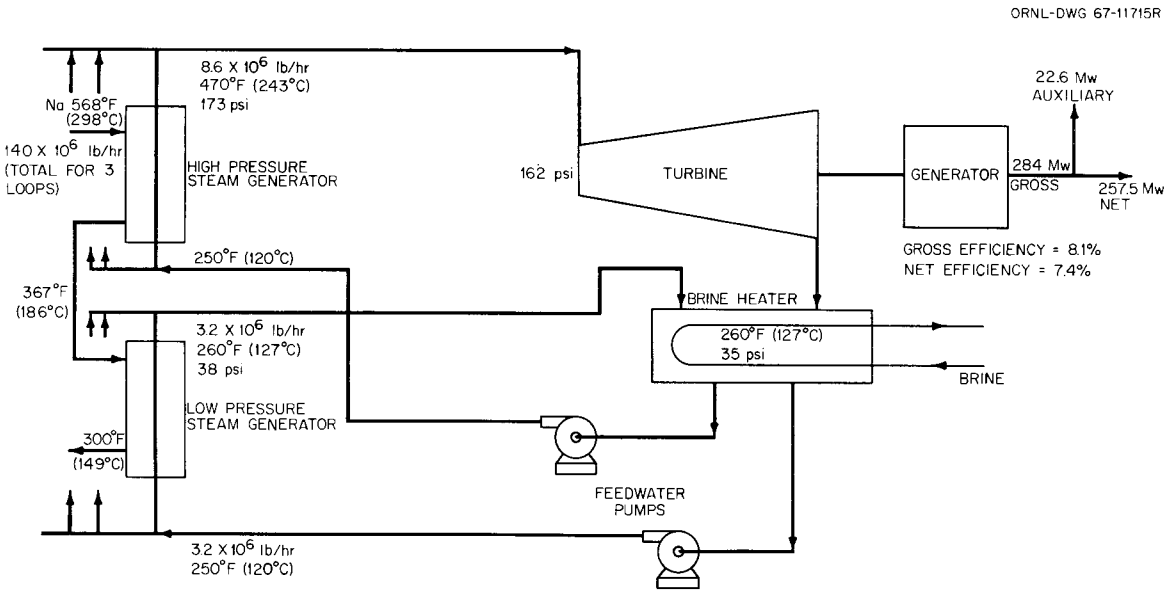

Fig. 3.8. Steam Cycle for Mixed-Fuel Process-Heat-Production Concept.

A distinguishing feature of the coolant system of the process-heat-production concept is the presence of both high- and low-pressure steam generators.[1,2] The dual-pressure cycle is of interest in order to generate a large fraction of the total steam at a pressure higher than that attainable with a single-pressure cycle. This is particularly appropriate for a process-heat-production system because the increased pressure represents a substantial improvement in the turbine pressure ratio (4.73 with the dual-pressure cycle in contrast to 1.24 for a single-pressure cycle), which leads to a substantial increase in the thermal efficiency of the system. It is also possible to bypass the low-pressure steam around the turbine directly to the brine heater. The turbine may therefore be smaller and less expensive. The higher temperature power systems tend to benefit less from this approach because a single-pressure system produces steam at adequately high pressures and temperatures. In addition, the low condensing pressure in the power cycle diminishes the effect of the higher pressure on the overall turbine pressure ratio.

3.4 Fission-Product Removal and Maintenance Concepts

The absence of fuel cladding permits a small but steady stream of fission products to enter the primary sodium system. It is necessary therefore to incorporate sodium cleanup devices in the system to limit the fission-product concentration in the primary sodium to acceptable levels. The design of the cover gas system also takes into account the expected presence of gaseous fission products in the gas blanket.

It is presently anticipated that normal sodium purification methods, such as cold trapping and hot trapping, will be adequate to reduce oxygen concentrations in the sodium sufficiently to avoid excessive oxygen buildup in the metallic fuel.

System maintenance will be affected by the expected level of fission products in the primary sodium. Experience at ORNL with circulating-fluid-fueled reactors (notably the MSRE and the HRE) has demonstrated that maintenance of highly contaminated systems can be handled. Further evidence of this comes from experience with the Dounreay Fast Reactor,[3] which has direct contact between the NaK coolant and metallic uranium-molybdenum fuel.

References

1. R. R. Matthews et al., Performance and Operation of the Dounreay Fast Reactor, Proceedings of the Third International Conference on the Peaceful Uses of Atomic Energy, Geneva, 1964, Vol. 6, pp. 23–30, United Nations, New York, 1965.

2. W. R. Wootton, A. J. Taylor, and N. G. Worley, Steam Cycles for Gas-Cooled Reactors, Proceedings of the Second International Conference on the Peaceful Uses of Atomic Energy, Geneva, 1958, Vol. 7, pp. 827–834, United Nations, New York, 1958.

3. W. R. Wootton, Steam Cycles for Nuclear Power Plant, Simmons-Boardman Publishing Corporation, New York, 1958.

4. PHYSICS

The parameters pertinent to the two reference designs used in the physics calculations are given in Table 4.1. The cores consist of two enrichment zones of approximately equal volume. The zoned core was selected in order to flatten the radial power distribution.

4.1 Calculational Methods

The fuel-cycle calculations were all done on an equilibrium basis with the MERC code. The reactivity worths of reactor materials, as well as prompt-neutron lifetimes and effective delayed-neutron fractions, were estimated with first-order perturbation theory by using the two-dimensional diffusion-theory code EXTERMINATOR-2. A combination of perturbation calculations made with EXTERMINATOR-2 and difference-of-k calculations made with the two-dimensional diffusion-theory code CITATION were used to determine the reactivity effect of partial sodium voiding. Doppler coefficients and fuel-expansion reactivity coefficients were also calculated with the CITATION code. The MODRIC 1-D diffusion-theory code was used for all other physics calculations.

For the MERC and MODRIC calculations, a two-dimensional synthesis was made by iterating between radial and axial calculations. The transverse buckling terms were adjusted until the leakage from the core for each group in the radial calculation matched the corresponding term in the axial calculation and vice versa.

Twenty-group cross-section sets were computed with the GAM-II code from the 100-group cross-section sets on the GAM-II data tape. The ^{232}Th, ^{234}U, ^{236}U, ^{238}U, ^{240}Pu, and ^{242}Pu cross sections were calculated by the GAM-II code to allow for Doppler broadening and homogeneous resonance self-shielding. All other nuclides were assumed to be dilute.

4.2 Equilibrium Fuel Cycle

The fuel-cycle calculations were made on an equilibrium basis. In these calculations it was assumed that the feed and discharge in the core

Table 4.1. Reactor Physics Parameters

	Process-Heat-Production Reactor	Power-Production Reactor
Reactor thermal power, Mw	3500	3500
Plant factor	0.9	0.9
Core geometry	Cylinder	Cylinder
Number of core zones	2	2
Core fuel material	Th-U-Pu alloy	Th-U-Pu alloy
Blanket fuel material	Depleted U metal	Depleted U metal
Dimensions, ft		
Core height	1.5	1.5
Diameter of inner core	5.0	5.8
Total core diameter	7.0	8.2
Radial blanket thickness	1.0	1.0
Radial blanket height	4.5	4.5
Axial blanket thickness	1.5	1.5
Region volumes, ft^3		
Core	57.9	79.2
Axial blanket	115.7	158.4
Radial blanket	122.6	139.5
Average core fuel burnup between reprocessings, Mwd/kg	100	100
Average core fuel burnup between refabrications, Mwd/kg	33.3	33.3
Average core fuel density, g/cm^3	12.4	12.4
Reactor composition, volume fractions		
Core and axial blanket		
Sodium	0.50	0.50
Fuel	0.47	0.47
Structure	0.03	0.03
Radial blanket		
Sodium	0.22	0.22
Fuel	0.75	0.75
Structure	0.03	0.03

and blankets were continuous and that the exposure was uniform. The core fuel material is a mixed thorium-uranium-plutonium alloy, and the blanket feed material is depleted uranium metal containing 0.3% ^{235}U.

Refabrication of the core fuel elements is done after average burnup intervals of 33 Mwd/kg. No credit was taken in the physics calculations for any loss of fission products during the refabrication operation.

When the core fuel reaches an accumulated burnup of 100 Mwd/kg, it is removed for reprocessing. The reprocessed material is recycled back to the core. A portion of the plutonium from the blanket discharge is used to maintain core criticality; the remainder is sold. The balance of the core makeup consists of thorium and depleted uranium in an appropriate ratio to retain the favorable metallurgical properties of the thorium-based alloy (see Chapt. 5).

The physics characteristics of the reference designs are given in Table 4.2; the neutron balances are given in Table 4.3; and the equilibrium inventories are given in Table 4.4. Figures 4.1 through 4.4 are

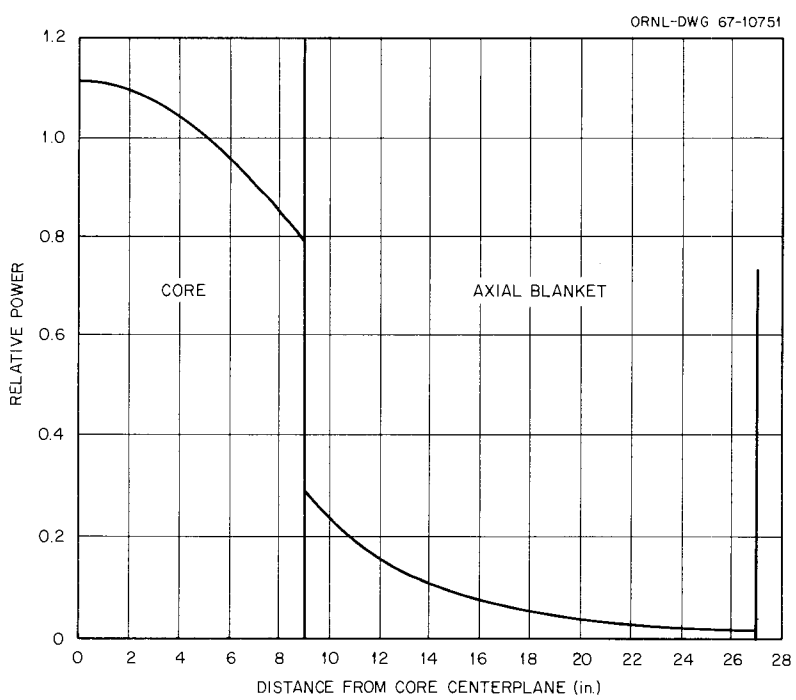

Fig. 4.1. Axial Power Distribution for Process-Heat-Production Reactor.

Table 4.2. Reactor Characteristics

	Process-Heat-Production Reactor	Power-Production Reactor
Power distribution, % of total		
Inner core	42.0	44.4
Outer core	37.2	37.9
Total core	79.2	82.3
Axial blanket	15.9	13.9
Radial blanket	4.9	3.8
Core enrichment, % heavy metal plus fission-product pairs		
Inner core	11.38	11.25
Outer core	14.31	13.84
Average	12.85	12.54
Blanket discharge enrichment, % heavy metal plus fission-product pairs[a]		
Axial blanket	3.18	2.48
Radial blanket	2.30	2.06
Peak blanket burnups, Mwd/kg		
Axial blanket	5.67	3.39
Radial blanket	7.78	6.58
Fissile inventories, kg[a]		
Inner core	544	739
Outer core	687	906
Axial blanket	496	521
Radial blanket	596	604
Processing	249	250
Fabrication	379	356
Total	2951	3376
Fissile sales, kg per day	1.876	1.869
Fuel yield, % per year at 0.90 load factor	23.2	20.2
Geometric doubling time, years[b]	3.0	3.4
Core conversion ratio		
Inner core	0.82	0.82
Outer core	0.65	0.67
Average	0.74	0.75
Total breeding ratio[c]		
Including blanket ^{235}U absorptions	1.60	1.60
Excluding blanket ^{235}U absorptions	1.64	1.64
Power peaking factors		
Core		
Axial	1.11	1.11
Radial	1.17	1.17
Age[d]	1.05	1.04
Axial blanket		
Axial	3.19	3.45
Radial	1.17	1.17
Age	1.43	1.40
Radial blanket		
Axial	2.77	2.85
Radial	3.61	3.68
Age	1.39	1.38

[a]Does not include ^{235}U from depleted uranium.

[b]Doubling time in calendar years of core plus blanket plus out-of-pile fissile inventory = 0.693/yield.

[c]Breeding ratio = (capture in ^{232}Th + ^{234}U + ^{238}U + ^{240}Pu less absorptions in ^{233}Pa)/(absorptions in ^{233}U + ^{235}U + ^{239}Pu + ^{241}Pu).

[d]Peak-to-average fission rate ratios in the fuel as a function of time in the core.

Table 4.3. Neutron Balances

Reactor	Neutron Event	Isotope	Percentage of Total Absorptions Plus Leakage[a] or Productions			
			Inner Core	Outer Core	Axial Blanket	Radial Blanket
Process heat production	Absorption	^{232}Th	11.77	8.55		
		^{233}Pa	0.23	0.12		
		^{233}U	10.82	7.84		
		^{234}U	0.79	0.56		
		^{235}U	0.29	0.20	0.58	0.23
		^{236}U	0.05	0.03		
		^{238}U	1.14	0.42	26.42	10.04
		^{239}Pu	3.73	5.23	3.52	0.93
		^{240}Pu	0.44	0.64	0.02	
		^{241}Pu	0.20	0.29		
		^{242}Pu	0.03	0.04		
		Fission products	0.72	0.53	0.09	0.02
		Steel	0.08	0.06	0.09	0.02
		Sodium	0.06	0.05	0.08	0.01
		Total	30.35	24.56	30.80	11.25
		Outer core		24.56		
		Axial blanket		30.80		
		Radial blanket		11.25		
		Leakage		3.04		
		Total		100.0		
	Fissions	^{232}Th	0.59	0.47		
		^{233}Pa	0.10	0.06		
		^{233}U	9.99	7.25		
		^{234}U	0.50	0.36		
		^{235}U	0.24	0.16	0.46	0.18
		^{236}U	0.02	0.01		
		^{238}U	0.24	0.10	2.40	0.81
		^{239}Pu	3.34	4.68	2.99	0.80
		^{240}Pu	0.24	0.35	0.01	
		^{241}Pu	0.18	0.25		
		^{242}Pu	0.01	0.02		
		Total	15.45	13.71	5.86	1.79
		Fissions = 36.81% of neutron events				
	Productions	^{232}Th	1.54	1.22		
		^{233}Pa	0.29	0.16		
		^{233}U	25.37	18.41		
		^{234}U	1.32	0.96		
		^{235}U	0.59	0.41	1.13	0.45
		^{236}U	0.05	0.03		
		^{238}U	0.67	0.27	6.67	2.27
		^{239}Pu	9.86	13.81	8.73	2.33
		^{240}Pu	0.79	1.16	0.03	
		^{241}Pu	0.55	0.78	0.01	
		^{242}Pu	0.07	0.07		
		Total	41.10	37.28	16.57	5.05

[a]Absorptions in control rods are not included in this balance but are accounted for in fuel-cycle costs.

Table 4.3 (continued)

Reactor	Neutron Event	Isotope	Percentage of Total Absorptions Plus Leakage[a] or Productions			
			Inner Core	Outer Core	Axial Blanket	Radial Blanket
Power production	Absorptions	^{232}Th	12.48	8.94		
		^{233}Pa	0.19	0.10		
		^{233}U	11.52	8.23		
		^{234}U	0.84	0.59		
		^{235}U	0.31	0.21	0.62	0.19
		^{236}U	0.05	0.04		
		^{238}U	1.23	0.52	27.04	8.23
		^{239}Pu	3.97	5.15	2.75	0.68
		^{240}Pu	0.46	0.60	0.01	
		^{241}Pu	0.21	0.27		
		^{242}Pu	0.03	0.04		
		Fission products	0.76	0.55	0.06	0.01
		Structure	0.08	0.06	0.10	0.02
		Sodium	0.07	0.05	0.08	0.01
		Total	32.20	25.35	30.66	9.14
		Outer core			25.35	
		Axial blanket			30.66	
		Radial blanket			9.14	
		Leakage			2.64	
		Total			100.0	
	Fissions	^{232}Th	0.63	0.49		
		^{233}Pa	0.09	0.05		
		^{233}U	10.65	7.61		
		^{234}U	0.53	0.38		
		^{235}U	0.25	0.17	0.49	0.15
		^{236}U	0.03	0.01		
		^{238}U	0.26	0.12	2.32	0.65
		^{239}Pu	3.55	4.61	2.33	0.58
		^{240}Pu	0.25	0.33	0.01	
		^{241}Pu	0.18	0.23		
		^{242}Pu	0.01	0.02		
		Total	16.43	14.02	5.15	1.38
		Fissions = 36.98% of neutron events				
	Productions	^{232}Th	1.62	1.27		
		^{233}Pa	0.24	0.13		
		^{233}U	27.02	19.32		
		^{234}U	1.41	1.00		
		^{235}U	0.64	0.44	1.21	0.37
		^{236}U	0.07	0.04		
		^{238}U	0.72	0.33	6.46	1.81
		^{239}Pu	10.47	13.61	6.80	1.70
		^{240}Pu	0.81	1.09	0.02	
		^{241}Pu	0.56	0.73		
		^{242}Pu	0.05	0.06		
		Total	43.61	38.02	14.49	3.88

Table 4.4. System Inventories

Reactor	Isotope	Equilibrium Inventory (kg)			
		Core	Axial Blanket	Radial Blanket	Out of Pile
Process heat production	^{232}Th	6,895			2,411
	^{233}Pa	60			22
	^{233}U	654			232
	^{234}U	179			64
	^{235}U	24	73	131	38
	^{236}U	20	2.9	3.3	8.4
	^{238}U	537	28,570	48,840	12,063
	^{239}Pu	474	495	596	356
	^{240}Pu	121	8	6	46
	^{241}Pu	18	0.2	0.1	6.3
	^{242}Pu	9	Negligible	Negligible	3
	Fission products	496	78	67	266
	Enrichment fractions[a]	0.129	0.017	0.012	0.042
Power production	^{232}Th	9,440			2,504
	^{233}Pa	65			18
	^{233}U	900			242
	^{234}U	247			67
	^{235}U	34	104	151	43
	^{236}U	28	3.1	3.4	8.6
	^{238}U	787	39,330	55,650	11,740
	^{239}Pu	625	521	604	331
	^{240}Pu	154	6.3	5.4	43
	^{241}Pu	22	0.1	0.1	6
	^{242}Pu	11	Negligible	Negligible	2.9
	Fission products	681	64	61	294
	Enrichment fractions[a]	0.126	0.013	0.011	0.040

[a]Blanket ^{235}U not included.

plots of the axial and radial power distributions for the reference reactors, and Fig. 4.5 is a graph of the peak neutron flux per full power day above a given neutron energy as a function of neutron energy.

The physics results given in Table 4.2 are based on continuous on-line refueling. For the process-heat- and power-production reactors, refueling after each 10 full-power days, as assumed in the economic evaluation (see Chapt. 9), would decrease the breeding ratios to 1.62 and 1.63, increase the fissile inventories to 2969 and 3395 kg, and decrease the

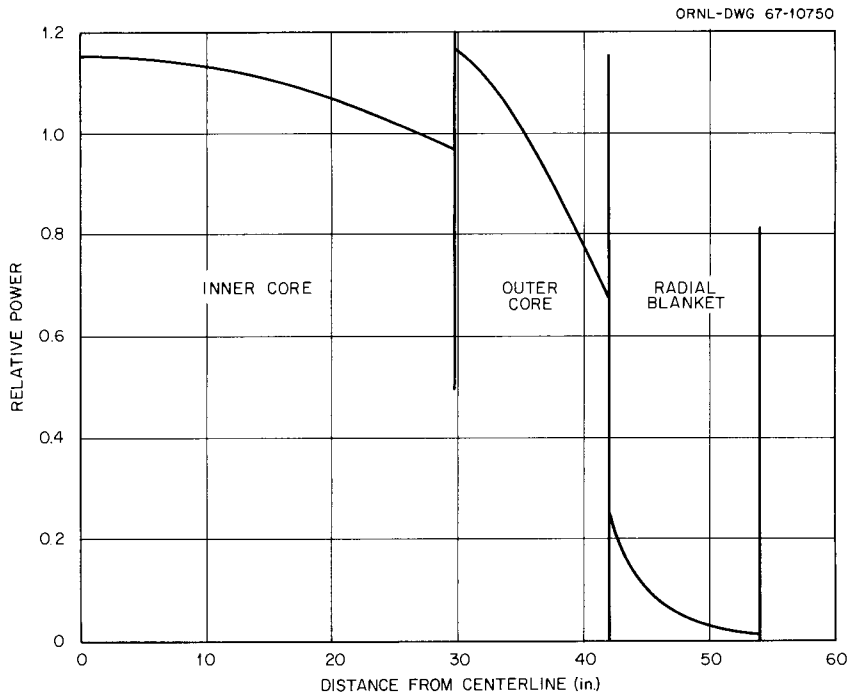

Fig. 4.2. Radial Power Distribution for Process-Heat-Production Reactor.

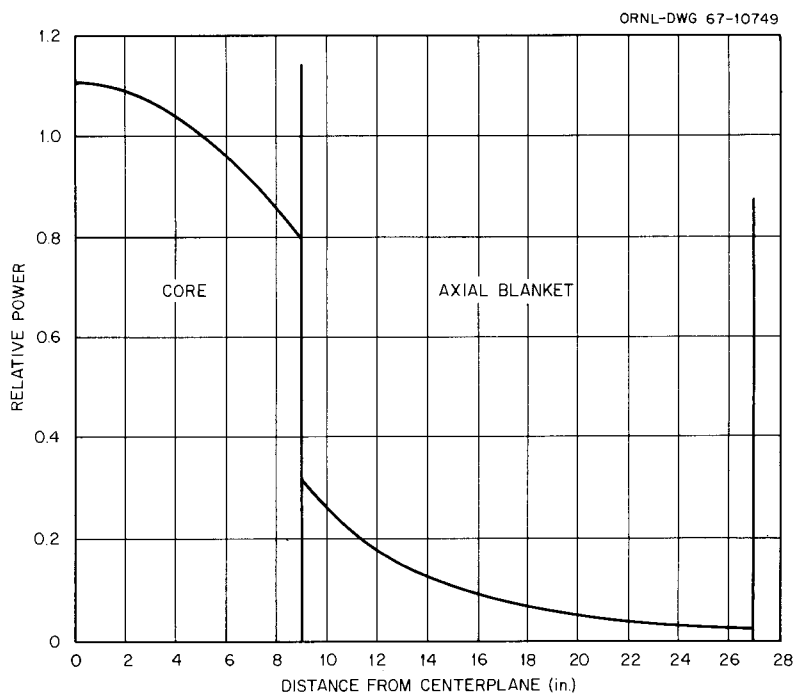

Fig. 4.3. Axial Power Distribution for Power-Production Reactor.

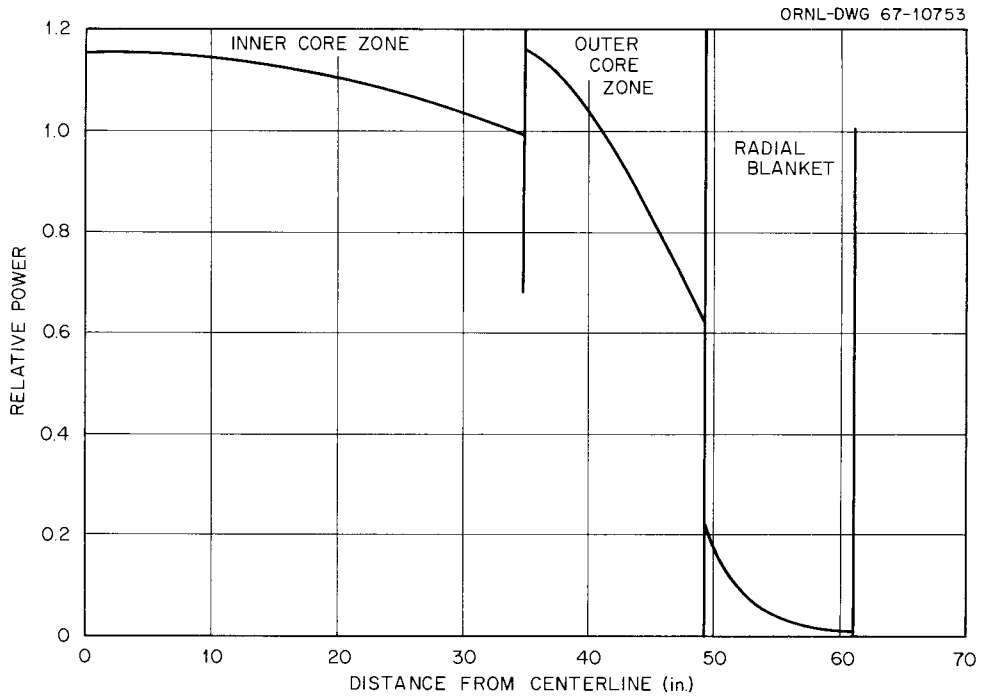

Fig. 4.4 Radial Power Distribution for Power-Production Reactor.

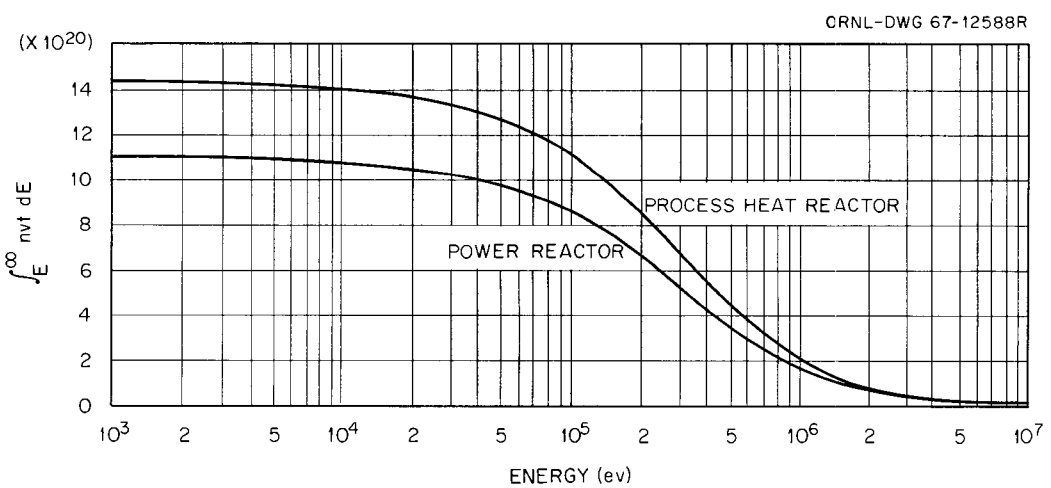

Fig. 4.5. Peak Neutron Flux per Full-Power Day Above a Given Neutron Energy as a Function of Neutron Energy.

net fissile production rates to 1.821 and 1.828 kg per day, respectively. These revised figures lead to doubling times of 3.1 years for the process-heat-production concept and 3.5 years for the power-production concept. The economic evaluation allows for the excess reactivity requirements of the intermittent off-stream refueling.

4.3 Reactivity Coefficients

Reactivity coefficients and various reactivity worths for the two reference designs are given in Table 4.5. In the calculation of the δk available between operating and melting temperatures, it was assumed that the melting point of the fuel was 1250°C. The fuel temperature increase was assumed to have the shape of the static power distribution so that the peak temperature would rise from 650 to 1250°C while the average fuel temperature would rise only from 445 to 907°C for the process-heat-production reactor and from 540 to 1002°C for the power-production reactor before melting of the central fuel element would begin.

A linear expansion coefficient of $1.2 \times 10^{-5}/°C$ was used in the calculations. Any phase changes that might occur in the uranium metal were neglected.

The Doppler coefficient, effective delayed-neutron fraction, and prompt-neutron lifetime were calculated for the power-production reactor. The process-heat-production reactor would be expected to have similar values.

Control is normally maintained by the use of B_4C rods positioned throughout the core. These rods are adequate to compensate for any partial sodium loss as well as for the normal requirements of shim control, temperature defect, and shutdown margin. In addition to this primary control system, another independent backup shutdown system is also provided. Fuel may be removed from the core by the lowering of clusters of fuel assemblies in the outer portion of the core. The number of B_4C rods and movable fuel assemblies needed, as well as the reactivity worths associated with control and shutdown for each of the reference reactors, are given in Table 4.6. The shutdown margin provided is thought to be more than adequate to compensate for any accidental reactivity insertion.

Table 4.5. Reactivity Worths

	Process-Heat-Production Reactor	Power-Production Reactor
Isothermal temperature coefficient, δk/°C		
Doppler	-0.27×10^{-5}	-0.24×10^{-5}
Fuel expansion	-0.10×10^{-5}	-0.08×10^{-5}
Sodium (from fuel expansion)	-0.01×10^{-5}	-0.01×10^{-5}
Total	-0.38×10^{-5}	-0.33×10^{-5}
Power coefficient at constant sodium inlet temperature, δk/Mw(th)		
Doppler	-2.12×10^{-7}	-1.33×10^{-7}
Fuel expansion	-0.82×10^{-7}	-0.59×10^{-7}
Sodium		
From fuel expansion	-0.04×10^{-7}	-0.03×10^{-7}
From sodium temperature rise	-0.28×10^{-7}	-0.30×10^{-7}
Total	-3.26×10^{-7}	-2.25×10^{-7}
Dependence of peak fuel temperature on power, °C/Mw(th)	0.1021	0.0724
δk available between operating and melting temperature		
Doppler	−0.00096	−0.00087
Fuel expansion	−0.00049	−0.00039
Sodium (from fuel expansion)	−0.00002	−0.00002
Total	−0.00147	−0.00128
Maximum reactivity rise on loss of sodium from one fuel assembly, δk	0.00008	0.00003
Reactivity change from complete loss of sodium from core plus axial blanket, δk	−0.0040	−0.0042
Reactivity rise upon loss of sodium from inner core plus its axial blanket, δk	0.0025	0.0020
Maximum reactivity rise from partial sodium voiding, δk	(a)	0.0065
Average reactivity worth of fuel element, δk	0.00137	0.00090
Maximum reactivity worth of fuel element, δk	0.00214	0.00145
Average control rod worth, δk	0.00094	0.00070
Central control rod worth, δk	0.00223	0.00133
Fuel depletion reactivity change, δk per day	-1.17×10^{-3}	-8.6×10^{-4}
Fuel expansion reactivity coefficient, δk/°C	-1.1×10^{-6}	-8.9×10^{-7}
Doppler coefficient		
At operating temperature, δk/°C	-2.6×10^{-6}	-2.4×10^{-6}
T·dk/dT	−0.00194[b]	−0.00194
Effective delayed-neutron fraction	0.004[b]	0.004
Prompt-neutron lifetime, sec	1.6×10^{-7} (b)	1.6×10^{-7}

[a]This value was not calculated.

[b]Estimated to be the same as for the power-production reactor.

Table 4.6. Control Worth

	Process-Heat-Production Reactor	Power-Production Reactor
Number of B_4C control rods	70	80
Net worth of B_4C rods, δk	0.0658	0.0563
Shim control, δk	0.0117	0.0086
Temperature defect, δk	0.0025	0.0029
Decay of ^{233}Pa, δk	0.0297	0.0241
Shutdown margin, δk	0.0219	0.0207
Number of movable fuel assemblies	23	50
Worth of movable fuel assemblies, δk	0.0207	0.0207

4.4 Sodium Voiding Effects

The reactivity change upon complete sodium voiding of the core and axial blanket was found to be negative for both reference reactors. Two conditions of partial sodium voiding were also studied. In the first the voiding was assumed to begin at the core center and propagate radially outward to the radial blanket. This reactivity change as a function of core radius is given in Figs. 4.6 and 4.7. The voiding of a core area implies voiding of the axial blanket above and below that area. The maximum δk that can be inserted by this manner of partial sodium voiding was found to be +0.25% δk for the process-heat-production reactor and +0.20% δk for the power-production reactor. For both reactors the maximum occurred with voiding approximately to the interface between the two core zones.

In the second sodium voiding condition the void was assumed to form in the central core zone at the midplane of the reactor and then expand axially toward both axial blankets. Since the first sodium voiding condition indicated that the positive reactivity change was maximum when the entire inner core zone but none of the outer core zone was voided of sodium, it was assumed that the axially expanding void had the diameter of the inner core zone. The reactivity change from this sodium voiding condition was calculated only for the power reactor and is given as a function of fraction of inner core voided in Fig. 4.8. These results

indicate that the power-production reactor could be as much as 65 cents above prompt critical for certain configurations of partial sodium voiding.

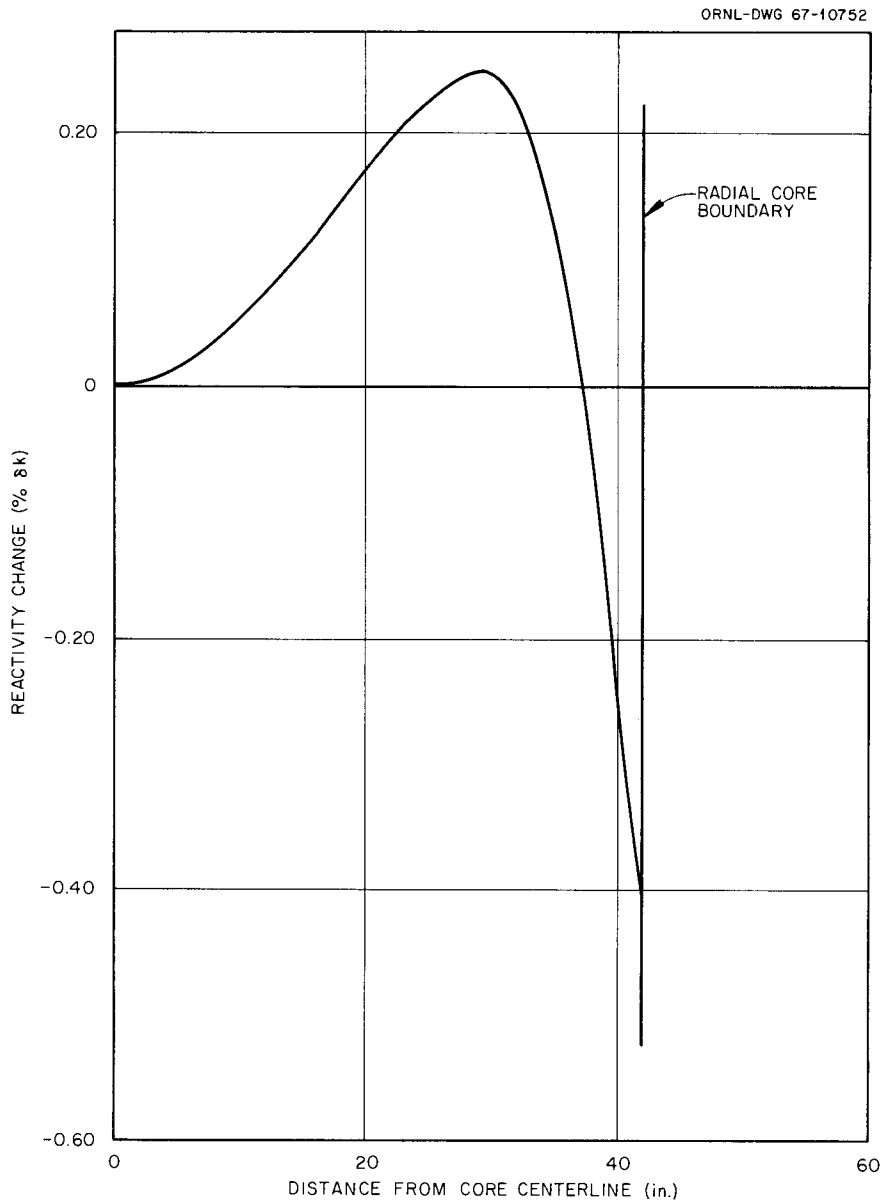

Fig. 4.6. Reactivity Change as a Function of Distance from Core Center Line Voided of Sodium in Process-Heat-Production Reactor.

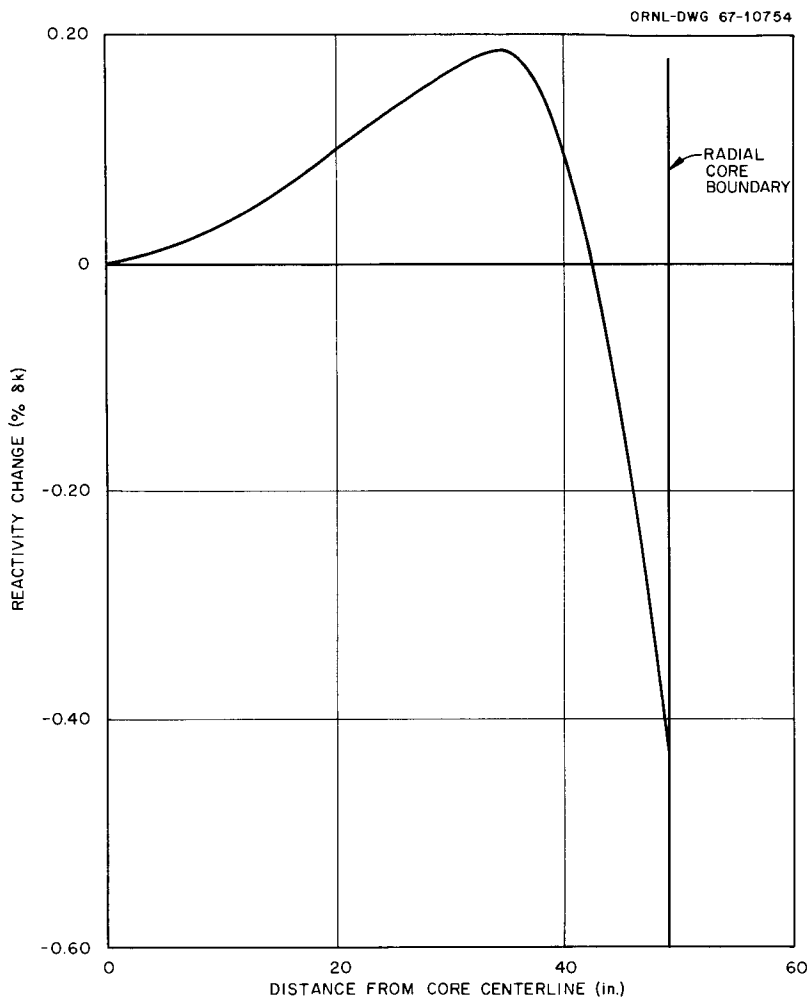

Fig. 4.7. Reactivity Change as a Function of Distance from Core Center Line Voided of Sodium in Power-Production Reactor.

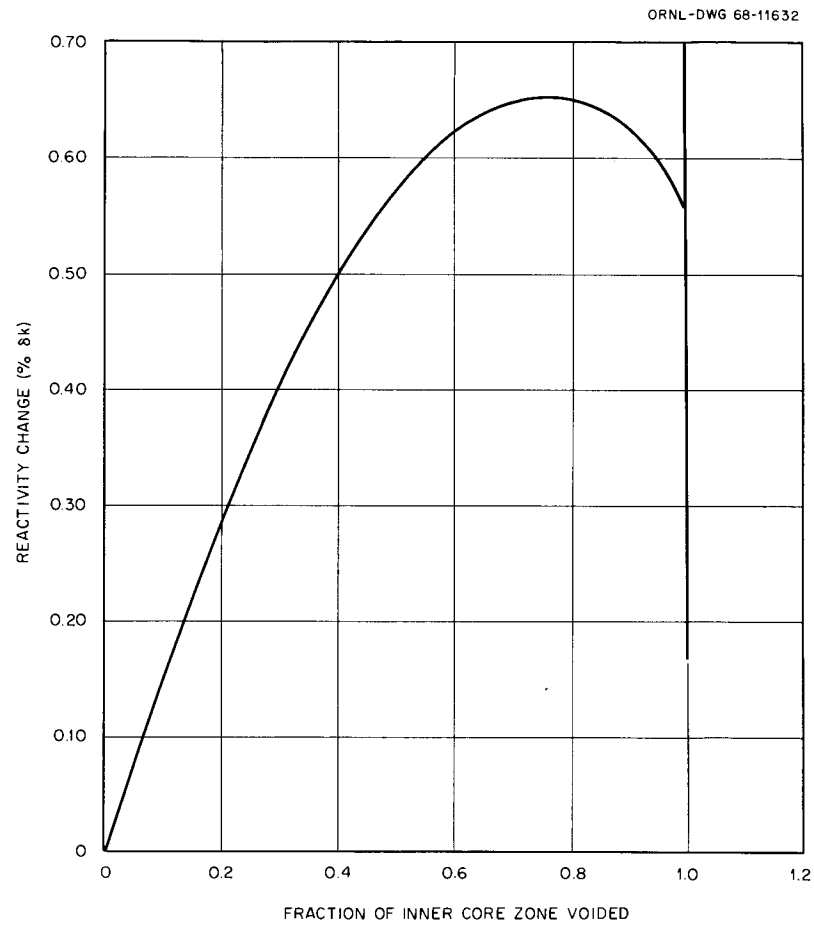

Fig. 4.8. Reactivity Change as a Function of Fraction of Inner Core Zone Voided of Sodium in the Power-Production Reactor.

4.5 Startup on ^{235}U

If it is decided to start up the reactor on ^{235}U, initial fissile loadings of 2200 and 2920 kg will be required for the process-heat- and power-production reactors, respectively. The initial breeding ratios are 1.18 and 1.19, respectively. As ^{233}U and plutonium breed in, these breeding ratios will rise and rapidly approach the equilibrium values.

5. CORE AND BLANKET FUEL PERFORMANCE UNDER IRRADIATION

The reference reactor designs utilize a thorium-based thorium-uranium-plutonium ternary alloy in the core and depleted uranium in the blankets. The performance of these materials in the core depends on temperatures and burnups. The bases for the anticipated performance of these materials are discussed in the following sections.

5.1 Core Fuel

5.1.1 Selection of Thorium-Based Alloy

The superior irradiation stability of thorium metal is widely recognized;[1-5] however, its poorer neutronic characteristics in comparison with ^{238}U have discouraged its consideration as a carrier for fast breeder reactor fuel. With an unclad fuel element, however, the relatively poor performance of thorium as a fertile material is mitigated by the higher volume fraction of fertile and fissile material. In addition thorium cores can be designed for desirable sodium void coefficients while still retaining desirable breeding characteristics.

The irradiation stability of thorium relative to uranium is a direct consequence of the following comparative properties:

1. Thorium has an isotropic crystal structure (FCC), and thus the prime cause for the poor irradiation stability of uranium metal is absent. (Thermal cycling of highly anisotropic alpha-uranium is believed to be an important contributing factor to breakaway swelling.)

2. Thorium undergoes no phase transitions from room temperature to 1275°C, whereas several phase transitions, beginning at 660°C, occur in uranium.

3. Thorium has a high melting point, 1750°C for the pure metal, and hence retains a substantial fraction of its room-temperature strength at moderate irradiation temperatures (e.g., 650°C for the present case).

In addition to irradiation stability, an important factor favoring thorium alloy fuels is their high thermal conductivity. At the maximum fuel design temperatures (i.e., 650°C for the thorium-based fuel and 350°C for the uranium-based fuel) and compositions it is estimated that thorium-

based fuels are approximately 80% more conductive than uranium-based fuels.*

5.1.2 Irradiation Characteristics of Thorium-Uranium Binary Alloys

Since uranium is only slightly soluble in thorium (1 wt % at 600°C), moderate additions of uranium to thorium would be expected to yield dispersion alloys with properties and characteristics similar to those of pure thorium. To test this, a number of irradiation experiments on thorium-uranium alloys have been run, with the most comprehensive being those of Kittel and his associates,[3] who covered the following ranges of conditions: temperatures up to 1000°C, burnups to 10 at. %, uranium concentrations from 0 to 31 wt %.

Figures 5.1 and 5.2, taken from Ref. 3, show photos of various irradiated specimens with compositions in the range 10 to 25 wt % uranium. Attention is called to the condition of the bottom-right specimen in Fig. 5.1, which was irradiated at 640°C to 4.5-at. % burnup, and to the top-right specimen in Fig. 5.2, which was irradiated at 650°C to 4.7-at. % burnup. Both these specimens were tested at approximately the selected maximum design conditions and seem to have survived well. The bottom photos in Fig. 5.2 illustrate failed specimens. As explained below the cause of failure seems to have been excessive uranium alloy concentration and not excessive temperature or burnup. In particular the bottom-right specimen exposure exceeded selected maximum design specifications in temperature level, burnup, and alloy concentration, but there was a comparatively mild mode of failure compared with that expected from alpha-uranium. The volume growth rates per unit burnup for these warped specimens are sufficiently low to be completely accounted for by fission-product buildin. Hence, although these specimens warped, they retained their physical integrity.

---

*Estimate based on Argonne National Laboratory data for U–10% Pu–10% Fs alloy and Atomics International data on Th–10% U alloy. It is assumed that the recycle plutonium present in the thorium fuel to the extent of 6.5 wt % resides primarily in the uranium phase and hence does not greatly alter the observed thermal conductivity.

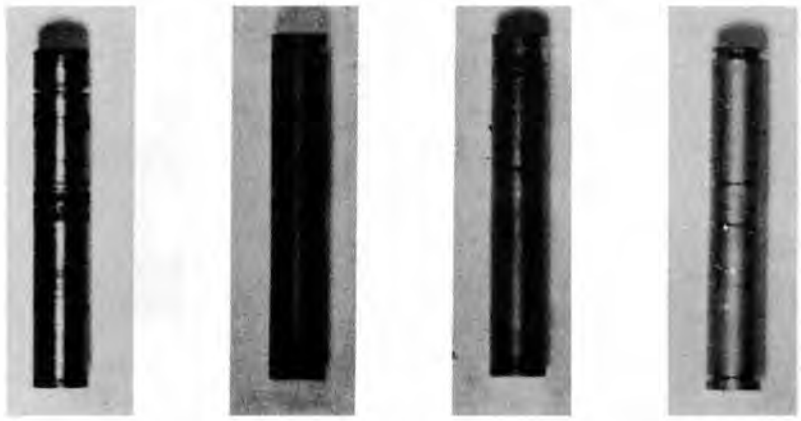

Specimen No.	ANL-42-8-1	ANL-42-2-1	ANL-42-3-1	ANL-42-5-1
Burnup, a/o	0.90	2.2	2.9	4.0
Max Irradiation Temp, °C	290	680	380	560
$\frac{\% \Delta \text{Vol}}{\text{a/o Burnup}}$	1.4	4.3	1.9	2.0

Postirradiation Condition of Typical Cast Thorium-10 w/o Uranium Alloy Specimens. Magnification 2X.

Specimen No.	CP-11-2	ANL-42-4-2	ANL-42-3-2	ANL-42-5-2
Burnup, a/o	0.47	1.4	3.3	4.5
Max Irradiation Temp, °C	665	410	450	640
$\frac{\% \Delta \text{Vol}}{\text{a/o Burnup}}$	3.9	2.2	1.8	2.5

Postirradiation Condition of Typical Cast Thorium-15 w/o Uranium Alloy Specimens. Magnification 2X.

Fig. 5.1. Postirradiation Conditions of Typical Cast Thorium-Uranium Alloy Specimens. (From Ref. 3)

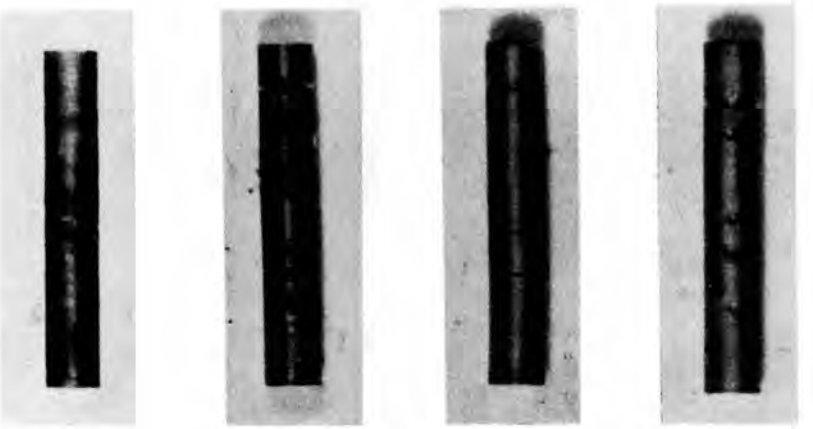

Specimen No.	CP-11-5	ANL-42-4-3	ANL-42-3-3	ANL-42-5-3
Burnup, a/o	0.46	1.5	3.5	4.7
Max Irradiation Temp, °C	540	420	460	650
% Δ Vol / a/o Burnup	4.0	1.7	2.2	2.9

Postirradiation Condition of Typical Cast Thorium-20 w/o Uranium Alloy Specimens. Magnification 2X.

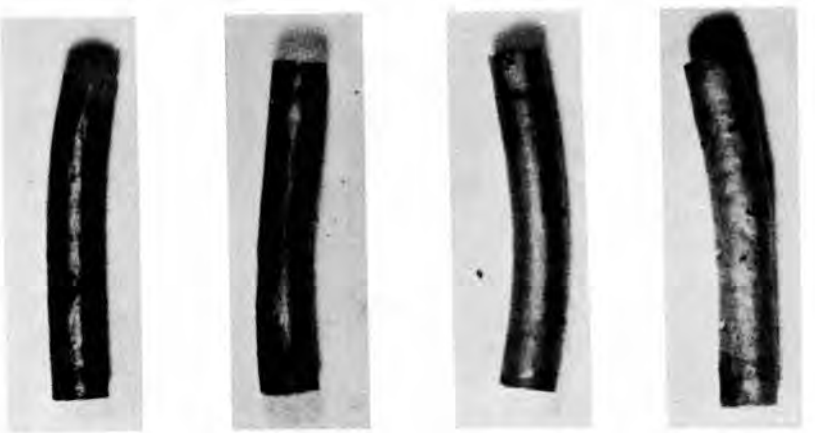

Specimen No.	ANL-42-8-4	ANL-42-4-4	ANL-42-7-4	ANL-42-1-4
Burnup, a/o	0.85	2.0	3.4	4.7
Max Irradiation Temp, °C	260	450	450	670
% Δ Vol / a/o Burnup	2.2	1.2	2.8	3.9

Postirradiation Condition of Typical Cast Thorium-25 w/o Uranium Alloy Specimens. Magnification 2X.

Fig. 5.2. Postirradiation Conditions of Typical Cast Thorium-Uranium Alloy Specimens. (From Ref. 3)

The following conclusions may be drawn from the Argonne National Laboratory experiments:

1. Thorium-uranium alloys did not exhibit "breakaway swelling" even under the most severe test conditions (1000°C, 10-at. % burnup, 31 wt % U). These high-temperature, high-burnup specimens were severely distorted, but their volume increase was a moderate 8.4% per at. % burnup. Even under these extreme conditions, physical integrity was maintained. In contrast, typical growth rates for metallic uranium undergoing irradiation failure may reach 150 vol % per at. % burnup. Such growth is indicative of void formation and disintegration of the fuel.

2. The addition of uranium did not alter the radiation stability of the alloy for concentrations up to 20 wt % uranium. Specimens with higher uranium contents showed a tendency for surface roughening and warping.

3. Metallographic examination showed the tendency for the uranium phase to collect around the thorium grain boundaries during irradiation. Since the cohesiveness of the alloy depends primarily on intergranular forces, extensive accumulation of uranium around the thorium grains would have a deleterious effect. This is the apparent cause for the relatively poorer performance of the alloys containing more than 20 wt % uranium.

4. The rate of volume increase on irradiation was 1.5 vol % per at. % burnup at temperatures below 450°C, and it rose to 2.5 vol % per at. % burnup at 650°C. At 800°C, the rate was 8 vol % per at. % burnup.

On the basis of these reported growth rates, a maximum irradiation temperature of 650°C was selected for the presented design. With the assumption that 10 vol % growth in the fuel can be accommodated by suitable fuel element assembly design, the maximum allowable burnup at 650°C maximum fuel temperature is 4 at. %.

5.1.3 The Thorium-Uranium-Plutonium Ternary System

The comparatively low melting point of plutonium, 640°C versus 1750 and 1132°C, respectively, for thorium and uranium, is a potential source of difficulty in the use of this ternary system as a core fuel. In general, compositions conducive to the formation of plutonium-rich phases would be unacceptable, since such phases would be expected to have melting points near the melting point of pure plutonium. Kelman and his

associates[6] have characterized the thorium-uranium-plutonium ternary system as essentially a combination of a high-melting thorium-rich solid solution in equilibrium with lower melting phases of predominantly uranium and plutonium alloys. The thorium-plutonium binary alloy is therefore rejected as an attractive core fuel, since low melting plutonium-rich phases may form as ^{233}U is bred in.* Kelman states that for plutonium concentrations of about 10 wt %, useful ternary alloys must contain from 10 to 20 wt % uranium in order to avoid plutonium-rich phases in the alloy. For lower plutonium concentrations, proportionately less uranium is required in the ternary alloy. The solidus and liquidus temperatures are given as 975 and 1525°C, respectively, for the 80-10-10 wt % composition and 940 and 1470°C for the 70-20-10 wt % alloy.

There have been irradiation tests performed on the ternary alloy at Argonne National Laboratory; however, postirradiation examination procedures have not yet begun. The specimens were clad, but axial growth was monitored radiographically. Very preliminary indications are that the Th–10% U–10% Pu and Th–20% U–10% Pu compositions irradiated at approximately 650°C grew at a rate of 8 to 10 vol % per unit burnup (at. %), which is three to four times the growth rate of the binary alloy under irradiation.[8] However, both compositions tested contained plutonium in excess of requirements for the reference design, while the Th–10% U–10% Pu alloy had, in addition, excessive uranium. The irradiation stability of the ternary composition should improve at lower dilutions of the thorium phase.

5.2 Blanket Fuel

Of the various types of uranium-alloy fuels that have been developed, the most appropriate seems to be the so-called "low-alloy" variety being investigated by the UKAEA at Harwell,[9] the Savannah River Laboratory,[10]

---

*The blanket rejection of the thorium-plutonium binary as a potential fuel material is perhaps too strong an opinion. It appears to be usable at temperatures up to 450°C with up to 10 wt % plutonium.[7] However, in view of the sparse data available for this alloy (only three irradiation results), the generalization of Kelman and his associates[6] still seems appropriate.

and the Pacific Northwest Laboratory of Battelle Memorial Institute.[11] These fuels contain less than 0.2 wt % alloy constituents and hence have excellent neutronic properties. The most extensively tested composition, the British "adjusted uranium," has withstood irradiation conditions almost identical to the requirements for the blanket material of the reference concept; namely, maximum temperature of approximately 600°C, burnup requirement of 0.2 to 0.35 at. %, no cladding constraint, sodium environment, fission rates up to 80 w/g.

Some of the irradiation test results for British adjusted uranium are presented in Fig. 5.3, which is reproduced from Ref. 9. Note that at the burnups needed for the present blanket fuel, volume increases are below 10% (the selected maximum allowable value) for all irradiation

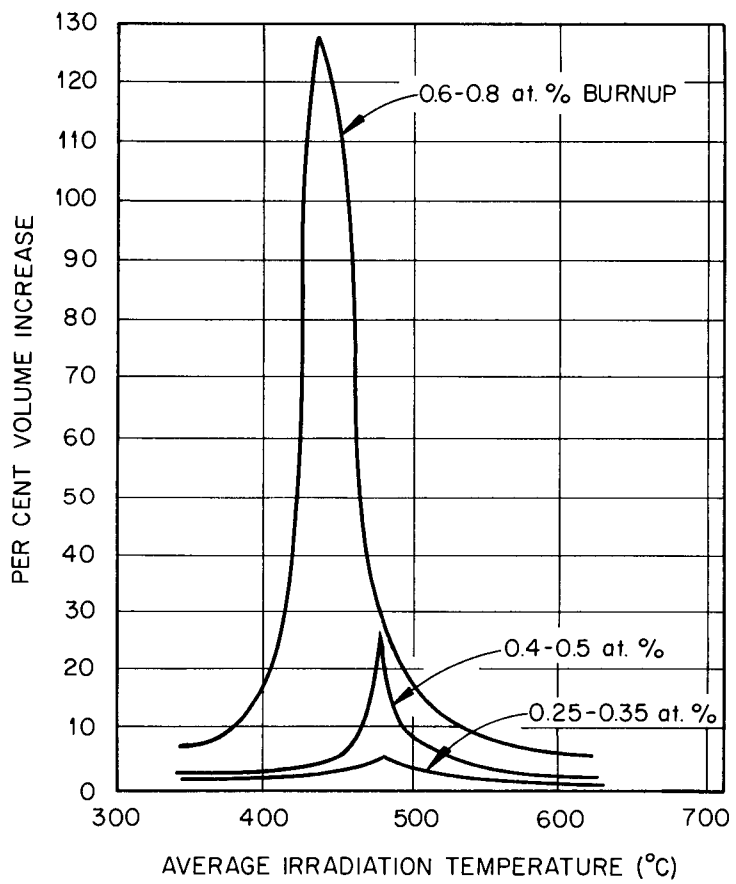

Fig. 5.3. Effect of Irradiation Temperature on Volume Increase of Adjusted Uranium Irradiated at Fission Rates from 15 to 80 w/g. (From Ref. 9)

temperatures. The power densities tested in the reported experiments covered the expected range that the blanket fuel will experience in the present design, the average value being 19 w/g in the axial blanket of the process-heat-production reactor, with power peaking increasing this to 78 w/g adjacent to the core. Barnes[9] reports that at 80 w/g, surface wrinkling is likely to occur, but no further information is given on the burnup levels that produce the wrinkling or how serious it is.

The irradiation test conditions differ, however, from the expected blanket environment in several respects. First, the fission power source was ^{235}U, whereas it would be in-bred ^{239}Pu and ^{238}U fissions in the blanket; second, the test sodium was stagnant and the oxygen level in the sodium was unspecified; and third, the flux was thermal.

Irradiation experiments at the Pacific Northwest Laboratory cover a wide range of fuel compositions in the "low-alloy" category, and in general, their results seem to corroborate those obtained at Harwell. However, the PNL low-burnup irradiation tests in the range from 0.2 to 0.35 at. % were incomplete at latest reporting.[11] Hence, the proven adjusted-uranium composition is the present choice, although alternatives are expected to be available soon. It is noted that a requirement for a lower burnup in the blanket imposes only a slight economic penalty, since the associated higher reprocessing costs are largely compensated by more rapid recovery and sale of bred plutonium.

5.3 Summary of Fuel Compositions and Design Conditions

The selected fuel compositions and design conditions are listed below:

1. for core

Nominal composition*	Th–15 wt % U–7 wt % Pu
Maximum temperature	650°C
Maximum burnup	4 at. %
Maximum expansion	10 vol %

*It is now recognized that 22 wt % (U + Pu) may be somewhat excessive from the point of view of fuel warpage under irradiation (see Sect. 5.1.2); however, some of the uranium, which is approximately 40% ^{238}U, could be removed with minor economic penalty while still retaining sufficient uranium for the required dilution of the plutonium phase.

2. for blanket

Composition (adjusted uranium)	400 to 1200 ppm Al, 600 ppm C, 300 ppm Fe, bal. U
Maximum temperature	600°C
Maximum burnup	0.3 at. %
Maximum expansion	10 vol %

References

1. G. G. Bentle, Study of the Thorium-Uranium Alloy System, Proceedings of the Second United Nations International Conference on the Peaceful Uses of Atomic Energy, Geneva, 1958, Vol. 6, pp. 156–161, United Nations, New York, 1959.

2. B. R. Hayward and G. G. Bentle, Effect of Burnup on Metallic Fuel Operating at Elevated Temperatures, ibid., Vol. 5, pp. 537–542.

3. J. H. Kittel et al., Effects of Irradiation on Thorium and Thorium-Uranium Alloys, USAEC Report ANL-5674, Argonne National Laboratory, 1963.

4. G. A. Last, Metallic Fuels, p. 9.1 in Quart. Progr. Rept. Jan., Feb., Mar. 1967, Reactor Fuels and Materials Development Programs, USAEC Report BNWL-435, Pacific Northwest Laboratory, 1967.

5. M. Bloomfield, Thorium, A Bibliography, USAEC Report NAA-SR-Memo-6180, Atomics International, 1961.

6. L. R. Kelman et al., Status of Metallic Plutonium Power-Breeder Fuels, Chapt. 22, pp. 458–484 in Plutonium 1965, Proceedings of the Third International Conference on Plutonium, London, 1965, Chapman and Hall, London, 1967.

7. J. A. Horak et al., The Effects of Irradiation on Some Binary Alloys of Th-Pu and Zr-Pu, USAEC Report ANL-6428, Argonne National Laboratory, 1962.

8. N. Beck, Argonne National Laboratory, personal communication to R. P. Wichner, Oak Ridge National Laboratory, Mar. 18, 1958.

9. R. S. Barnes et al., The Irradiation Behaviour of Uranium and Uranium Alloy Fuels, Proceedings of the Third United Nations International Conference on the Peaceful Uses of Atomic Energy, Geneva, 1964, Vol. 11, pp. 218–226, United Nations, New York, 1965.

10. W. R. McDonnel and C. L. Angerman, Effect of Microstructure on the Cavitational Swelling of Dilute Uranium Alloys, in Symposium on

Radiation Effects, Asheville, North Carolina, USAEC Report CONF-650904-4, 1965.

11. R. D. Leggett and B. Mastel, Postirradiation Examination of Uranium and Uranium Alloys, pp. 6.3–6.5 in Quart. Progr. Rept. Jan., Feb., Mar. 1967, Reactor Fuels and Materials Development Programs, USAEC Report BNWL-435, Pacific Northwest Laboratory, 1967.

6. THERMAL AND HYDRAULIC ANALYSES

The objective of the steady-state thermal and hydraulic analyses was the selection of a core configuration for a given set of volume fractions in which maximum temperatures would not exceed the specified metallurgical limit and the coolant pressure drop would be acceptably low. In addition, a maximum coolant velocity of 32 fps was imposed below which problems of local cavitation and effects of excessive local hydrodynamic forces should be minimized.

Two versions of the same basic plan were studied. In the process-heat-production concept, in comparison with the power-production concept, lower coolant temperatures create higher temperature driving forces for heat removal with given identical maximum allowable fuel temperatures, and thus higher specific powers are obtainable. A radially flat coolant distribution was selected to minimize the pressure drop in the process-heat-production reactor, but for the power-production reactor, high thermal efficiency was a primary goal, and to achieve this a radially distributed mode of core cooling was selected that allowed the exit coolant temperature to approach more closely the maximum fuel temperature. The penalty for this is an increased pressure drop approximately equal to the square of the radial power peaking factor.

The thermal and hydraulic characteristics of the two concepts are summarized in Table 6.1.

6.1 Assumptions and Method of Calculating Temperature Distributions

The axial power distribution is assumed to be a chopped cosine. Physics calculations give the extrapolation length as 21 cm and the product of the age and radial power peaking factors as 1.24 for the two-zone core.

A heat balance yields the axial coolant temperature distribution directly. For the power-production concept, the axial coolant temperature distribution is independent of radial location because the radial flow distribution compensates for the radial power variation. Thus the

Table 6.1. Thermal and Hydraulic Characteristics

	Process-Heat-Production Reactor	Power-Production Reactor
Reactor thermal power, Mw	3500	3500
Coolant temperatures, °C		
Inlet	170	345
Exit	350	525
Core characteristics		
Thermal power, Mw	2772	2880
Geometry	Cylinder	Cylinder
Volume, ft^3	57.9	79.1
Length, ft	1.5	1.5
Diameter, ft	7.0	8.2
Specific power, w/g	290	220
Coolant hole distance across flats, cm	0.75	0.62
Coolant hole web thickness, cm	0.33	0.275
Maximum fuel temperature, °C	650	650
Location of maximum fuel temperature, in. from inlet	13.8	15.7
Average power density, w/cm^3	1690	1284
Average power density in fuel, w/cm^3	3400	2570
Power peaking factor		
Axial	1.12	1.12
Radial	1.23	1.22
Peak power density, w/cm^3	2300	1740
Peak power density in fuel, w/cm^3	4981	3731
Heat flux, w/cm^2		
Average	751	472
Peak	1037	642
Volume fractions		
Fuel	0.47	0.47
Sodium (total)	0.50	0.50
Sodium in coolant holes	0.423	0.423
Sodium in can for transverse growth	0.067	0.067
Sodium between cans	0.01	0.01
Steel	0.03	0.03
Ratio maximum thermal stress at midplane to tensile strength of fuel	0.61	0.31
Axial blanket characteristics		
Thermal power, Mw	546	465
Volume, ft^3	115.8	158.2
Length, ft	1.5	1.5
Power peaking factor		
Axial	3.19	3.45
Radial	1.30	1.30
Average power density, w/cm^3	166	104
Power density in fuel, w/cm^3		
Average	332	208
Peak	1377	933
Maximum fuel temperature, °C	600	600
Primary coolant loop		
Power distribution	Flat	Radial
Mass flow, core and axial blankets, kg/sec	14,021	14,635
Maximum velocity, m/sec	10.4	10.1
Reactor pressure drop, atm	3.90	4.13
Reactor pumping power, Mw(e)	9.33	10.8
Coolant Reynolds number	185,000	202,000
Coolant Peclet number	1243	1027
Coolant Nusselt number	12.5	11.5

exit coolant temperature is also constant. Conversely, the process-heat-production concept, with its flat flow distribution, yields radially dependent axial temperature profiles and exit coolant temperatures. For this case, attention is focused on the hottest channel.

The fuel surface temperature at each point was calculated from the known local power density, the assumed fuel configuration dimensions, and the heat transfer coefficient estimated from the equation[1]

$$Nu = 5 + 0.025\ Pe^{0.8}\ ,$$

where Nu and Pe are the Nusselt and Peclet numbers.

The temperature rise in the fuel from the channel surface to the central hot spot was calculated at each axial elevation from a two-dimensional approximation; axial heat conduction was neglected. The hexagonal symmetry pattern was approximated by circular arcs, as indicated in Fig. 6.1. Heat was assumed to flow radially inward from the arc through the hot spot, m, to a concentric arc passing through the surface point, b. The linear increase of thermal conductivity with temperature was taken into account.

ORNL-DWG 67-10747

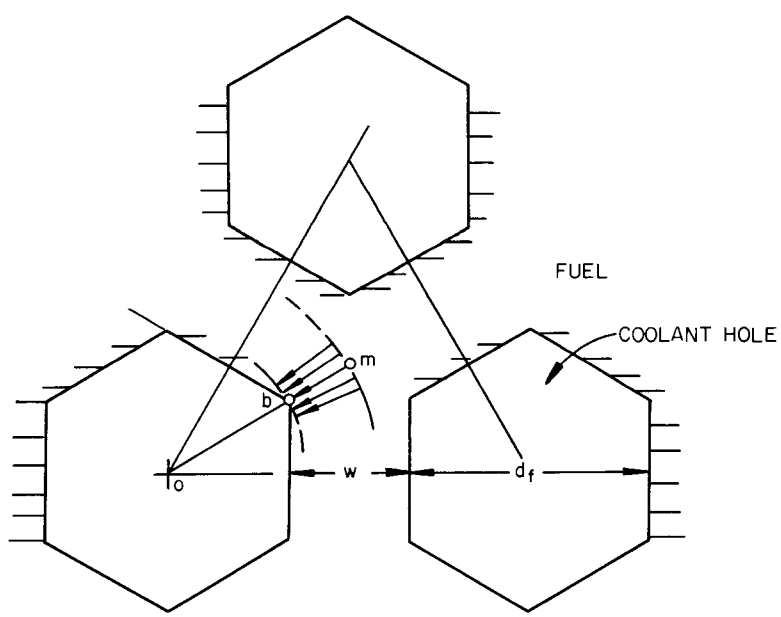

Fig. 6.1. Fuel-Coolant Heat-Conduction Model.

6.2 Pressure Drop Estimates

The reactor pressure drop was calculated by summing the irreversible flow losses through the core. Recoverable gravity effects were ignored, and thus the values given in Table 6.1 represent friction losses only. The standard smooth-tube friction factor was used to obtain the viscous losses in the coolant holes, and the hydrualic-mean diameter was used to calculate the Reynolds number.

In order to minimize variations with time in the core coolant flow caused by changes in the surface roughness of the fuel, flow constrictors are provided at the entrance of each fuel assembly. These are sized so that approximately 75% of the total core pressure drop occurs at the inlet orifices. Thus the velocity of the coolant in the core is made insensitive to variations of the viscous losses within the core. The inlet orifice pressure drop turns out to be a factor of 4 or 5 times greater than would be expected for inlet and outlet losses with no flow constrictor.

For the power-production case, the pressure drop was calculated only for the central channel, which has the highest flow rate. At the other radial locations, flow orifices were sized to yield equal pressure drop for the appropriate flow rate.

6.3 Engineering Peaking Factors

The fuel element design specifies a stagnant sodium-filled volume within the container to accommodate the expected 10% volume expansion of the fuel. In addition, 1 vol % of the core was assumed to be composed of sodium-filled dead-spots between containers formed by the container bearing surfaces. These, plus the 3 vol % metal for the fuel element containers, were taken into account by appropriate factors applied to the temperature distribution and flow equations.

Other engineering factors involving primarily variations in fuel composition, fuel thermal conductivity variation with irradiation, and fuel element dimensional tolerances are not known. Their eventual inclusion will have the effect of diminishing the required coolant hole size.

6.4 Computation of Coolant Hole Size

A compution routine called MXTEMP was encoded for trial and error selection of the proper coolant hole size. A series of distances across flats was assumed, and the axial variation of the maximum fuel temperature was calculated for each. The highest maximum fuel temperature was determined in each case, and the coolant hole size was selected that yielded the value closest to the given metallurgical limit.

6.5 Results of the Thermal and Hydraulic Calculations

Results of the thermal and hydraulic calculations are presented in Table 6.1, and the axial temperature distributions along the central channels are given in Figs. 6.2 and 6.3. The reported values of the maximum

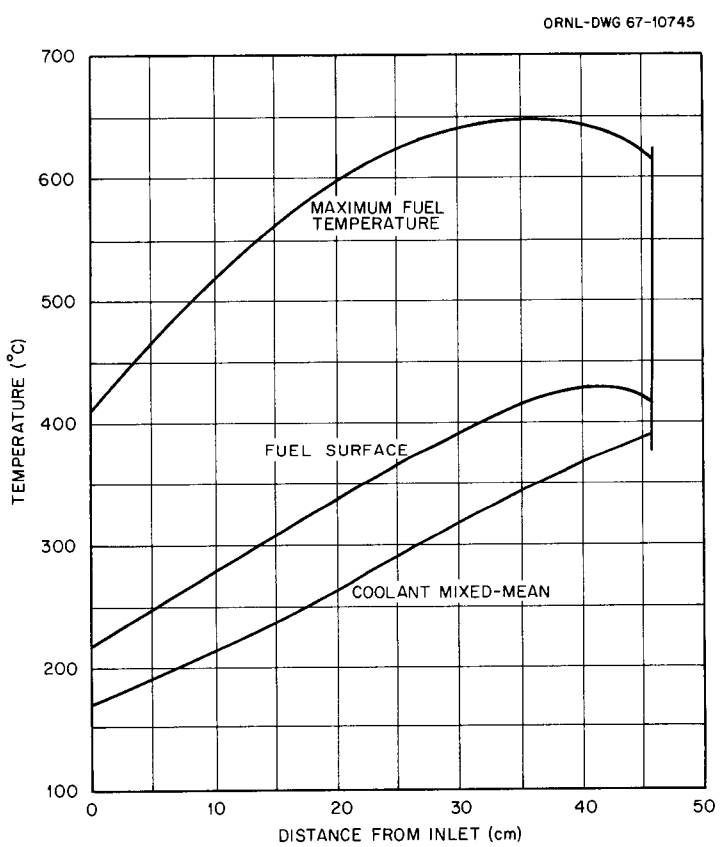

Fig. 6.2. Axial Temperature Distributions in Central Channel of Process-Heat-Production Reactor.

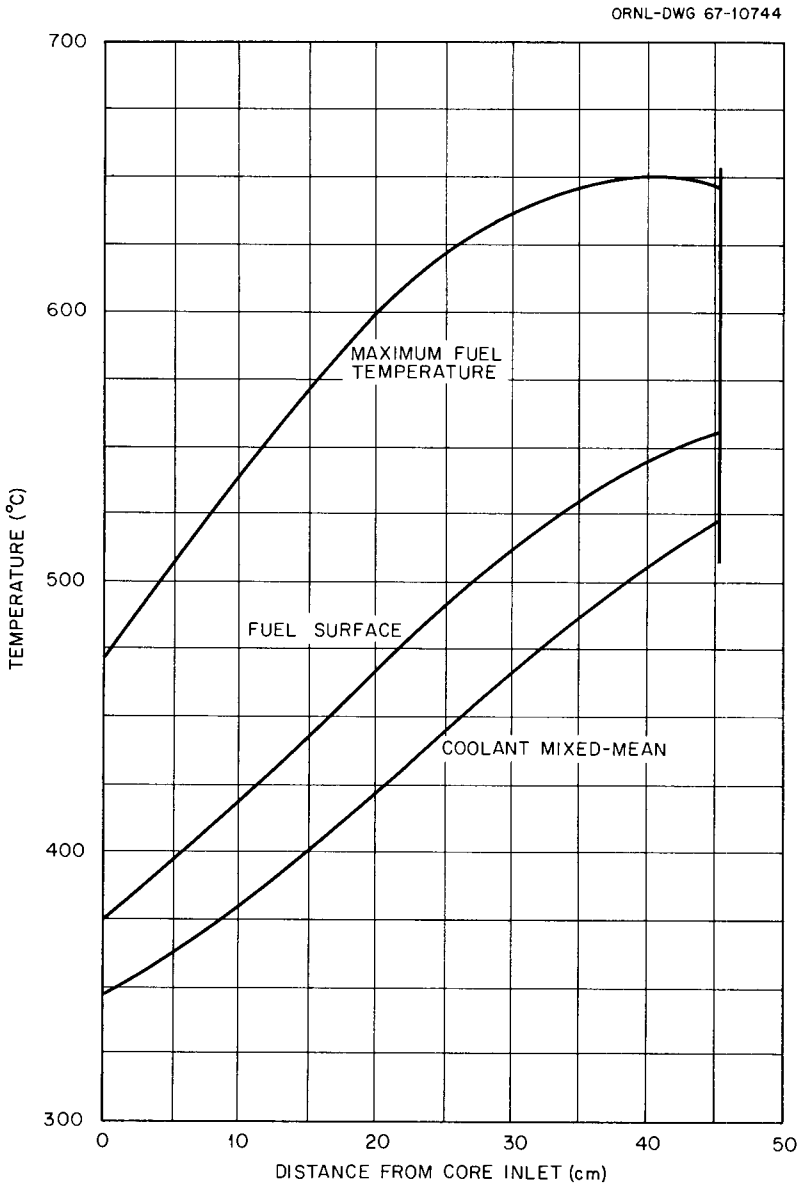

Fig. 6.3. Axial Temperature Distribution in Central Channel of Power-Production Reactor.

thermal stress were estimated by assuming a cylindrical geometry for the hexagonal unit cell in the fuel. Of primary concern is the maximum tensile stress that will be generated at the surface of the coolant hole. Values are reported in the table relative to the estimated tensile strength of the fuel. The thermal stresses are 61 and 31% of the tensile strength for the process-heat- and power-production reactors, respectively, as

evaluated from the long circular cylinder equation and physical property values[2,3] typical for commercially pure thorium at room temperature, as given in Table 6.2. Physical properties for type 304 stainless steel and uranium are also given in Table 6.2 for comparison. A more thorough analysis would investigate the stress conditions at the corners of the hexagonal coolant hole where the thermal stresses will be appreciably higher than for the assumed circular hole. If such stresses prove to be excessive, alternate fuel element geometries will be considered. Based on this geometric approximation and the uncertain physical property values for the fuel at the specified temperatures, the thermal stresses seem reasonable.

Some comment is in order on the reported high heat fluxes in the core. These values, which range from 1.5×10^6 Btu/hr·ft^2 (470 w/cm^2) to 3.3×10^6 Btu/hr·ft^2 (1040 w/cm^2), are higher than usually designed for and exceed values often thought of as "burnout limits." While these high heat fluxes render the system sensitive to heat transfer surface fouling, there is no question of boiling burnout, since surface temperatures must exceed liquid saturation temperatures before boiling burnout

Table 6.2. Room-Temperature Properties of Thorium, Uranium, and Type 304 Stainless Steel

	Thorium	Uranium	Type 304 Stainless Steel
Melting point, °C	1749	1132	1427
Density, g/cm^3	11.6	19.0	7.9
Thermal conductivity, Btu/hr·ft·°F	21.8	17.2	9.4
Linear thermal expansion coefficient, μin./in.·°C	12	13–15[a]	10
Modulus of elasticity, psi	7×10^6–10^7	24×10^6	28×10^6
Poisson's ratio	0.26	0.21	0.28
Tensile strength, psi	32,000	56,000[a]	85,000
Yield strength, psi	21,000	28,000[a]	30,000

[a]Average values for cast metal.

can occur. In the present design, the static pressure at the core exit is estimated to be 1.6 atm, which corresponds to a saturation temperature of 940°C for the sodium coolant. Anticipated fuel surface temperatures, as may be seen from Figs. 6.2 and 6.3, are 446 and 556°C for the process-heat- and power-production reactors, respectively, and thus are substantially below the saturation value. In fact, even the maximum internal fuel temperature of 650°C is well below the minimum saturation temperature of the coolant in the core. The high heat fluxes result from the assumed heat-flow model, the temperature driving forces, the coolant velocity and physical properties, the channel and fuel-web dimensions, and the thermal conductance of the fuel. Most important are the latter two — thin fuel web and high thermal conductivity. (The value of thermal conductivity given for the fuel alloy is twice that of uranium carbide and 13 times that of uranium oxide.)

6.6 Effect of Fuel Growth on Maximum Fuel Temperature

If it is assumed that the fuel grows to its maximum design value of 10 vol % in an isotropic fashion, that is, each linear dimension increases by 3.33%, it can be shown that the ratio of the temperature rise in the fuel after expansion to that before expansion is given by

$$\frac{\Delta t_{f2}}{\Delta t_{f1}} = \frac{(PD)_2}{(PD)_1} \frac{b_2^2}{b_1^2} ,$$

where the sub 2 refers to the condition after the expansion, PD is the power density in the fuel, and b is the distance from the coolant hole surface to the fuel hot spot. With the assumption that the specific power (w/g) remains constant* upon expansion, the power density decreases. Hence,

$$\frac{\Delta t_{f2}}{\Delta t_{f1}} = 0.9(1.033)^2 = 0.96 ;$$

*The specific power will actually decrease 5 to 10% as the core fuel expands because of a decrease in fissile atom density.

that is, a 10-vol % fuel expansion will diminish the temperature rise in the fuel by 4%.

If it is assumed that the volumetric flow rate in the coolant channel remains constant upon fuel expansion, the velocity will drop because the flow channel diameter will be 3.33% larger (neglecting the slight thickening of the fuel web). This will diminish the heat transfer coefficient and tend to elevate the fuel-to-coolant temperature difference, Δt_{fc}. However, the effect is negligible for a 10-vol % expansion, as shown below.

The ratio $\Delta t_{fc2}/\Delta t_{fc1}$ (the temperature rises after and before fuel expansion, respectively) may be evaluated from

$$\frac{q_{s2}}{q_{s1}} = \frac{h_2}{h_1} \frac{A_{s2}}{A_{s1}} \frac{\Delta t_{fc2}}{\Delta t_{fc1}} ,$$

where q_s is the convective rate, A_s the heat transfer area, and h the heat transfer coefficient. The left-hand side is unity, since the power level remains constant, and the area ratio is $(1.033)^2$. To evaluate the drop in the heat transfer coefficient the coolant Nusselt number is assumed to be proportional to the Reynolds number to the 0.8 power, from which it can be shown that h_2/h_1 has a value of $1/(1.033 \times 1.033^{0.8})$. Thus the effect of increased heat transfer area slightly exceeds the effect of the lower coefficient, and

$$\frac{\Delta t_{fc2}}{\Delta t_{fc1}} = \frac{1.033^{0.8}}{1.033} = 0.99 .$$

Hence, the maximum fuel temperature will diminish approximately 3% on a 10-vol % isotropic fuel expansion.

6.7 Effect of a Plugged Coolant Hole

To obtain an indication of the consequences of a coolant hole becoming completely plugged while the reactor is operating at full power, an infinite slab geometry was assumed for the web. If the variation of fuel thermal conductivity with temperature is neglected, the profile in

the web initially has the parabolic shape shown in Fig. 6.4, with a maximum in the center, t_{fm}. Upon sudden insulation of the right face, the profile quickly takes the shape designated by curve-II with the maximum at the right face, t_{f2}. The surface temperature at the left face rises from t_{s1} to t_{s2} to accommodate the double heat load. If it is further assumed that the mixed-mean coolant temperature and heat transfer coefficient remain constant at the left face, it can be shown that the maximum fuel temperature rise, $t_{f2} - t_{fm}$, is given by

$$t_{f2} - t_{fm} = q_f \frac{l}{2} \left(\frac{1}{h} + \frac{3l}{4k}\right) ,$$

and Δt, the time in seconds required to reach the new steady-state profile, is

$$\Delta t = \frac{\rho c_p l}{2} \left(\frac{1}{h} + \frac{l}{2k}\right) .$$

ORNL-DWG 67-10748

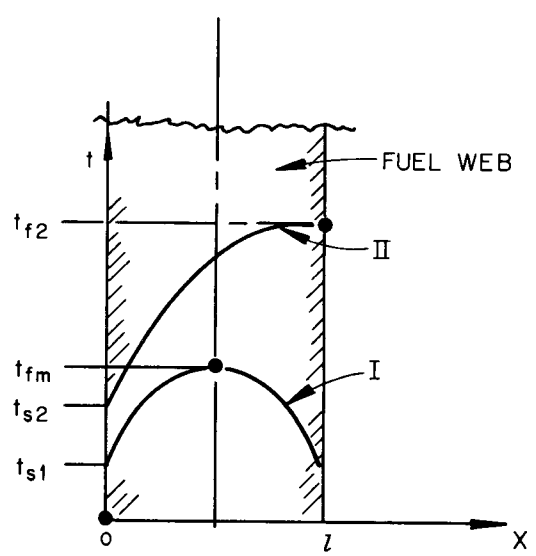

Fig. 6.4. Temperature Rise Upon Insulation of One Face of a Fuel Element. Curve I — before plug forms. Curve II — after plug forms and insulates surface at right.

Table 6.3 gives the results of the calculations for the two designs. The expected fuel temperature rise is 582°C for the process-heat-production reactor, which yields a new maximum temperature of 1232°C that is above the solidus temperature of 960°C. Hence some melting may be expected. In the power-production reactor, the lower power density and thinner web relieve the situation somewhat, and the new maximum temperature does not quite reach the solidus temperature.

Table 6.3. Results of Analysis of Effect of Plugged Coolant Hole[a]

	Process-Heat-Production Reactor	Power-Production Reactor
Web thickness, cm	0.333	0.275
Fuel power density, w/cm^3 (max)	4680	3510
Initial maximum fuel temperature, °C	650	650
Solidus temperature, °C	960	960
Liquidus temperature, °C	1500	1500
Estimated rise in maximum fuel temperature due to plugging, °C	582	304
Time required to reach new maximum, sec	0.13	0.09
New maximum temperature, °C	1232	954

[a]Assumptions: $h = 2.9\ cal/cm^2 \cdot sec \cdot °C$, corresponding to $Nu = 11.4$; for the fuel, $k = 0.09\ cal/cm \cdot sec \cdot °C$ and $\rho c_p = 0.35\ cal/cm^3 \cdot °C$.

It should be mentioned that cross-flow passages could be provided to interconnect the coolant channels and minimize the consequences of a plugged hole. However, they might complicate fuel fabrication and decrease the sodium volume fraction available for coolant passages. Cross-flow coolant passages were not included in the designs, but further study may indicate their desirability.

6.8. Effect of Loss of Coolant Pumping Power

In the event of failure of the coolant pumping power supply, calculations show that moderately sized flywheels on the pump shafts could serve to keep the primary coolant well mixed for appreciable times. Figure 6.5 shows the relative flow rates in the primary coolant loop during the coastdown period. Curve A represents the situation with no attached flywheel and with the motive force for flow being due solely to recovery of the rotational kinetic energy of the motor armatures. Curves B, C, and D show the calculated coastdown flows relative to the rated flow for cases with light, medium-weight, and heavy flywheels attached to the pump shafts. The dimensions and masses of these flywheels, given in Table 6.4, were selected for illustrative purposes; however, the 6-m diameter is well below the bursting diameter of approximately 10 m for a carbon-steel flywheel rotating at 450 rpm, and the heaviest flywheel may be

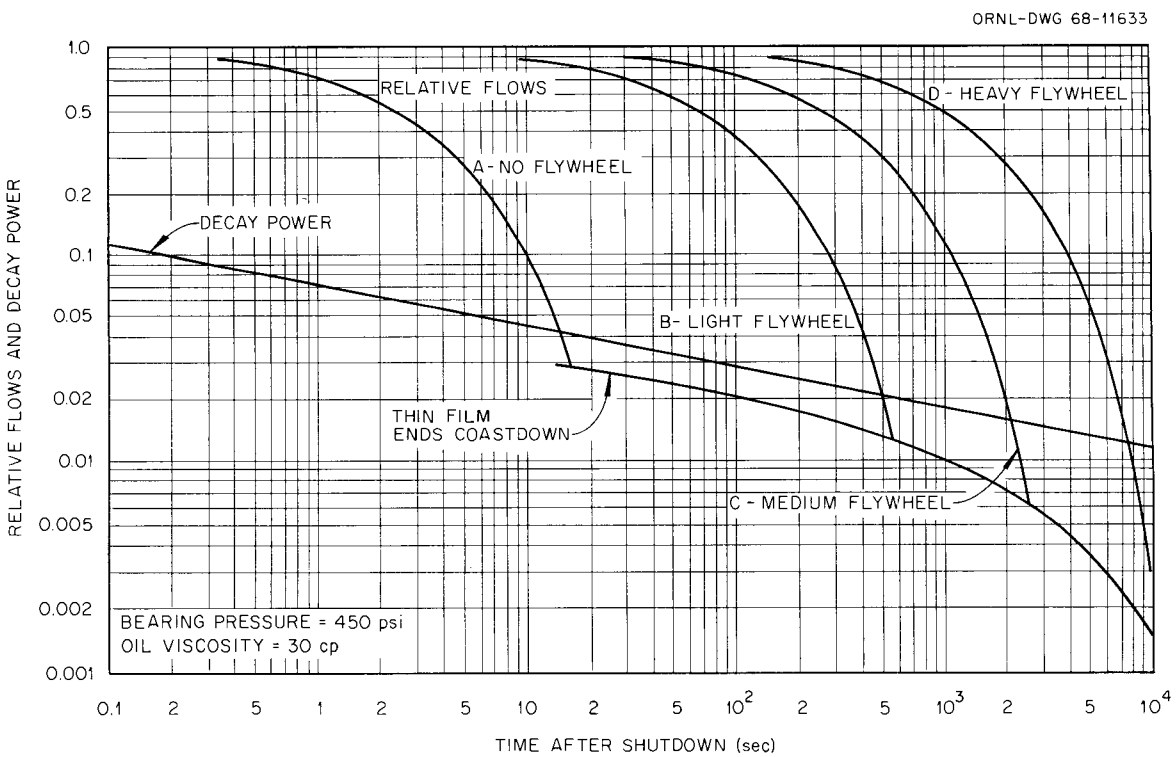

Fig. 6.5. Relative Coastdown Flow Versus Time After Shutdown for Various Flywheel Sizes.

Table 6.4. Flywheel Characteristics

	Armature[a]	Flywheels[b]		
		Light	Medium Weight	Heavy
Average diameter, m		6	6	6
Thickness, m		0.1	0.4	0.8
Height, m		1	1	2
Mass, kg	10,000	15,000	60,000	240,000
Polar moment, $kg \cdot m^2$	5,000	133,000	533,000	2,160,000

[a]Approximate value for a 5000-hp induction motor.

[b]The flywheels are assumed to be cylinders with thin annular cross sections. The mass and moment associated with the structural attachments to the shaft are assumed to be negligible.

supported by a Kingsberry bearing of size and load pressure well within the range listed in Ref. 4.

The ratio of decay power to rated thermal power, as given by the Way-Wigner equation, is superimposed on the flow coastdown curves in Fig. 6.5. For the time after shutdown in which the relative coastdown flow exceeds the relative decay power, it may be expected that sufficient coolant flow is available to preclude formation of localized hot spots in the core. In this interval of time, termed the "useful coastdown duration," the decay heat gradually elevates the temperature of all the materials comprising the primary coolant loop. If the temperature rose to no more than approximately 800°C, no serious damage to either fuel or structure would occur. From Fig. 6.5 it may be seen that the useful coastdown duration is 15 sec with no attached flywheel. This may be increased to 500 sec by attaching light flywheels to the primary pump motor shafts; to 2100 sec by using medium-weight flywheels; and to 7800 sec by using heavy flywheels. Both the loss of impeller efficiency with flow rate and the retarding effect of the thrust bearings on the rotation rate have been accounted for in the calculation.[5] The dashed line that terminates the coastdown flow curves in Fig. 6.5 represents the estimated point at which the thrust-bearing lubrication may be lost.

Table 6.5 lists the estimated heat absorption of the primary coolant loop from the operating temperature to 800°C for both the process-heat- and power-production reactors. For the process-heat-production case, 139.6 full-power seconds of heat is absorbed by the primary loop to elevate it to 800°C. It would take 2.9 hr for the decay heat to have a similar effect. Values for the power-production reactor are somewhat lower because the initial temperature is higher.

A natural-convective heat sink could be provided to prevent the temperatures from ultimately exceeding 800°C.

Table 6.5. Primary Loop Heat Capacity

	Process-Heat-Production Reactor	Power-Production Reactor
Mass of sodium in primary loop, kg		
Reactor vessel	200,000	
Loop piping	102,000	
Heat exchanger	162,000	
Total	464,000	
Mass of steel associated with primary loop, kg		
Reactor vessel and internals	250,000	
Loop piping	47,000	
Heat exchanger	440,000	
Total	737,000	
Mass of heavy metal in core and blanket, kg	88,000	108,000
Heat absorption to 800°C, Mwhr		
Sodium	87.3	59.0
Structure	50.9	34.4
Heavy metal	1.4	1.4
Total	139.6	94.8
Heat capacity, full-power seconds	143.6	97.5
Time required for decay heat to raise primary loop to 800°C, hr	2.9	1.8

6.9 Effect of Surface Film

The high heat fluxes present in the core render the system sensitive to surface fouling. Because of the great affinity of the thorium-based material for oxygen, there will probably be a film of ThO_2 covering the core fuel; however, out-of-pile tests indicate the film to be tenacious and impervious,[6] as expected from its Pilling and Bedworth ratio of 1.28.* Films of this type cannot grow very thick because they form an effective barrier to oxygen diffusion. Typically, the thickness may be of the order of 1 μ. At a heat flux of 1037 w/cm^2, with $k = 0.05$ w/cm·°C (the value for ThO_2 at 400°C), the film temperature drop would be 2°C.

Hence, while there is no direct evidence on the subject, oxide-film-induced temperature rises are not expected to be a serious problem for thorium-based fuels.

---

*See Table 7.2 and discussion in Chapter 7.

References

1. R. A. Seban and T. T. Shimizaki, Heat Transfer to a Fluid Flowing Turbulently in a Smooth Pipe with Wall at Constant Temperature, Paper 50-A-128 ASME Conf. (1950).

2. F. L. Cuthbert, Thorium Production Technology, p. 16, Addison-Wesley, New York, 1958.

3. Metals Handbook, 8th ed., American Society for Metals, 1961.

4. C. Carmichael (Ed.), Kent's Mechanical Engineer's Handbook, 12th ed., p. 436, Wiley, New York, 1966.

5. R. P. Wichner, Flywheel Augmented Flow Coastdown for the 3500 Mwt Unclad Metal-Fueled Reactor (UMBR), USAEC Report ORNL-TM-2132, Oak Ridge National Laboratory, 1968.

6. H. M. Finniston and J. P. Howe (Eds.), Metallurgy and Fuels, p. 233, McGraw-Hill, New York, 1956.

7. REACTOR CHEMISTRY

Basic questions related to the use of unclad metal fuel in a sodium-cooled reactor concern the amount of fuel material and fission products that become dispersed into the sodium coolant and the ultimate disposition of the material lost in the primary cooling system. The answers to these questions are given preliminary consideration in this chapter.

In summary, successful use of unclad nuclear fuel depends primarily on its compatibility with the coolant. Both thorium and uranium metal are reported to be compatible with pure liquid sodium, and in general, any corrosion of these metals by sodium is caused by and limited by the amount of the oxygen impurity present. It is anticipated that corrosion of the fuel can be controlled by limiting the access of oxygen to the system and, if necessary, removing or inactivating the oxygen by chemical means, such as by using hot traps or a soluble getter.

7.1 Corrosion

The chemical problems of the reactor system may be considered by referring to Table 7.1, which lists the free energies of reaction in kilogram calories per gram-atom of oxygen of several elements reacting with sodium oxide. Each element listed can reduce the oxides of those below it in the list. The oxides of those elements that have positive values for the free energy of the listed reactions would be reduced to the metallic state by sodium. Also listed in the table are some of the Pilling and Bedworth critical density ratios. This ratio is the molecular volume of the oxide divided by the volume of the equivalent amount of metal. Those metals that have a ratio approximately in the range 1.0 to 1.5 can have tenacious, impermeable oxide surfaces (for example, aluminum under ambient conditions rapidly becomes inert as it forms an oxide coat that has a Pilling and Bedworth critical density ratio of 1.29 to 1.45); those with ratios below 1 tend to have porous oxide surfaces; and those with ratios above about 1.5 tend to have oxide surfaces that spall because of mechanical deformation and thus expose fresh metal to oxidation.

Table 7.1. Free Energies of Reaction of Several Elements With Sodium Oxide and the Pilling and Bedworth Ratios

Reaction	Free Energy Change, $\Delta G_{800°K}$ (kcal/g-atom of oxygen)	Pilling and Bedworth Ratios
$Na_2O + Ca \rightarrow CaO + 2\ Na$	-58.5	0.648
$2/3\ Pr \rightarrow 1/3\ PrO_3$*	-57	1.106
$1/2\ Th \rightarrow 1/2\ ThO_2$	-56	1.28
$2/3\ Nd \rightarrow 1/3\ Nd_2O_3$*	-55	1.11
$2/3\ Sm \rightarrow 1/3\ Sm_2O_3$*	-54	1.81
$2/3\ Ce \rightarrow 1/3\ Ce_2O_3$*	-52	1.19
$2/3\ La \rightarrow 1/3\ La_2O_3$*	-52	1.11
$Be \rightarrow BeO$	-52	1.71
$Mg \rightarrow MgO$	-52	0.784
$Sr \rightarrow SrO$*	-50	0.65
$2/3\ Y \rightarrow 1/3\ Y_2O_3$*	-48	1.45
$2\ Li \rightarrow Li_2O$	-45	
$Ba \rightarrow BaO$*	-42.6	0.684
$U \rightarrow UO$		1.43
$1/2\ U \rightarrow 1/2\ UO_2$	-41	1.97
$1/2\ Zr \rightarrow 1/2\ ZrO_2$*	-41	1.54
$1/2\ Pu \rightarrow 1/2\ PuO_2$	-34.4	
$3/8\ U \rightarrow 1/8\ U_3O_8$	-18	2.67
$1/3\ U \rightarrow 1/3\ UO_3$	-9	2.74
$1/2\ Nb \rightarrow 1/2\ NbO_2$*	-5.6	
$2\ Rb \rightarrow Rb_2O$*	+20	
$1/2\ Mo \rightarrow 1/2\ MoO_2$*	+20	
$Fe \rightarrow FeO_2$	+21	
$3/4\ Fe \rightarrow 1/4\ Fe_3O_4$	+21	
$Sn \rightarrow SnO$*	+24	
$1/2\ C \rightarrow 1/2\ CO_2$	+24.5	
$2\ Cs \rightarrow Cs_2O$*	+27	
$1/3\ Mo \rightarrow 1/3\ MoO_3$*	+28	
$C \rightarrow CO$	+28	
$Ni \rightarrow NiO$	+33	
$1/2\ Ru \rightarrow 1/2\ RuO_2$*	+61	

*Indicates fission products.

7.1.1 Thorium

The oxygen concentration in the sodium and the temperature have critical effects on the corrosion of thorium metal. When low oxygen pressures are applied to the thorium metal in the temperature range up

to 727°C, the rate of the oxide film formation drops off rapidly and the rate of oxygen pickup is reduced.[1-3] In addition, thorium oxide has fair resistance to corrosion by sodium up to 815°C.[4] Under low oxygen potentials a thin film of oxide forms on the thorium surface that is almost impervious to further corrosion. This thin film appears to have a structure more dense than that of bulk thorium oxide. However, under high oxygen concentrations, the film continues to increase in thickness until a phase change occurs that forms the normally observed bulk thorium oxide, and the film is transformed to a scale. Under some conditions this scale can spall. When the temperature is raised above 925°C, the thorium surface becomes reactive, presumably because of the surface mobility of the oxide layer.[1]

In summary, while thorium has a high affinity for oxygen under favorable conditions, it may develop a tenacious and impervious oxide film on contact with liquid sodium with a low oxygen content. This indicates that the oxide layer offers substantial protection toward further corrosion. Such behavior is typical of several metals that have high affinities for oxygen and a Pilling and Bedworth critical density ratio slightly above 1, coupled with the existence of a single oxide compound without any phase transitions within the temperature range. For the reference reactor conditions, thorium, by itself, appears to be sufficiently resistant to corrosion by the oxygen contaminant in the sodium. However, the behavior of the fuel alloy would require experimental verification and, if necessary, readjustment of composition to insure corrosion resistance.

7.1.2 Uranium

Although pure sodium and uranium are compatible, the presence of impurities, oxygen in particular, can cause adverse effects. Donaldson[5] reports the results of Thorley and Tyzack (1961) and other unpublished work obtained in the UKAEA, which show the effect of temperature, velocity, oxygen content, and fuel composition on corrosion rates. Without adequate oxygen removal, even at temperatures as low as 200°C, the corrosion rate of uranium is high. Oxide formation on the uranium surface appears to be

a prerequisite to corrosion. Table 7.2 shows the effect of alloying the uranium on the corrosion rate.

Table 7.2. Corrosion Rates of Uranium and Uranium Alloys in Sodium in Tests Carried Out Under Zirconium Hot-Trapping Conditions[a]

	Temperature (°C)	Na Velocity (fps)	Corrosion Rate (mils/month)
Uranium	600	25	2.13
U-1/2% Cr	600	25	2.41
U-1/2% Mo	600	25	2.71
U-10% Mo	600	25	1.56

[a]Oxygen concentration estimated to be about 1.5 ppm.

Pearlman[3] also concludes that corrosion rates depend very strongly on impurities, particularly oxygen; UO_2 and UO have been identified as dispersed corrosion products in dynamic sodium systems. The sequence of chemical interactions that can occur with uranium metal and sodium oxide causing the formation of a series of uranium oxides that become progressively more friable as the oxygen content increases would explain the high corrosion rates in the experiments cited. The fact that corrosion is negligible in static systems verifies that corrosion can be prevented by limiting the access of oxygen to the uranium surface.

Additional work has shown that the character of the film that forms on uranium metal is dependent on the temperature, as well as the oxygen content of the sodium. With cold trap temperatures of 175, 140, and 105°C, the temperatures at which a tenacious film formed were 425, 350, and 325°C, respectively, and the film increased in tenacity with temperature.[6]

Mogard[7] showed that inactivation of the oxygen in sodium in a static test by simple in-situ gettering with calcium essentially eliminated the oxide formation on uranium metal when calcium was in excess but not when the calcium and oxygen were in stoichiometric ratio.

The work of Isaacs[8,9] at the Atomic Energy Board in the Republic of South Africa and, subsequently, at Brookhaven National Laboratory, also is pertinent. He found that soluble getters remove oxygen from sodium more rapidly than uranium does at 300 to 400°C. Thus they reduce the effective oxygen concentration. Also, the rate of weight gain of uranium tabs (reported to be almost independent of time and temperature) in low-oxygen sodium appears to offer a simple method for monitoring the oxygen concentration in sodium.

7.2 Compatibility Data from Dounreay Reactor Experiment

Reliable compatibility data have been gathered for a large operating system, the Dounreay Fast Reactor (DFR). The DFR uses enriched U-7% Mo fuel elements in the form of hollow cylinders, 0.7 in. OD and 0.3 in. ID, clad on the outside with niobium and on the inside with vanadium. The cladding restrains warping of the fuel, and yet, since the ends of the element are vented to the primary coolant and the fresh fuel is separated from the outer cladding by a 0.1-in. space, a flow of NaK with a velocity at the start of fuel life of about 10 fps is permitted to pass over the fuel alloy surface. Fission products can therefore pass into the coolant, restricted only by the properties of the fuel alloy. The coolant flow within the cladding removes any fission-product gas deposits and also promotes heat transfer.

According to information furnished by the DFR staff,[10] the U-7% Mo fuel metal becomes coated with 2 to 3 mils of adherent oxide.* The exact composition of the surface layer is not known but is presumed to contain more UO_2 than UO and also some carbon. Because of the gettering action of the uranium fuel the oxygen level in the NaK coolant is low, probably much less than 10 ppm. The available cold traps are not used for oxygen contamination control because of the fuel gettering capability. A

---

*With an average in-pile lifetime for blanket material of about one year, a 1-mil-thick layer of uranium dioxide on the surface of the blanket metal of the reference process-heat-production concept is approximately equivalent to an in-leakage rate to the primary coolant circuit of 6.5 liters/hr of oxygen (STP).

disturbance of the system causes the oxygen concentration to increase, but gettering by the fuel quickly returns it to normal levels. The uranium content of the coolant is estimated at 10^{-3} ppm, but none has been detected. No major operational problems attributable to the use of vented metal fuel and fuel-coolant contact have been cited.

Chemically, the Dounreay Fast Reactor is similar to the proposed reactor. Some of the factors that may have an effect on the corrosion rate are compared in Table 7.3.

Table 7.3. Comparison of Characteristics of Dounreay Fast Reactor and Proposed Process-Heat-Production Reactor

	DFR	Process-Heat-Production Reactor
Fuel	U-7% Mo	Th-15% U-7% Pu
Fuel surface-to-volume ratio, cm^2/cm^3	3.94	3.44
Maximum fuel temperature, °C	840	650
Coolant	NaK	Na
Coolant flow velocity past fuel surface, fps	~10	30
Coolant inlet temperature, °C	200	170
Coolant outlet temperature, °C	400	350

7.3 Corrosion Control

In the long run, the rate of oxygen inleakage to the primary system will determine the severity of the interaction with uranium. The large mass of blanket metal provides a large sink into which the oxygen from the coolant will slowly diffuse. Thus the system will clean itself up unless the inleakage is high.

The three different methods that may be applied to enhance the compatibility between the fuel and blanket alloys directly in contact with

liquid sodium coolant are

1. complete removal of oxygen from the coolant by using a soluble getter or sacrificial reaction trap,
2. passivation of the fuel alloy surface,
3. formation of tenacious oxide films on the fuel and blanket metal surfaces and allowing the gettering action of these metals to remove the contaminants that leak into the system.

Application of the first method would require a greater amount of fundamental and development work than application of the third which, in essence, is the method applied in the Dounreay Fast Reactor, where the exposed fuel is used to clean up the coolant, with no reported ill effects.

To remove all the contaminant oxygen from the sodium coolant would require the use of a sacrificial reaction trap or a soluble getter, such as calcium or magnesium.[11-14] Methods of adding the getter to the sodium and of removing the insoluble getter oxide have been studied but not applied to large systems. Since the presence of the getter in the system may introduce new problems, it would be advantageous to know more about the properties of the getter and its oxide in the sodium as a function of temperature.

Some metals can be passivated by the formation of a mechanically stable and chemically inert surface layer. Thus, the stability of the nitrided surfaces of uranium and thorium on exposure to sodium oxide was considered.

The uranium nitride, UN, is stable in liquid sodium up to 820°F (438°C) (Refs. 15 and 16) and appears to be stable toward low concentrations of sodium oxide dissolved in sodium at moderate temperatures, approximately 300°C, according to thermodynamic data. The apparent mechanical stability of the nitride surface on uranium is indicated by the Pilling and Bedworth critical density ratio of 1.39, a value which in many systems is associated with a stable surface.

The calculated free energy change for the interaction between thorium nitride, Th_3N_4, and sodium oxide showed that thorium oxide is expected to form with the liberation of nitrogen. Thus, the method is not expected to be effective for use with thorium because of the pronounced affinity

of thorium for oxygen. Thorium metal, however, may be sufficiently resistant to corrosion because of the type of oxide layer that forms on its surface (see Sect. 7.1.1).

A combination of the second and third method may be applied in the reference reactor using the high-thorium-content fuel alloy. The uranium blanket alloy may be treated with nitrogen to form a stable nitride surface, which would retard corrosion by oxidation. Should some oxidation of the uranium metal occur, the presence of the nitride may enhance the stability of the more dense and tenacious uranium monoxide by the formation of a solid solution.[16,17]

In the Dounreay Fast Reactor the U-7% Mo alloy in contact with the flowing NaK at 600°C becomes covered with an adherent oxide film that does not erode. If the presence of molybdenum is essential for this behavior, the uranium blanket elements may be plated with molybdenum by vapor-phase deposition, or a suitable alloy may be selected. Molybdenum hexafluoride is volatile, like uranium hexafluoride, and the reaction

$$MoF_6 + U \rightarrow Mo + UF_6$$

may be used to deposit a layer of molybdenum onto the surface. The molybdenum then diffuses into the metal to develop a surface composition similar to the fuel alloy used in the Dounreay Fast Reactor.

7.4 Fission-Product Transport

Fission products may be transported from the fuel into the coolant by two different mechanisms: recoil at the instant of fission or diffusion after fission. Because of the low temperature, the amount of fission products transferred by diffusion may be assumed to be negligible, particularly when compared with the amount that recoils across the fuel-coolant interface, as discussed below.

A liquid sodium coolant in contact with fissioning uranium metal fuel will receive those fission fragments that recoil across the fuel coolant interface. The maximum range of fission products in uranium metal is given as 12.6 mg/cm^2 (~0.007 mm).[18] With bare metal fuel having a 1/8-in. web thickness, about 0.07% of the fission products are estimated

to recoil into the coolant. If the nature of the fuel surface were known, a more accurate evaluation of the recoil distance and the amount of fission products released could be made by using the data of Frank[19] for the selected fuel assay and the possible oxide surfaces. The fission products transported by recoil and accumulated are estimated to amount to about 1.4 ppm or less in the sodium coolant of the proposed reactor each year. This small amount is expected to be chemically insignificant.

Although the amount of fission-fragment recoil into the coolant is low in the case under consideration, it is desirable to know, or at least estimate, the effect these recoils will have on the transport of the fuel into the coolant. For the system being considered, the metal in contact with liquid sodium is expected to have a thin oxide layer because of the presence of oxygen impurity in the sodium. Studies of the recoil process across a uranium dioxide surface exposed in a vacuum show that about 4.5 atoms of uranium accompany each fission fragment.[20] Applying this value to an all-uranium system gives the result that about 12 ppm of uranium would appear in the sodium coolant each year, corresponding to a fuel loss of 5 g fissile per day. Very probably the amount of transported metal would be much less than this, inasmuch as uranium has not been detected in the Dounreay Fast Reactor coolant. It is noted that the reference design has a fuel with properties primarily determined by a thorium oxide surface rather than uranium dioxide and that the fuel surface is exposed to pressurized sodium rather than vacuum. These factors are expected to reduce the amount of fuel material transferred into the coolant by fission fragment recoil.

Plutonium and uranium may be expected to behave similarly. A low level of fissile material has been reported in the BR-5 reactor coolant.[21] The reactor was fueled with vented elements containing plutonium dioxide. After a 5% burnup of the fuel, the 50 alpha counts of sodium per second observed in the coolant indicated a plutonium content of 2×10^{-6} ppm.

The solubility of plutonium metal in sodium at 700°C is estimated from direct experimental data to be 1 to 2 ppm.[22] The plutonium was molten at this temperature, so no stable protective oxide layer could form on the surface. The proposed reactor will be fueled with solid metal

elements, and the surfaces of the elements will be covered by oxide films. The solubilities of the fuel materials will be governed by the solubilities of their oxides in the sodium.

7.5 Fission-Product Behavior

Fission-product behavior may be predicted by referring to Table 7.1. Those fission products whose free energies of reaction with sodium oxide are more negative than the free energy of uranium (strontium, lanthanum, and barium) may be expected to form insoluble oxides that will deposit at low-temperature points in the coolant system. Metallic fission products whose free energies of reaction are greatly positive will remain in the metallic state, and those which are normally insoluble in sodium may be expected to deposit on structural surfaces, while others such as cesium and rubidium are expected to remain in solution. The xenon and krypton will find their way into the cover gas, and their daughters are expected to deposit onto available solid surfaces. The free energy of formation of NaI is such that, upon release, iodine would not be expected to find its way to the gas phase but would react with and remain dissolved in the sodium. The NaI would not be expected to be reduced by other fuel or structural materials in the system.

The behavior of these fission products can be inferred from the results of fuel cladding failures during work with the Sodium Reactor Experiment[23] in July 1959, when 5 to 10 megacuries of fission products was released to the primary coolant system. The cold traps continued to operate after the failure and were found, on analysis of the sodium, to have provided efficient cleanup of all nongaseous fission products, except cesium and iodine. Sodium decontamination factors by all modes other than decay were less than 10 for cesium and iodine, 10^2 to 10^3 for ruthenium and zirconium, and more than 10^3 for cerium and strontium. Some of this effect was due to the presence of carbonaceous particles produced by radiolysis of tetralin, which was inadvertently introduced. Specific activities of the carbonaceous material were not selective and ranged from 10^3 to 10^4 times the specific activity of the filtered sodium in which it was contained. Only xenon and krypton were found in the

helium cover gas. Deposits of fission products on the walls of the system consisted primarily of strontium, cerium, niobium, and ruthenium. After cooling for four months ^{137}Cs and, possibly, ^{125}Sb still remained in the sodium; however, their activities were of the same relative magnitude as the unavoidable ^{22}Na and thus were not expected to hamper future operations.

Similar behavior was observed in the Enrico Fermi reactor in the October 5, 1966 event.[24] In this case, fission products were released into the primary coolant system. Within a few days after the incident, plateout losses of fission products from the liquid sodium were as large as 93% for ^{89}Sr and ^{90}Sr, 75% for ^{140}Ba, and 84% for ^{140}La, but only 8% for ^{137}Cs. The krypton and xenon were observed almost immediately in the cover gas of the coolant system, from which they partly escaped into the reactor containment vessel.

The behavior of fission products released into the sodium coolant of the Russian fast-neutron reactor, BR-5, has been reported.[21] The vapor-phase transport of ^{137}Cs activity was observed where accumulation on colder surfaces occurred. Also, the ^{137}Cs activity deposited onto the colder surfaces in contact with the coolant, such as cold traps, and reentered the coolant when the temperatures increased. The following activities were observed to have deposited with increasing tenacity: ^{137}Cs, ^{140}Ba-^{140}La, and ^{95}Zr-^{95}Nb.

7.6 Sodium Activation

In addition to the fission products that can recoil into the coolant, ^{24}Na (with a 14.9-hr half-life formed by an n,γ reaction of ^{23}Na) controls* the activity level of the primary coolant during operation. The relative contributions to the activity of the primary coolant due to fission products and sodium activation as a function of time after shutdown are shown in Fig. 7.1. The data in Fig. 7.1 are based on equilibrium

*The primary ^{24}Na gamma energies are 1.38 and 2.76 Mev.

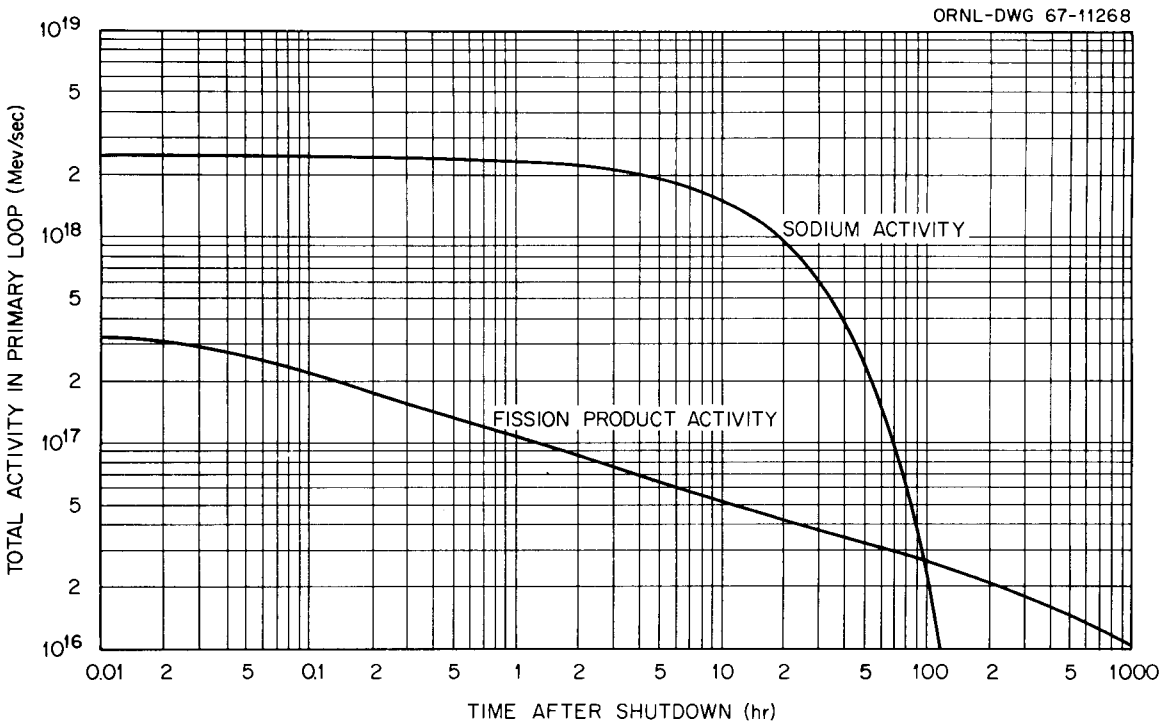

Fig. 7.1. Contributions to Primary Sodium System Activity Due to ^{24}Na and Fission Products from Fission Recoil.

conditions at the start of shutdown, 0.07% fission-product release, and no fission-product cleanup.*

7.7 Coolant Impurities

An estimate of the impurities that can be expected to appear in the sodium coolant can be made from previous experiments. In an extended investigation of mass transfer in a sodium circulating system with 10 to 50 ppm oxygen, the following[25] ranges of constituents were found:

Constituents	Concentration (ppm)
Ca	<20
Cr	0.0–3.0

*Fission-product activity in the coolant due to fissioning of plutonium or uranium in the coolant is negligible relative to that from other activity sources.

Constituents	Concentration (ppm)
Fe	1.0–10
K	129–366
Ni	0.5–2.5
Mo	0.2–1.5
C (elemental)	5–60
C (other)	50–250

Of particular interest is the carbon, which apparently can exist in several forms in the system.

These investigations resulted in the conclusions that the first few months of operation provided very different corrosion conditions compared with those of a "seasoned" system. Also any changes in operating conditions can cause "unseasoned" effects.

Contamination levels observed in the primary sodium system of the Enrico Fermi[24,26] reactor may be indicative of the amounts expected in other similar liquid sodium systems. The ranges of the contaminant concentrations are listed below:

Contaminant	Concentration (ppm)
Total C	50–200
Total O	7–15
H (non OH)	0.1–0.4
H (as OH)	0.1–1.4
Cr	<0.2
Fe	0.3–2.4
Ni	<0.2–0.6

Also, the argon cover gas of the sodium system contained about 1100 ppm nitrogen. The contaminant concentration in the sodium was found to increase when the temperature of the system was increased.

The impurities, oxygen, carbon, and hydrogen, can exist in several different species in the liquid sodium.[27] The distribution among the different species is dependent on the forms in which the impurities first enter the system and the subsequent temperature conditions. It would be prudent to anticipate each of the species that have been found; for example, carbon is found distributed as carbonate, carbide, graphite, and,

apparently, a carbonyl form that, on analysis, appears as the water-soluble sodium salt of hexahydroxy benzene. Hydrogen also can exist in two forms in the system — as the hydroxide and as the hydride.

Temperature fluctuations are expected to cause changes in the chemical behavior of the coolant by three different mechanisms: (1) by changing the solubilities of substances deposited on surfaces in contact with the coolant, (2) by changing the rate at which impurities diffuse into the coolant from the containment structure, and (3) by causing the species to undergo changes from one to another, such as changing carbon dioxide to carbon and oxygen or the hydroxyl ion to hydrogen and oxygen.

If coolant dump tanks are provided, these could be used also as holdup tanks for the helium cover gas in which the radioactive fission gases could decay before the gas was passed through the activated charcoal traps to remove the denser gases such as nitrogen and residual krypton and xenon. In an inadvertent fuel meltdown, the volume of gas released could amount to 90 to 5000 standard liters of gas, depending on the irradiation history. This added amount of gas could be readily accommodated by the dump tank space.

7.8 Materials of Contruction of Coolant Loops

Of the materials available, the austenitic stainless steels best meet the requirements for the containment of liquid sodium and have been used in nine reactors cooled with liquid sodium or NaK.[4] Experimental work will be needed to verify that the mass transfer rates are satisfactorily low and to determine whether columbium stabilization (such as in type 347 stainless steel) is needed.

The low-chromium-content steels can be used under some circumstances, but carbon transfer in the sodium system limits their use. Carbon steels have been used to reduce costs for noncritical applications, such as fill tanks and cold traps, but temperatures are restricted to 800 to 900°F (427 to 482°C).[28]

Both uranium and plutonium are known to form low-melting alloys with iron and nickel. However, material transport or direct contact is a prerequisite to such interactions, and neither condition is likely to be

present in the system being considered. Since the solubility of the uranium is apparently below detection, no significant amount of fuel is expected to reach the structure by mass transport. In addition, the uranium, in gettering the oxygen from the sodium, will be chemically and physically separated from the bulk sodium by a thin oxide film. The solubility of the iron in the sodium is also expected to be very low, since its solubility depends upon the oxygen content of the gettered sodium.

References

1. H. M. Finniston and S. P. Howe (Eds.), Progress in Nuclear Energy, Series V, Metallurgy and Fuels, McGraw-Hill, New York, 1956.

2. F. L. Gett and A. Draycott, The Compatibility of Beryllium with Liquid Sodium and NaK in Dynamic Systems, Proceedings of Second United Nations International Conference on the Peaceful Uses of Atomic Energy, Geneva, 1958, Vol. 7, pp. 125-131, United Nations, New York, 1958.

3. H. Pearlman, Corrosion of Uranium, Thorium and Uranium Alloys in Sodium and Organics, in Fuel Elements Conference, Paris, November 18-23, 1957, USAEC Report TID-7546, pp. 565-587, March 1958.

4. K. Goldmann and B. Minushkin, Sodium Technology, pp. 321-425 in Reactor Technology Selected Reviews - 1965, L. E. Link (Ed.), USAEC Report TID-8541, January 1966.

5. D. M. Donaldson, Compatibility Problems in Fast Reactors, pp. 89-121 in Progress in Nuclear Energy, Series IV, Vol. 5, Technology Engineering and Safety, C. M. Nicholls (Ed.), McGraw-Hill, New York.

6. H. F. Isaacs, Brookhaven National Laboratory, unpublished.

7. H. Mogard, Observations on the Corrosion of Uranium in Liquid Sodium, Proceedings of the First United Nations International Conference on the Peaceful Uses of Atomic Energy, Geneva 1954, Vol. 9, pp. 318-320, United Nations, New York, 1955.

8. B. Minushkin and H. S. Isaacs, The Chemistry of Oxygen in Sodium, paper presented at the 16th USAEC Corrosion Symposium, May 6-8, 1968, Battelle Memorial Institute, Columbus, Ohio.

9. H. S. Isaacs, The Gettering of Oxygen in Sodium by Uranium, paper presented at the 16th USAEC Corrosion Symposium, May 6-8, 1968, Battelle Memorial Institute, Columbus, Ohio.

10. Letter from W. Cunningham, Great Britain, to R. L. Philippone, USAEC, June 21, 1967.

11. S. Siegel, Basic Technology of the Sodium Graphite Reactor, Proceedings of the First United Nations International Conference on the Peaceful Uses of Atomic Energy, Geneva, 1954, Vol. 9, pp. 321-330, United Nations, New York, 1955.

12. M. Davis and A. Draycott, Compatibility of Reactor Materials in Flowing Sodium, Proceedings of Second United Nations International Conference on the Peaceful Uses of Atomic Energy, Geneva, 1958, Vol. 7, pp. 94-110, United Nations, New York, 1958.

13. F. L. Bett and A. Draycott, The Compatibility of Beryllium with Liquid Sodium and NaK in Dynamic Systems, Proceedings of Second United Nations International Conference on the Peaceful Uses of Atomic Energy, Geneva, 1958, Vol. 7, pp. 125-131, United Nations, New York, 1958.

14. W. L. Anderson, Removal of Carbon from Liquid Sodium Systems, USAEC Report NAA-SR-6386, Atomics International, 1961.

15. J. Bugl and A. A. Bauer, Corrosion and Oxidation Characteristics of Uranium Mononitride, p. 463 in Nuclear Metallurgy, Vol. X, International Symposium on Compounds of Interest in Nuclear Reactor Technology, J. T. Waber, P. Chiotti, and W. N. Miner (Eds.), The Metallurgical Society of the American Institute of Mining, Metallurgical and Petroleum Engineers, 1964.

16. R. F. Dickerson, A. F. Gerds, and D. A. Vaughan, Metallographic Identification of Nonmetallic Inclusions in Uranium, Trans. Am. Inst. Mining and Metallurgical Engrs., 206: 456-460 (1956).

17. R. E. Rundle, N. C. Baenziger, A. S. Wilson, and R. A. McDonald, The Structure of the Carbides, Nitrides, and Oxide of Uranium, J. Am. Chem. Soc., 70: 99-105 (1948).

18. E. Segre and C. E. Wiegand, Stopping Power of Various Substances for Fission Fragments, Phys. Rev., 70: 808-811 (1946).

19. P. W. Frank, Recoil Range of Fission Fragments, Bettis Technical Review, Reactor Technology, WAPD-BT-30, pp. 47-52, Westinghouse Electric Corporation, 1964.

20. M. D. Rogers, Ejection of Uranium Atoms from Sintered UO_2, J. Nucl. Mat., 22: 103-105 (1967).

21. A. I. Leipunskii et al., 5-Year Operation Experience in Reactor BR-5, Proceedings of Third United Nations International Conference on Peaceful Uses of Atomic Energy, Geneva, 1964, Vol. 6, pp. 51-61, United Nations, New York, 1965.

22. J. C. Clifford, Behavior of Liquid Pu-Co-Ce Alloys in Contact with Sodium, II. Liquid Metal Equilibra, USAEC Report LA-3545-MS, Los Alamos Scientific Laboratory, July 5, 1967.

23. R. S. Hart, Distribution of Fission Product Contamination in the SRE, USAEC Report NAA-SR-6890, Atomics International, Mar. 1, 1962.

24. Atomic Power Development Associates, Inc., and Power Reactor Development Company, October 5, 1966, Fuel Damage Incident at the Enrico Fermi Atomic Power Plant — Status as of February 24, 1967, Report NP-16750.

25. R. W. Lockhart, L. E. Pohl, and R. S. Young, Sodium Mass Transfer Investigations, pp. 189—208 in Proceedings of Sodium Components Information Meeting in Palo Alto, Calif., August 20—21, 1963, USAEC Report SAN-8002, May 1964.

26. Atomic Power Development Associates, Enrico Fermi Atomic Power Plant Reports for October 1966, EF-38; November 1966, EF-39; December 1966, EF-40.

27. V. M. Sinclair, J. L. Drummond, and A. W. Smith, The Analysis of Carbon in Sodium, UKAEA TRG Report 1185(D), Feb. 7, 1966.

28. C. B. Jackson (Ed.), Sodium-NaK Supplement, Liquid Metals Handbook, USAEC Report TID-5277, July 1, 1955.

8. FABRICATION AND REPROCESSING

In order to make a preliminary assessment of fuel-cycle costs, it is necessary to select core and blanket element fabrication and processing methods and to estimate their respective costs. The cost estimates derived are functions of the size of the reactor industry served, the location of the fabrication and processing facilities, the type of facility (i.e., design to serve a single reactor type or a variety of reactor types), spent element cooling time, and shipping time. A detailed analysis of these factors is beyond the scope of this report.

Although many uncertainties remain, a reference fuel cycle was selected that is believed to be reasonably appropriate for the unclad-metal-fueled concept. It consists of on-site core and blanket processing by the salt transport process, on-site core element fabrication, and off-site blanket element fabrication.

It should be noted that the feasibility and potential of the concept are not dependent on the reference fuel-cycle system selected; however, alternative systems would be expected to be somewhat more expensive. The magnitudes of the effect on reactor economics of certain alternatives are discussed in Section 9.3.

8.1 Core Element Fabrication Cycle

In the absence of mechanical restraint from cladding, it is desirable to limit the fuel burnup to a level that will not produce more than about 10-vol % growth. For the design fuel temperature used, this limitation requires fuel refabrication at average burnups of about 33 Mwd/kg. To accommodate this need, an on-site fuel refabrication facility is assumed to be directly coupled to the reactor plant. Elimination of the need to remove and replace fuel cladding simplifies the on-site operations required. In addition, an on-site facility reduces the out-of-pile inventory and eliminates the cost of shipping the fuel to and from a central plant. To take full advantage of such an arrangement, it was assumed that the exposed fuel would be introduced to the refabrication plant after a 15-day cooling period. The short decay period and the nature of

the fuel and refabrication process require that the facility be shielded and remotely operated and that an inert atmosphere be maintained in the fuel-handling and -processing cells.

The primary purpose of the refabrication process is to remove the accumulated fission gas from the fuel and to reform the element to its initial size and density. In the fuel-refabrication facility, the fuel assemblies are dismantled, the shielding and blanket portions of the assemblies are put into temporary storage, and the core fuel elements are refabricated. During the refabrication process, one-third of the exposed fuel is sent to an on-site reprocessing plant, where the remaining fission products are removed. Recycle material from the reprocessing plant and sufficient makeup material are blended with the remaining two-thirds of the exposed fuel in the refabrication plant to produce a new fuel element of equilibrium composition. The refabricated core elements and the shielding and blanket elements are then reassembled and returned to the reactor.

The relationship between the reactor, the refabrication facility, and the reprocessing plant is shown in Fig. 8.1. The daily refabrication rates for plants servicing either a process-heat- or a power-production reactor complex are listed in Table 8.1.

Table 8.1. Summary of Fuel Fabrication and Processing Throughputs for a Three-Reactor Complex Producing 10,500 Mw(th)

	Throughput (kg per operating day)	
	Process-Heat-Production Reactor	Power-Production Reactor
Fabrication throughput		
Core	83.4	86.7
Blanket	101.4	122.5
Processing throughput		
Core	27.8	28.9
Blanket	101.4	122.5

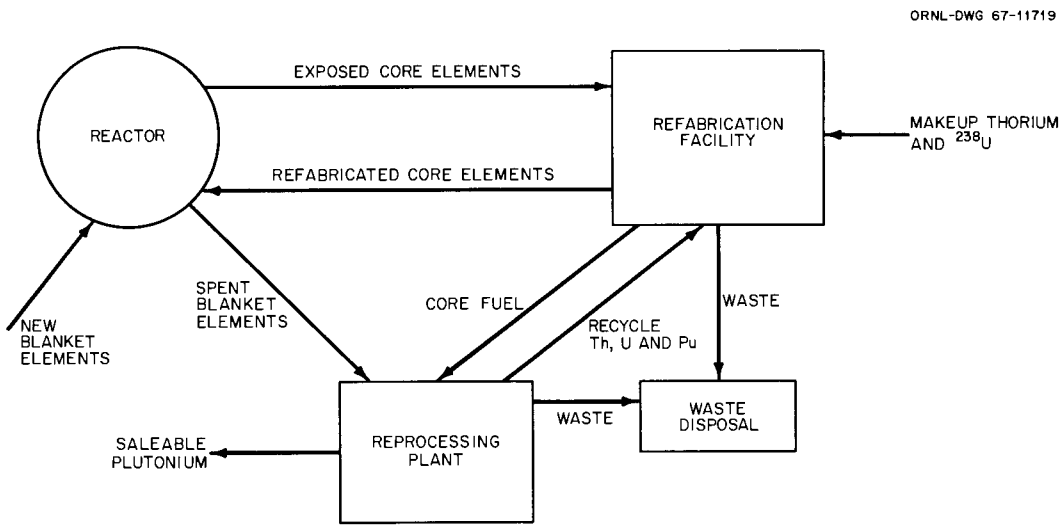

Fig. 8.1. Mixed Fuel-Cycle Flow Diagram.

8.2 Core Element Fabrication Methods

The equilibrium core fuel is a thorium-based Th–15 wt % U–7 wt % Pu ternary alloy containing noble-metal fission products. The geometric form of the fuel is shown in Fig. 3.3, and the dimensions of the fuel elements are given in Table 3.1.

Consideration was given to two general methods of fabricating the fuel elements. These methods, melt casting and powder metallurgy, were compared in an attempt to assess the relative merits of each for this particular application. Experience with the melt casting of thorium-uranium alloys has shown that segregation of the uranium occurs with normal casting procedures. This, coupled with the fact that suitable crucible and mold materials would need to be developed, makes melt-casting processes appear less attractive than powder metallurgy techniques. Vacuum-arc melting in a chilled copper mold would eliminate the mold material problem but would increase segregation problems, as well as require subsequent forming operations.

Powder-metallurgy techniques offer a way around the difficulties inherent in the melt-casting process. Production of the metal powder is accomplished by hydriding and dehydriding the spent fuel alloy. The

powders may then be formed into the fuel element shape by one of several standard powder metallurgy methods. Discussions of this method with personnel at the Union Carbide Nuclear Company Y-12 Plant, with Battelle Memorial Institute, and with the ORNL Metals and Ceramics Division indicate that the process may be technically feasible.

Although no work has been done with this particular alloy, each of the primary constituents has been successfully hydrided and dehydrided.[1] The optimum temperature for the formation of uranium hydride is between 200 and 250°C. At 250°C a charge of 100 g of clean uranium shavings is completely converted to the hydride in about 30 min; a massive piece of metal of the same weight requires 1 1/2 to 2 hr for complete hydriding. The uranium hydride may be readily reduced by heating to 300 to 400°C under reduced pressure.

The formation of thorium powder from massive metal requires, first, the formation of the dihydride, ThH_2, at 600 to 650°C at 1 atm hydrogen pressure. During this step the charge swells but does not break up into a powder. The higher hydride, Th_4H_{15}, is then formed at 250°C. The charge exfoliates and breaks up into a coarse powder during this operation. The higher hydride is decomposed next at 500°C under a pressure of 1 atm of hydrogen, and the lower hydride is decomposed at 700°C at a low (<1 mm Hg) pressure. A 10-lb charge of thorium shavings can be converted to powder in 8 to 12 hr by this process. Large pieces of massive metal have also been converted to powder, but the time required is somewhat longer.

Within the realm of powder metallurgy technology, there exist several promising methods for producing the desired fuel element configuration. These methods are briefly described below.

1. Extruded tube method. In this process, individual hexagonal tubes may be extruded, either from a powder-binder mixture or from a predensified billet. The extruded tubes would be partially sintered, assembled to form a complete element, and then diffusion bonded together during the final sintering process. The major uncertainties with this process are the effect of the binder on the material properties and the integrity of the tube-to-tube bond. Indications are that dimensional tolerances within the acceptable range can be maintained with this method.

2. Cold pressing, sintering, and recoining method. This approach would produce short, full cross sections (1/2 to 4 in. high) of the fuel element. These sections would then be stacked, one on top of another, to the proper height. The process steps include cold pressing of the powder followed by alternate sintering and coining operations until the desired density is achieved. The major uncertainty with this method is the height of the unit that can be formed. If the individual pieces are too short, additional care is required to insure proper axial alignment of the coolant channels.

3. Hot pressing method. With this method the same shape would be produced as in method 2. Here, however, the parts are heated and densified in the molds without separate sintering and coining operations. The difficulty with this approach lies in the fact that hot pressing is, historically, an expensive process.

4. Extruded element method. This process would produce a complete cross-section element of the full core height by extruding either a predensified billet or a powder-binder mixture. Die life is uncertain if a predensified billet is used, and nonuniform shrinkage may be a problem if the powder-binder mixture is chosen.

The preliminary nature of this study has not allowed a thorough investigation of these alternatives. Method No. 1 for producing bundles of individually extruded tubes was chosen as the basis for a refabrication cost study. The results of this study are summarized in Chapter 9, Table 9.2, and details of the cost study are presented in Appendix B.

8.3 Blanket Element Refabrication

Since the blanket elements are depleted uranium and would require no special facilities or handling techniques, it was assumed that the blanket fuel elements would be fabricated in a central facility serving a 70,000-Mw(th) industry (2000 kg per operating day). A blanket element fabrication cost of $5.23/kg was estimated based on the information contained in Appendix B.

8.4 Reprocessing

The salt-transport process under development at Argonne National Laboratory is appropriate for metal fuel reprocessing; therefore it was the process assumed for fuel reprocessing in this preliminary concept study. In applying this process to uranium-plutonium fuels, dehydrided metal powder from the fuel element refabrication facility is dissolved in molten copper-magnesium, contacted with one molten halide salt to remove the reactive fission products (Cs, Rb, Sr, Ba, rare earths, and, presumably, also Kr, Xe, I_2, Se, and Te if they were not removed during the dissolution step), and then contacted with a second molten halide salt that will extract the plutonium and uranium (together or in sequence) while leaving the nonreactive fission products (Zr, Nb, Mo, noble metals, etc.) behind. The second halide salt is contacted with molten zinc-magnesium, which transfers the uranium and plutonium back into the metallic phase. The zinc and magnesium are volatilized in a retorting operation that leaves behind metallic uranium and plutonium, which would be remelted preparatory to fuel fabrication. Argonne National Laboratory has demonstrated all the steps of the process on a modest engineering scale but has not yet made an actual pilot plant demonstration of the integrated process. While experimental development of the salt transport process has been directed toward uranium-plutonium fuels, studies at Argonne and elsewhere[2] indicate that the process would be applicable to thorium-bearing fuels as well.

On-site fuel processing cost estimates for the above processes are summarized in Chapter 9, Table 9.2. The estimates are based on extrapolation and/or interpolation of 1966–67 Argonne estimates for uranium-plutonium fast breeder reactor fuels, and it is assumed that the cost for processing uranium-plutonium-thorium core fuel will be the same as for uranium-plutonium core fuel (see App. C). The estimates are speculative, since the process is in the early stages of development. The effect on overall concept economics of a requirement for off-site aqueous reprocessing is minor, as discussed in Section 9.3.

References

1. H. H. Hausner, Powder Metallurgy in Nuclear Engineering, pp. 38–45, American Society for Metals, 1958.

2. P. Chiotte and J. S. Klepfer, Transfer of Solutes Between Liquid Alloys in Material Contact with Fused Salt, Application to Fuel Reprocessing, Ind. Eng. Chem., Proc. Des. Dev. Quart., 4(2): 232 (April 1965).

9. ECONOMICS

Cost projections were made for a single-unit reactor of 3500-Mw(th) capacity. Although the on-site fuel fabrication and processing plants are sized to serve a three-reactor complex, the effect on reactor capital cost of multiple reactors sited together is not included. On the same basis the effect of scaling up the reactor to a 10,000-Mw(th) single-unit core rating is treated separately in Section 9.8.

9.1 Economic Factors

Economic factors used to estimate product costs for the mixed-fuel concept are given in Table 9.1. The value of plutonium is based on the projected cost given for ^{235}U and its effectiveness relative to ^{235}U when used in a thermal reactor.

Table 9.1. Economic Factors Used to Estimate Product Costs

Cost of natural uranium as U_3O_8, \$/lb	8
Cost of unirradiated thorium as ThO_2, \$/lb	5
Separative work cost, \$/kg	26
Value of fully enriched uranium, \$/g ^{235}U	11.17
Value of fissile plutonium, \$/g	9.30
Value of ^{233}U for inventory charges, \$/g	9.30
Value of depleted uranium, \$/kg	3.08
Cost of conversion of U_3O_8 to UF_6, \$/kg	2.70
Reactor thermal capacity served by on-site fuel fabrication and reprocessing plant, Mw	10,500
Reactor capacity factor	0.9
Spent element cooling time, days	15
Processing time, days	30
Fabrication time, days	30
Total losses, % of material processed	1.2
Fixed charge rate on fuel inventory, %/year	
Public financing	5
Private financing	10
Fixed charge rate on plant capital, %/year	
Public financing	7
Private financing	12

9.2 Plant Availability

A plant availability factor of 0.9 was used to assess reactor economic potential. The following assumptions permitted the selection of this value:

1. An annual nine-day shutdown for preventive maintenance accounts for 2.5% downtime.

2. Approximately five days per year (1.5%) is allotted for unscheduled system maintenance incremental to maintenance during refueling.

3. A 16-hr refueling period following each 10 days of full-power operation contributes a 6% loss in plant availability. This is based on a 3-hr power-reduction period, a 20-min cycle for each fuel element transfer,* and a 5-hr startup period. These time periods were based on the results of a survey (see App. D) of the refueling schedules and methods presently anticipated for several sodium-cooled fast breeder reactors. It is assumed that two fuel transfer machines will operate simultaneously during the fuel transfer period.

9.3 Fuel-Cycle Costs

Unit fuel-fabrication and -processing costs used in the design study are given in Table 9.2. These costs are based on estimates of the capital and operating costs for the processes involved and the material throughputs given in Table 8.1. Additional information describing the basis for these unit cost estimates is included in Appendices B and C for refabrication and reprocessing, respectively. The reprocessing and fabrication plant facilities are sized to serve a three-reactor complex with single-unit ratings of 3500 Mw(th).

The fuel-cycle costs based on the economic factors given in Table 9.1 and the unit fabrication and processing costs given in Table 9.2 are presented in Table 9.3. The negative fuel-cycle costs reflect the result that, for the economic factors assumed, the value of the bred fuel exceeds all other positive elements of fuel-cycle cost.

---

*Based on 22 and 25 fuel elements for the process-heat- and power-production reactors, respectively.

Table 9.2. Summary of Unit Fabrication and Processing Cost Estimates for a Three-Reactor Complex

	Unit Cost ($/kg)			
	Process-Heat-Production Reactor		Power-Production Reactor	
	Public Financing	Private Financing	Public Financing	Private Financing
Fabrication				
Core (on-site)	27.0	32.4	25.9	31.6
Blanket (off-site)	5.2	5.2	5.2	5.2
Processing				
Core (on-site)	47.8	57.8	47.3	57.2
Blanket (on-site)	36.0	43.5	34.5	41.7

Table 9.3. Summary of Fuel-Cycle Cost Estimates

Cost Component	Process-Heat-Production Reactor		Power-Production Reactor	
	Public Financing	Private Financing	Public Financing	Private Financing
Inventory, ¢/MBtu	1.48	2.96	1.69	3.38
Processing, ¢/MBtu	1.73	2.09	1.95	2.36
Fabrication, ¢/MBtu	0.99	1.18	1.03	1.23
Plutonium credit, ¢/MBtu	(6.45)[a]	(6.45)	(6.45)	(6.45)
Net fuel cycle cost				
¢/MBtu	(2.25)	(0.23)	(1.78)	0.52
Mills/kwhr(e)			(0.166)	0.048
Annual fuel-cycle cost for 3500-Mw(th) reactor, $ million	(2.12)	(0.22)	(1.68)	0.49

[a]Parentheses denote gain.

If it is found impractical to fabricate core fuel containing fission products, the reference fuel cycle can be changed to allow for processing before each fabrication of the fuel element. The net fuel-cycle cost in this instance is −1.6 cents per MBtu, or 0.7 cents per MBtu more than the reference cost for the 3500-Mw(th) capacity plant under public financing. Similarly if the fuel reprocessing is done at some privately owned central facility with aqueous rather than pyrochemical processing, the net fuel-cycle cost for the process-heat-production reactor is −1.9 cents per MBtu or 0.3 cents per MBtu more than the reference gain. In this estimate a 22% annual charge rate was applied to the central reprocessing plant capital and an additional 60 days cycle time was allowed for shipping and storage.

9.4 Capital Costs

The capital cost estimates* for the 3500-Mw(th) reference reactors are summarized in Table 9.4; detailed estimates are given in Appendix E. An attempt was made to account for unusual costs associated with the concept. For example, extra allowances of $2 million and $1 million were included for maintenance equipment costs and the reactor coolant treatment systems for the process-heat- and power-production reactors, respectively. The nuclear "island" estimates include all equipment, land, improvements, and indirect costs required to produce steam, and the turbine "island" estimates include all costs necessary to convert the prime steam into power. In the power-production concept the turbine exhaust is at full condensing conditions, while the turbine exhausts at 127°C (260°F) for the process heat-production reactor. The capital costs of the on-site fuel-fabrication and -processing plants are included in the fuel-cycle cost and not in the reactor plant cost.

---

*The speculative nature of all cost estimates for advanced concepts is recognized, but it is nonetheless noteworthy that the capital cost of the unclad-metal-fueled reactor is no more than that for other sodium-cooled fast breeder reactors, since its high power density and sodium temperatures permit a compact design.

Table 9.4. Summary Capital Cost Estimates for 3500-Mw(th) Reactors

	Process-Heat-Production Reactor		Power-Production Reactor	
	Public Financing	Private Financing	Public Financing	Private Financing
Nuclear island				
Total cost, $ million	103.0	106.4	105.3	108.8
Unit cost, $/kw(th)	29.4	30.4	30.1	31.1
Fixed annual cost due to investment, $ million	7.2	12.8	7.4	13.1
Turbine island				
Gross electrical output, Mw	284	284	1332	1332
Total cost, $ million	25.9	26.8	69.0	71.3
Gross unit cost, $/kw(e)	91.2	94.4	51.8	53.5
Fixed annual cost due to investment, $ million	1.81	3.22	4.83	8.56
Total facility				
Total cost, $ million	128.9	133.2	174.3	180.2
Fixed annual cost due to investment, $ million	9.0	16.0	12.2	21.6

The capital cost estimate for the process-heat-production concept is based on conventional materials and design practices for high-temperature reactors. However, since it is possible that carbon steel could be used in part for the low-temperature reactor, a cost estimate for a carbon steel system (instead of stainless steel) was made for the process-heat-production reactor that showed a possible 10% reduction in the nuclear plant cost. Another significant capital cost saving that may be considered for a process-heat-production concept is the elimination of the steam generator. For the concepts considered, elimination of steam-generation equipment would reduce nuclear plant costs by about 15%. However, since studies of direct-cycle brine heating to identify the possible applications and incentive for such designs are incomplete, steam-generator costs are included in the process-heat-production system capital costs.

9.5 Operating and Maintenance Costs

Annual operating and maintenance costs, taken from Ref. 1, are given in Table 9.5. The estimates are intended to include costs for labor (with a 20% allowance for fringe benefits and a 25% allowance for general and administrative expense), materials, supplies, services, and coolant makeup.

Table 9.5. Estimated Annual Operating and Maintenance Costs for 3500-Mw(th) Plant

	Costs (millions of dollars)	
	Process-Heat-Production Reactor	Power-Production Reactor
Nuclear island	1.23	1.23
Turbine island	0.17	0.55
Total	1.40	1.78

9.6 Nuclear Insurance

The annual insurance cost was calculated as

$$\text{Annual cost (\$)} = 130{,}000 + 30 \times \text{Thermal rating (Mw)} .$$

The cost of nuclear insurance is therefore $235,000 for the 3500-Mw(th) capacity plant.

9.7 Heat and Power Costs

Based on the data of Sections 9.2 through 9.5 the total cost of providing steam at 127°C (260°F) from the process-heat-production concept and of producing power from the power-production concept are given in Tables 9.6 and 9.7. In determining the cost of 127°C (260°F) heat from the process-heat-production concept, a credit for power produced in excess of that required for the reactor plant was applied that was based on the power cost estimates for the power-production concept. The unit

Table 9.6. Heat Cost Summary[a] for 3500-Mw(th) Process-Heat-Production Reactor Operating at a Plant Factor of 0.9

Annual production: 127°C (260°F) steam, 86.4×10^6 MBtu
Gross power, 2.24×10^9 kwhr, 284 Mw
Net power, 2.04×10^9 kwhr, 258 Mw

	Annual Cost (millions of dollars)	
	Public Financing	Private Financing
Nuclear island		
Capital	7.2	12.8
Operating and maintenance	1.23	1.23
Fuel	(2.12)[b]	(0.22)
Insurance	0.24	0.24
Total	6.55	14.05
Turbine island		
Capital	1.81	3.22
Operating and maintenance	0.17	0.17
Total	1.98	3.39
Credit for surplus power production	(2.43)	(4.49)
Total	6.10	12.95
Cost of 127°C (260°F) steam, ¢/MBtu	7.06	15.0

[a]On-site fuel-fabrication and -processing facilities sized to serve 10,500-Mw(th) capacity.

[b]Parentheses denote gain.

cost of the power conversion equipment for the process-heat-production design is relatively high, primarily because of the small amount of power produced. For this reason the power credit applied just offsets the incremental costs of producing the power and does not significantly influence the estimated cost of 127°C (260°F) heat to the evaporator. For the process-heat-production concept this surplus power would normally be more than adequate for evaporator and product-water pumping needs.*

*As a guideline, evaporator and product-water pumping power requirements for a low-temperature (120°C) evaporator designed to utilize the heat available from a 3500-Mw(th) process-heat-production reactor might fall in the range 100 to 200 Mw(e).

Table 9.7. Heat and Power Cost Summary[a] for 3500-Mw(th) Power-Production Reactor Operating at a Plant Factor of 0.9

Annual production: Prime steam, 94.2×10^6 MBtu
Gross power, 10.5×10^9 kwhr, 1332 Mw
Net power, 10.1×10^9 kwhr, 1280 Mw

	Annual Cost (millions of dollars)	
	Public Financing	Private Financing
Nuclear island		
Capital	7.37	13.1
Operating and maintenance	1.23	1.23
Fuel	(1.68)[b]	0.49
Insurance	0.24	0.24
Total	7.16	15.06
Turbine island		
Capital	4.83	8.56
Operating and maintenance	0.55	0.55
Total	5.38	9.11
TOTAL	12.5	24.2
Unit product costs		
Prime steam, ¢/MBtu	7.60	16.0
Power, mills/kwhr	1.24	2.40

[a]On-site fuel-fabrication and -processing facilities sized to serve 10,500-Mw(th) capacity.

[b]Parentheses denote gain.

The heat and power costs given in Table 9.6 indicate that in 3500-Mw(th) capacities and with public financing (7% annual capital recovery factor) the process-heat-production concept is potentially capable of producing 127°C (260°F) steam for a self-contained single-purpose plant for about 7.1 cents per MBtu.

Further, if the unclad fuel proves to be suitable for use with the higher coolant temperatures assumed for the power-production concept, the

low prime steam and power costs indicate that the concept is potentially attractive for central station power (or dual-purpose plant) applications.

9.8 Effect of Scaleup to 10,000-Mw(th) Single-Core Ratings

The cost projections presented in the following were developed to indicate the effect of the process-heat-production concept on large water-desalting complexes. Past studies[2] under the ORNL Nuclear Desalting Program have considered the feasibility and effect on cost of scaling up four different 1000-Mw(e) single-unit power plant designs to 10,000-Mw(th) single-unit ratings. In that work successful development of the components necessary for the 1000-Mw(e) designs was assumed. It was also assumed that the refueling concept for the 10,000-Mw(th) plant would not differ significantly from that for the 1000-Mw(e) plant.

A result from that work is that unit capital costs for the nuclear steam-generating facilities, as well as for the complete power-production plants, would be expected to decrease if the thermal capacity were increased to 10,000 Mw. Based on the scaleup studies the expected percentage decrease in unit costs in scaling up the reference designs from 3500- to 10,000-Mw(th) ratings are given in Table 9.8. If those percentage reductions are applied to the capital and operating costs for the 3500-Mw(th) reference designs and the unit fuel fabrication and processing costs are as given in Table 9.9, which reflects a material throughput for three 10,000-Mw(th) reactors, the product costs for the reference designs that result are as given in Table 9.10.

References

1. T. D. Anderson and M. L. Myers, Capital and O&M Cost Data for Fast Breeder Reactors, memo to E. A. Mason, AISP-I-130, Sept. 12, 1967.

2. T. D. Anderson, H. A. Sindt, and I. Spiewak, Costs of Power from Nuclear Desalting Plants, Chem. Eng. Progr., 63(4): 41–45 (April 1967).

Table 9.8. Percentage Reduction in Unit Costs Anticipated Upon Reference-Design Scaleup from 3500 to 10,000 Mw(th)

	Reduction in Unit Cost (%)
Nuclear island	
Capital	31
Operating and maintenance	44
Turbine island	
Capital	9
Operating and maintenance	22

Table 9.9. Summary of Fabrication and Processing Costs for Three 10,000-Mw(th) Plants

	Unit Cost ($/kg)			
	Process-Heat-Production Reactor		Power-Production Reactor	
	Public Financing	Private Financing	Public Financing	Private Financing
Fabrication				
Core (on-site)	19.22	23.94	20.00	25.20
Blanket (off-site)	5.23	5.23	5.23	5.23
Processing				
Core (on-site)	37.90	45.80	37.50	45.30
Blanket (on-site)	30.00	36.30	27.70	33.50

Table 9.10. Projected Product Costs from Reference Designs Scaled Up to 10,000-Mw(th) Single-Unit Ratings[a]

	Process-Heat-Production Reactor		Power-Production Reactor	
	Public Financing	Private Financing	Public Financing	Private Financing
Annual production				
Prime steam, MBtu			270×10^6	
127°C (260°F) steam, MBtu	247×10^6			
Net power, kwhr	5.84×10^9		28.9×10^9	
Annual costs, $ million				
Nuclear island				
Capital	14.2	25.2	14.5	25.8
Operating and maintenance	2.0	2.0	2.0	2.0
Fuel	(7.5)[b]	(2.3)	(6.3)	(0.4)
Insurance	0.5	0.5	0.5	0.5
Total	9.2	25.4	10.7	27.9
Turbine island				
Capital	4.7	8.4	12.6	22.3
Operating and maintenance	0.4	0.4	1.2	1.2
Total	5.1	8.8	13.8	23.5
Credit for power production	(4.7)	(9.6)		
TOTAL ANNUAL COST	9.6	24.6	24.5	51.4
Unit costs				
Prime steam, ¢/MBtu			4.0	10.3
127°C (260°F) steam, ¢/MBtu	3.9	10.0		
Power, mills/kwhr			0.85	1.78

[a]On-site fuel-fabrication and -processing facilities sized to serve 30,000-Mw(th) capacity.

[b]Parentheses denote gain.

APPENDICES

Appendix A

DESCRIPTION OF ALTERNATE CONCEPTS OF THE UNCLAD-METAL-FUELED FBR — THE U-Pu-Fs AND Th-^{233}U FUELED REACTORS

1. General Characteristics of the U-Pu-Fs and Th-^{233}U Fueled Reactors

Two alternate concepts of the unclad-metal-fueled fast breeder reactor were studied. In the uranium-plutonium-fission fueled concept the penalty caused by the low burnup capability of uranium-based-alloy fuels containing plutonium would be partially ameliorated by providing an on-site fuel refabrication plant to reconstitute the fuel several times between each full chemical processing step. Vacuum melting would be carried out to remove the volatile fission products, and the reactive rare earths plus strontium and barium would be removed from the melt through the use of zirconium oxide[1] or halide salt[2] reagents. Plutonium and the noble fission products would accumulate to some equilibrium level dependent on the fission production rate and the rate of removal to the chemical processing plant. By this means effective burnups of 100 Mwd/kg between complete chemical processings would be achieved over several recasting steps. The equilibrium core fuel would be of the U-Pu-Fs type, which has been extensively irradiation tested at Argonne National Laboratory.

While the economics of the U-Pu-Fs fueled concept appear to be quite attractive, difficulties are encountered in the design. First, most of the available irradiation tests described in the literature were carried out in a high-burnup high-temperature regime in which most of the tested specimens failed. Very little information is available for low burnups, and there is none on the expected increase in temperature capability at low burnups. To be designed on the basis of proven capability, the fuel would be limited to an irradiation temperature of approximately 350°C. While this situation is resolvable by further irradiation testing, the consequences of exceeding the irradiation limit are severe because of the well-known catastrophic mode of failure of alpha-phase uranium alloys under irradiation. Thus not only are the operability limits unclearly

defined but they must not be exceeded at all costs. In contrast, thorium-based fuel alloys could probably withstand an inadvertent excessive exposure without gross change.

2. Unclad U-Pu-Fs Fueled Reactor Characteristics

2.1 Description

A summary of reactor parameters for all four of the concepts studied is presented in Table A.1. Note that because of the temperature limitation the U-Pu-Fs fueled concept is primarily a process-heat producer that generates some saleable electricity. Its average core specific power of 71 w/g is the lowest of the four cases, and its core geometry differs also in that it has an annular shape with a high length-to-width ratio. The small width minimizes the radial peaking factor and forms a high-leakage core that tends also to minimize the positive sodium loss coefficient. The height was extended to maximize the core expansion reactivity loss. The higher power densities of the other concepts precluded this sort of a core design. For them, a pancake shape was required to reduce coolant velocities to acceptable levels. The pancake shape also has high leakage and, hence, the good sodium-loss characteristics of the annular design, but the expansion reactivity loss is diminished and radial fuel zoning must be adopted to lower the radial peaking factor.

Note that the blanket materials for the U-Pu-Fs and mixed-cycle concepts are identical.

2.2 Reactor Physics

Reactivity coefficients and worths are listed in Table A.2; however, such a listing resolves no question regarding the safety of the reactor. Transient analyses under various assumed operational and accident conditions would be required to determine the inherent safety of the reactor.

2.3 Fuel Performance

The core fuel alloy material termed "fissium" is a particularly convenient combination of metals, being what is left of the fission products

Table A.1. Unclad-Metal-Fueled Fast Breeder Reactor Characteristics — Comparison of Mixed-Cycle Concepts with U-Pu-Fs and Th-^{233}U Versions

	Process-Heat-Production Reactor		Power-Production Reactor	
Appendix E Case No.	4	2	3	1
Fuel	U-Pu-Fs	Th-U-Pu	Th-^{233}U	Th-U-Pu
Reactor thermal power, Mw	3500	3500	3500	3500
Coolant inlet temperature, °C (°F)	170 (338)	170 (338)	370 (698)	345 (653)
Coolant outlet temperature, °C (°F)	290 (554)	350 (662)	550 (1022)	525 (977)
Core specific power, w/g heavy metal	71	287	211	217
Net efficiency [net Mw(e)/Mw(th)], %	4.35[a]	7.35[a]	39.8	36.6
Process heat at 127°C (260°F) and 35.4 psia, Btu/hr	11.3×10^9	10.96×10^9		
Doubling time, years (geometric)	5.75	3.0	5.7	3.4
Core characteristics				
Percentage of total power	86.0	79.2	88.5	82.3
Geometry	Annular	Cylinder	Cylinder	Cylinder
Number of fuel zones	1	2	2	2
Volume, ft^3	209	57.9	79.2	79.2
Height, ft	3.0	1.5	1.5	1.5
Diameter, ft (OD for annular core)	13.1	7.0	8.2	8.2
Fuel composition (nominal), wt %	U–8 Pu–10 Fs	Th–7 Pu–10 U	Th–13 ^{233}U	Th–7 Pu–10 U
Maximum burnup, Mwd/kg	8	40	40	40
Maximum fuel temperature, °C (°F)	350 (662)	650 (1200)	650 (1200)	650 (1200)
Average power density, w/cc	511	1700	1250	1280
Maximum power density, w/cc	816	2342	1751	1754
Coolant channel distance across flats, cm	0.55	0.75	0.56	0.62
Maximum ratio of thermal stress to tensile strength	0.10	0.64	0.24	0.31
Void fractions				
Fuel	0.47	0.47	0.47	0.47
Sodium	0.50	0.50	0.50	0.50
Structure	0.03	0.03	0.03	0.03
Core specific power, w/g heavy metal	71	287	211	217
Core fissile specific power, w/g fissile metal	832	2220	1620	1720

[a]Cycle efficiency based on turbine exhaust at 127°C (260°F).

Table A.1 (continued)

	Process-Heat-Production Reactor		Power-Production Reactor	
Core characteristics (continued)				
Inventories, kg				
Total fissile plus fertile	44,900	8,990	10,380	12,300
Fissile	3,830	1,320	1,660	1,650
Axial blanket				
Percentage of total power	5.0	15.9	9.1	13.9
Volume, ft^3	139.5	115.7	158.4	158.4
Thickness, ft	1.0	1.5	1.5	1.5
Fuel	Depleted U[b]	Depleted U[b]	Thorium	Depleted U[b]
Maximum burnup, Mwd/kg	3.0	3.0		3.0
Maximum fuel temperature, °C (°F)	600 (1112)	600 (1112)		600 (1112)
Void fractions				
Fuel	0.47	0.47	0.47	0.47
Sodium	0.50	0.50	0.50	0.50
Structure	0.03	0.03	0.03	0.03
Radial blanket				
Percentage of total power	8.5	5.0	2.3	3.8
Volume, ft^3	439	123	140	140
Thickness, ft	1.0	1.0	1.0	1.0
Fuel	Depleted U[b]	Depleted U[b]	Thorium	Depleted U[b]
Maximum burnup, Mwd/kg	3.0	3.0		3.0
Maximum fuel temperature, °C (°F)	600 (1112)	600 (1112)		600 (1112)
Void fractions				
Fuel	0.75	0.75	0.75	0.75
Sodium	0.22	0.22	0.22	0.22
Structure	0.03	0.03	0.03	0.03
Breeding characteristics				
Core conversion ratio	1.18	0.74	0.64	0.75
Total breeding ratio	1.93	1.60	1.34	1.60

[b] Low-alloy type.

Table A.1 (continued)

	Process-Heat-Production Reactor		Power-Production Reactor	
Breeding characteristics (continued)				
Fissile sales,[c] kg/day	2.52	1.88	1.03	1.87
Fuel yield, % per year	12.0	23.2	12.1	20.2
Doubling time, years (geometric)	5.75	3.0	5.70	3.4
Thermal and hydraulic data				
Turbine throttle steam condition				
Temperature, °C (°F)	168 (335)	243 (470)	447 (836)	367 (692)
Pressure, psi	110	173	2000	1450
Evaporator steam condition				
Temperature, °C (°F)	127 (260)	127 (260)		
Pressure, psi	35.4	35.4		
Net cycle efficiency, %	4.35[a]	7.35[a]	39.8	36.6
Reactor inlet temperature, °C (°F)	170 (338)	170 (338)	370 (698)	345 (653)
Reactor outlet temperature, °C (°F)	290 (554)	350 (662)	550 (1022)	525 (977)
Intermediate heat exchanger inlet temperature, °C (°F)	149 (300)	149 (300)	349 (660)	324 (615)
Intermediate heat exchanger outlet temperature, °C (°F)	238 (475)	297 (568)	497 (928)	473 (883)
Maximum fuel temperature, °C (°F)	350 (662)	650 (1200)	650 (1200)	650 (1200)
Number primary coolant loops	4	3	3	3
Number secondary coolant loops	4	3	3	3
Sodium flow per primary loop, gpm	98,000	83,000	91,300	91,000
Sodium flow per secondary loop, gpm	116,000	102,000	112,000	111,000
Primary loop pressure drop, psi	135	86	98	91
Nominal primary loop pumping power, hp per pump	7700	4300	5200	4800

[c] ^{233}U for the Th-^{233}U version, Pu for all others.

Table A.2. U-Pu-Fs Fueled Concept Reactor Physics Data

Average energy of fission neutrons, kev	374
Effective delayed neutron fraction	0.004
Isothermal temperature coefficient, $\delta k/°C$	-0.8×10^{-5}
Power loss coefficient at constant sodium inlet temperature, $\delta k/Mw(th)$	-3.0×10^{-7}
"Fuel depletion" reactivity loss, $\delta k/day$	8.3×10^{-5}
Reactivity change between operating temperature and fuel melting, δk	-0.0029
Reactivity change on sodium loss from core and axial blanket	0.0155
Maximum reactivity change on sodium loss from one core assembly	0.0009
Maximum reactivity worth of one core fuel assembly	0.00175
Worth of all control rods, δk	0.0236
Average worth per control rod, δk	0.001
Number of control rods	138
Control rod material	$^{10}B_4C$

after the xenon, krypton, and cesium are boiled off at 1300°C and the rare earths, strontium, and barium are separated from the melt by oxidation. The following seven elements remain with the fuel in the stated weight ratios:

	Weight Ratio
Molybdenum	42.1
Ruthenium	33.2
Technetium	15.8
Rhodium	6.0
Palladium	1.5
Zirconium	1.3
Niobium	0.1

These elements build up to an equilibrium concentration after repeated recastings.

Fissium has the same effect as pure molybdenum in slowing the rate of the gamma-to-alpha transition, and hence gamma stabilization is feasible. However, the irradiation tests on alloys containing plutonium were all carried out on a fuel initially composed of alpha crystals, and earlier tests without plutonium showed no improved performance for the gamma-quenched specimens in irradiation tests carried out below the gamma transition temperature. Thus the fissium alloys are alpha-phase fuels and behave typically; that is, they grow slowly at first, at a rate between 3 and 6 vol % per at. % burnup, and then catastrophically fail at a level of burnup that depends primarily on the irradiation temperature.

While unrestrained fissium alloy fuels have demonstrated only marginally acceptable properties as power reactor fuels because of their low-temperature capability and have been abandoned for that purpose by Argonne National Laboratory, they may be suitable for a process-heat-production reactor for the following reasons:

1. Irradiation test data are available for plutonium-containing fissium fuels. While these data emphasize the high-temperature high-burnup regime, where most of the specimens failed, and are somewhat deficient in the area of greatest interest (temperatures below 400°C and burnups below 1 at. %), it is nevertheless possible to interpolate an operating regime that incorporates the allowable burnup and temperature for plutonium-containing fissium fuels. In fact, this is the only fuel type for which such data exist (i.e., for unclad fuels with an initial plutonium loading).

2. The temperature capability of the fissium fuels is adequate for process-heat-production reactors.

3. The fissium fuel is well suited to the proposed concept. The proposed repeated recasting of the core material will, in fact, automatically yield the fissium composition. The equilibrium level is estimated to be approximately 10 wt %, a composition for which much test data exist.

Reports by Smith[3] and Horak[4] summarize the results of the U-Pu-Fs irradiation testing program at Argonne National Laboratory. Representative data from these reports are presented in Fig. A.1, where it may be

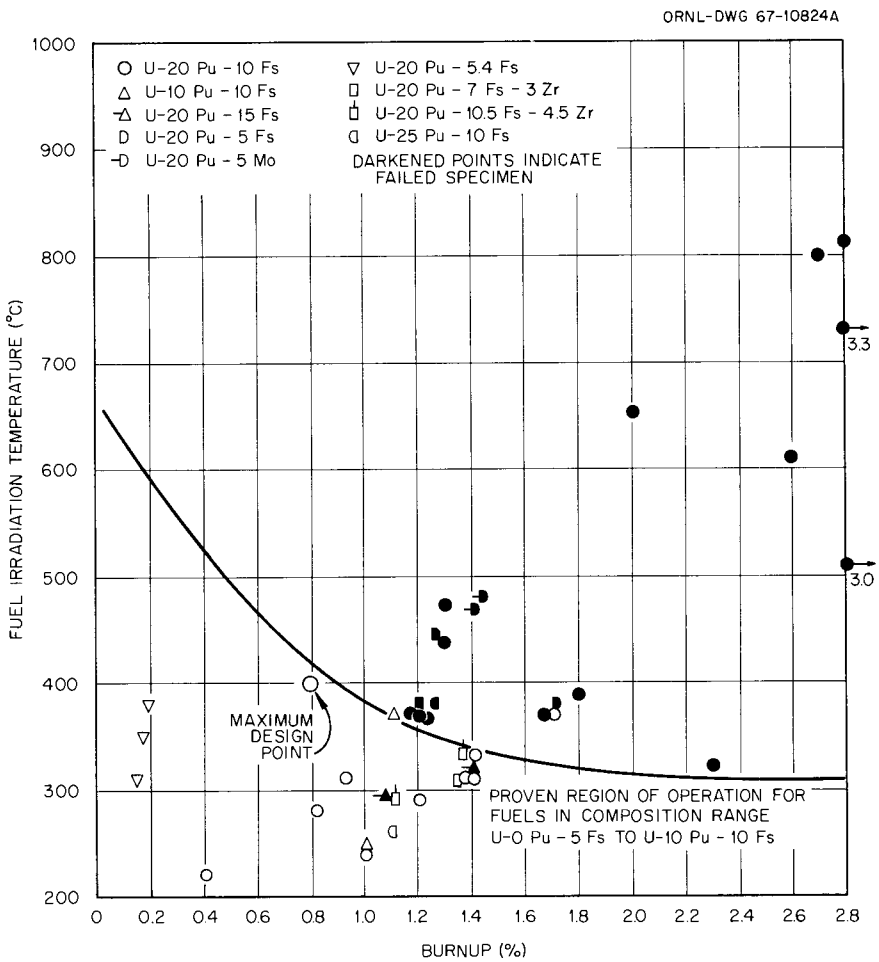

Fig. A.1. Summary of Data from U-Pu-Fs Alloy Irradiation Tests.

noted that the particular fuel composition is denoted by the shape of the data point. Failed specimens are indicated by darkened points. The open points indicate tests for which the specimen met the following criteria: (1) less than 10 vol % expansion and (2) a volume expansion rate of less than 10% per at. % burnup.

The allowable temperature-burnup operating regime is shown below the interpolated line separating the failed and unfailed specimens. The present design point for maximum burnup and fuel temperature is 0.8 at. % at 350°C and is shown to be within the allowable region. Note that most of the data points delineating the allowable operating regime are for fuels containing 20 wt % plutonium. The maximum plutonium concentration

expected is closer to 10 wt %, and such a composition should possess relatively better characteristics.

2.4 Fuel Cycle and Fabrication

The fuel-cycle calculations were made on an equilibrium basis, and in order to take advantage of existing calculational codes, certain simplifying assumptions were made. A simplified material flow diagram is shown in Fig. A.2. It was assumed that the feed and discharge of uranium and plutonium in the core and blanket were continuous and that the exposure was uniform. When the core fuel reached a cumulative burnup of 100 Mwd/kg, it would be sent to the processing plant after an average exposure of 2000 days, which corresponds to a fissile plutonium buildup of 2.5%. No provisions were made in the calculations for any removal of fission products during the repetitive core-fuel remelting operation, which if taken into account would result in improved nuclear performance.

As noted from Table A.1, the outstanding characteristic of the proposed reactor is the plutonium production, which is a direct consequence of eliminating the fuel cladding. The overall breeding ratio is 1.93 and

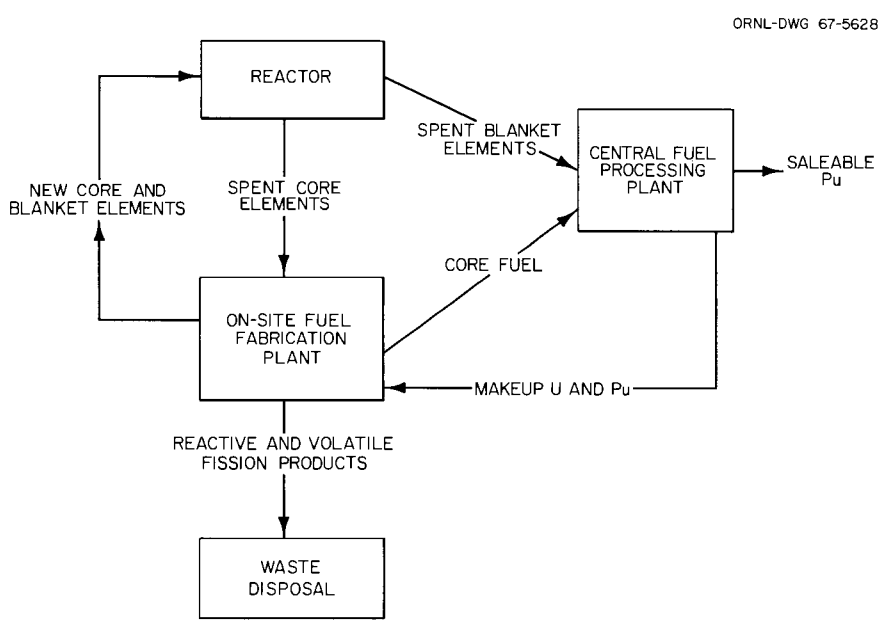

Fig. A.2. U-Pu-Fs Fuel-Cycle Flow Diagram.

the core region has a conversion ratio of 1.18. Calculations concerning initial startup with ^{235}U indicate that the initial loading would be all the fuel that would be required, since the system reactivity would increase steadily after startup.

The geometric form of the fuel slug is similar to that shown in Fig. 3.3. The preferred fabrication method is casting in either expendable graphite molds or permanent metallic molds. A major uncertainty is the compatibility of the mold with the alloy melt. Alternate fuel fabrication methods are discussed in Ref. 5.

The fuel fabrication facility was assumed to serve a desalting complex consisting of three 3500-Mw(th) reactors with an on-line factor of 0.9. With an average fuel exposure of 6.310 Mwd/kg, a fabrication rate of 1230 kg per calendar day would be required. Based on a fuel-slug height of 2 in. and a fuel density of 17.5 g/cm^3, about 308 fuel slugs per day would be fabricated and provided as recharge to the reactor. This corresponds to 18 fuel assemblies per day. Compensation for equipment downtime and fluctuations in the actual processing load was accommodated by operation of the facility on the basis of a five-day week. It was also estimated that a 10-day period was required from introduction of the spent fuel element to the refabrication facility until that fuel material was again available for either storage or recharge to the reactor. The refabrication process flowsheet is shown in Fig. A.3.

2.5 Steam System for U-Pu-Fs Fueled Concept

Thermal and hydraulic flow diagrams for the primary and secondary coolant loops and the steam generator—turbine system for the U-Pu-Fs fueled concept are shown in Figs. A.4 and A.5. The thermal output to the brine heater as 127°C (260°F) 35.4-psia process heat steam is 3300 Mw (11.25×10^9 Btu/hr) or 94% of the reactor thermal power. Selection of the dual-pressure steam cycle for the process-heat-production concepts enables significant improvement in the production of power by easing the pinch-point problem that arises in the single-pressure system steam generator. The system produces 152 Mw of power in excess of reactor plant auxiliary power requirements; this power excess would normally be adequate for evaporator and product-water pumping power needs.

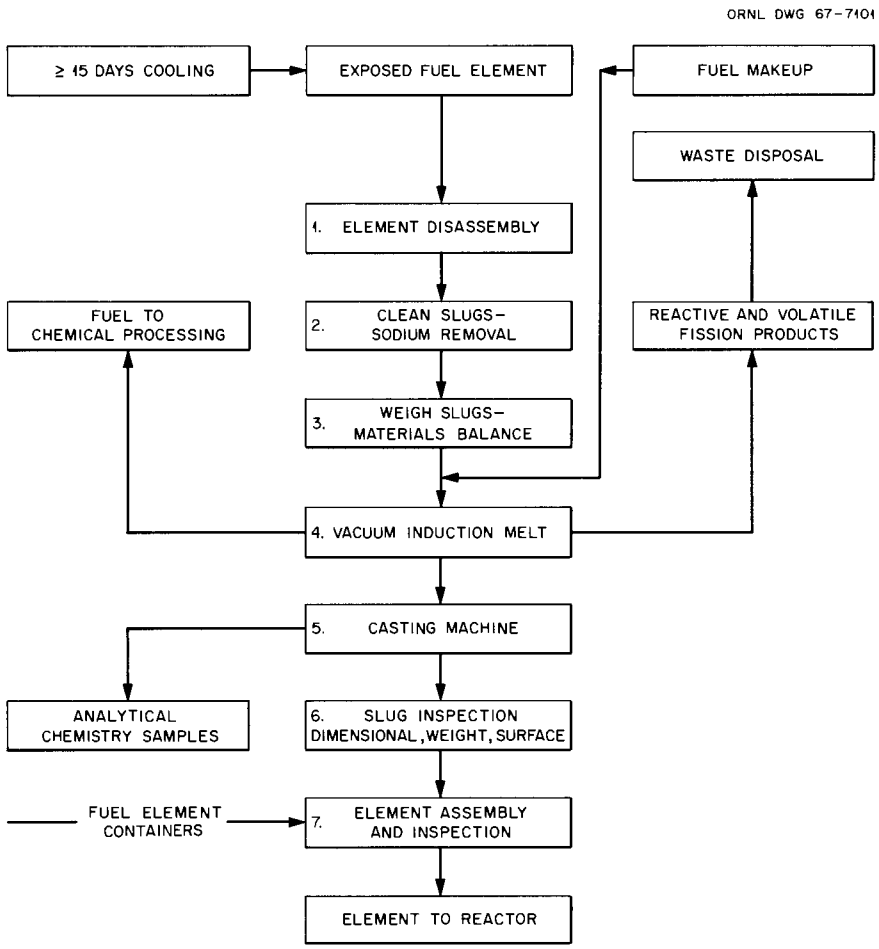

Fig. A.3. Fabrication Plant Flowsheet Based on Casting Machine Concept.

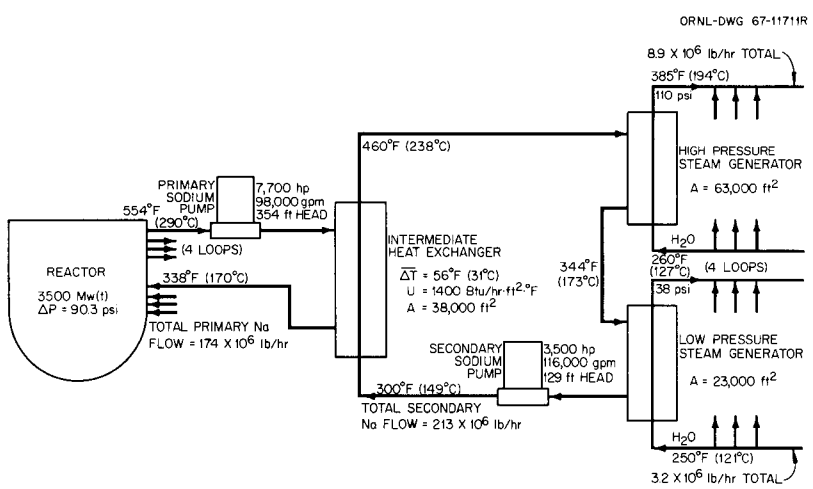

Fig. A.4. Flow Diagram of Primary and Secondary Coolant Loops of U-Pu-Fs Fueled Concept.

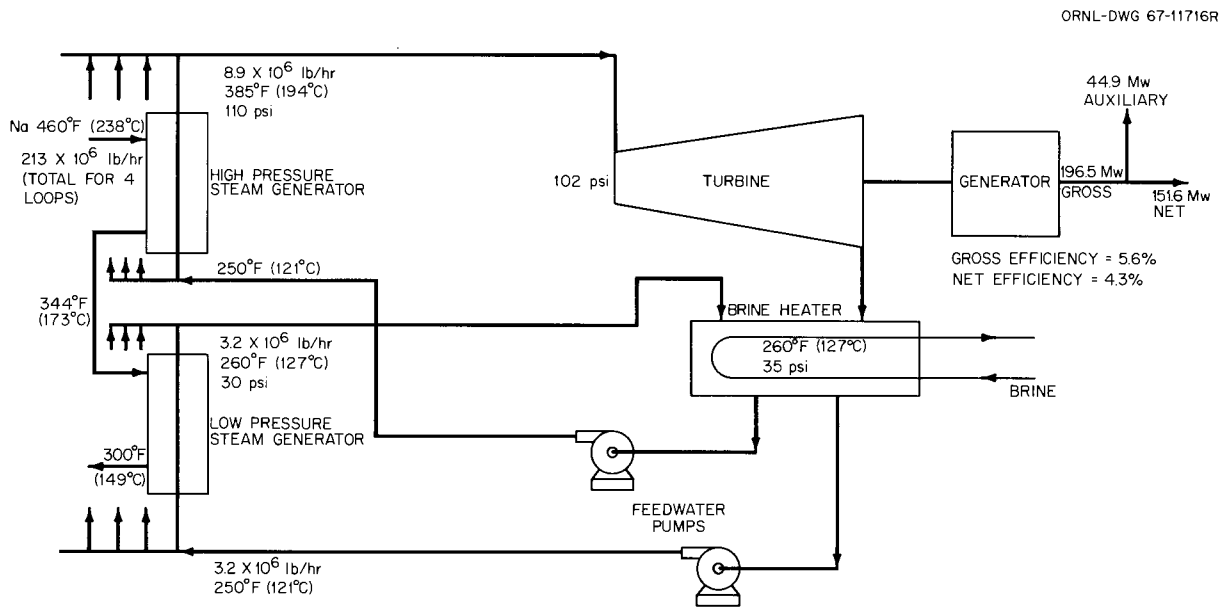

Fig. A.5. Steam Cycle for U-Pu-Fs Fueled Concept.

2.6 Summary Cost Data

Estimated fuel-cycle costs for the U-Pu-Fs fueled design, based on the unit fabrication and processing costs and other economic factors given in Table A.3, are presented in Table A.4. A summary of reactor annual and unit costs is given in Table A.5 for a 3500-Mw(th) capacity at a 0.9 plant factor. Detailed capital cost estimates are given in Appendix E, and operating costs are discussed in Section 9.5.

3. Unclad Th-^{233}U Fueled Reactor Characteristics

Salient reactor characteristics for the unclad Th-^{233}U fueled concept of the fast breeder reactor are presented in Table A.1. The thorium blankets give the Th-^{233}U system a thermal efficiency capability comparable to that for ceramic-fueled FBR's and higher than that for the corresponding mixed-cycle concept, which is limited by a uranium blanket temperature capability. Data on the Th-^{233}U system are presented for a high-temperature reactor designed for power production; however, it could also be suitably designed for process-heat production. For the present case the maximum fuel temperature is limited to 650°C to take advantage

Table A.3. Economic Factors for the U-Pu-Fs and Th-^{233}U Fueled Concepts

	U-Pu-Fs Fueled Reactor	Th-^{233}U Fueled Reactor
Value of fissile Pu, $/g	9.30	
Value of ^{233}Pa and ^{233}U, $/g		16.75[a]
Value ^{235}U, $/g	11.17	11.17
Cost of depleted uranium, $/kg	3.08	
Cost of thorium as ThO_2, $/lb		5
Fixed charge rate on fuel inventory, % per year		
Public ownership	5	5
Private ownership	NU[b]	NU
Fixed charge rate on off-site central processing plant, %	22	NU
Fixed charge rate for on-site plant capital,[c] % per year		
Public ownership	7	7
Private ownership	NU	NU
Reactor plant factor	0.9	0.9
Refueling method	Continuous, on line	Continuous, on line
Total losses, % per reprocessing pass	1.2	1.2
Time for off-site chemical processing, days	180	NU
Time for on-site chemical processing, days	NU	45
Time for on-site refabrication, days	30	30
Assumed capacity of off-site fuel processing plant, MT/day	10	NU
Thermal capacity served by on-site reprocessing and fabrication plants (three-reactor complex), Mw	10,500	10,500
On-site fabrication throughput, kg per calendar day		
Core	1230	250
Blankets		208
Fabrication charges, $/kg		
Core	8.38	23.74
Blanket	5.23	5.23
Processing charges, $/kg	18.60	35.50
Shipping charges, $/kg		
Core	14.00	
Blankets	3.00	

[a]Applicable to a thermal reactor economy.

[b]Not used.

[c]An additional separate allowance for interim replacements was included for the on-site fuel fabrication facilities.

Table A.4. U-Pu-Fs Fuel-Cycle Cost

Cost Component	Unit Cost (¢/MBtu)
Inventory	3.8
Metal preparation, processing, and shipping	1.5
Fabrication	1.6
Plutonium credit	(9.1)[a]
Net fuel-cycle cost	(2.2)

[a]Parentheses denote gain.

Table A.5. Summary of U-Pu-Fs Fueled Reactor Costs

Annual production	
127°C (260°F) steam, MBtu	89.0×10^6
Gross power	
kwh(e)	1.55×10^9
Mw(e)	197
Net power	
kwh(e)	1.20×10^9
Mw(e)	152
Investment, $ millions	
Nuclear island	128.3
Turbine island	22.7
Total	151.0
Annual costs, nuclear island, $ millions	
Capital, at 7% per year	8.98
Operating and maintenance	1.23
Fuel	(2.08)[a]
Insurance	0.24
Total	8.37
Annual costs, turbine island, $ millions	
Capital, at 7% per year	1.59
Operating and maintenance	0.11
Total	1.70
Annual credit[b] for surplus power production, $ millions	(1.62)
Total annual cost, $ millions	8.45
Cost of 127°C (260°F) steam, ¢/MBtu	9.5

[a]Parentheses denote gain.

[b]1.2×10^9 kwhr per year at 1.35 mills/kwhr; 1.35 mills/kwhr is the approximate incremental cost of on-site power production.

of the lower growth rates at lower irradiation temperatures; even so, the calculated gross thermal efficiency is 41.5%.

Costs and physics characteristics were calculated for continuous on-line refueling, so no control poison was considered in the calculations. The effect of shim control was not estimated for this thorium-fueled alternative.

In the equilibrium fuel cycle the core fuel is reprocessed when a burnup equivalent to 100 Mwd/kg is reached. The average enrichment of the blanket discharge material is 2.4% for the radial blanket and 3.1% for the axial blanket. It was assumed that the uranium processed from the core and blankets would be mixed. The feed to the core needed to maintain criticality would be taken from this mixture and the remaining uranium would be sold. Thorium would be used as makeup feed to both core and blankets.

The estimated fuel-cycle costs are given in Table A.6. These calculated costs were based on the various unit costs and other economic data given in Table A.3. A summary of reactor annual and unit costs is given in Table A.7 for a 3500-Mw(th) capacity at a 0.9 plant factor. Detailed capital cost estimates are given in Appendix E and operating costs are discussed in Section 9.5.

Thermal and hydraulic flow diagrams for the primary and secondary coolant loops and the steam generator—turbine system are shown in Figs. A.6 and A.7.

Table A.6. Th-^{233}U Fuel-Cycle Cost

Cost Component	Unit Cost	
	¢/MBtu	Mills/kwh(e) (net)
Inventory	2.8	0.24
Processing	1.3	0.11
Fabrication	0.9	0.08
^{233}U credit	(6.6)[a]	(0.57)
Net fuel-cycle cost	(1.6)	(0.14)

[a]Parentheses denote gain.

Table A.7. Summary of Th-^{233}U Reactor Costs

Annual productions	
Prime steam, MBtu	94.2×10^6
Gross power	
kwh(e)	11.4×10^9
Mw(e)	1451
Net power	
kwh(e)	11.0×10^9
Mw(e)	1394
Investment, $ millions	
Nuclear island	109.1
Turbine island	63.2
Total	172.3
Annual costs, nuclear island, $ millions	
Capital, at 7% per year	7.64
Operating and maintenance	1.23
Fuel	(1.51)
Insurance	0.24
Total	7.60
Annual costs, turbine island, $ millions	
Capital, at 7% per year	4.42
Operating and maintenance	0.59
Total	5.01
Total annual cost, complete plant, $ millions	12.61
Unit costs	
Prime steam, ¢/MBtu	8.1
Power, mills/kwh(e)	1.1

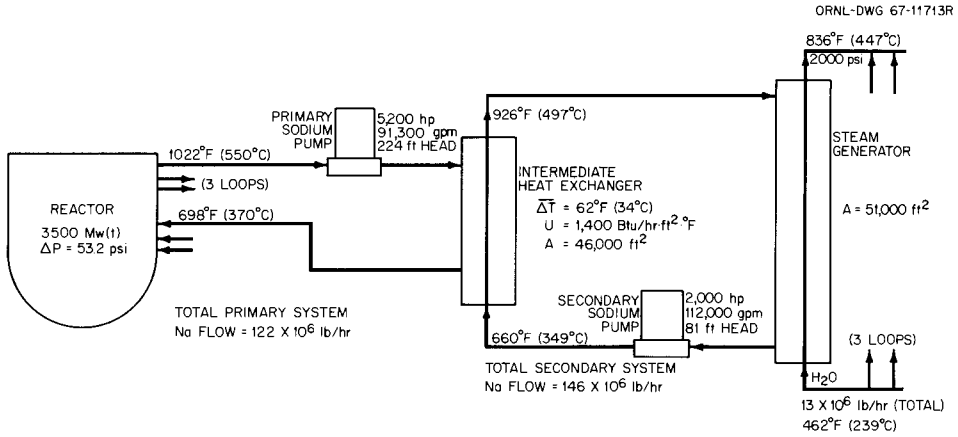

Fig. A.6. Flow Diagram of Primary and Secondary Coolant Loops of Th-^{233}U Fueled Reactor.

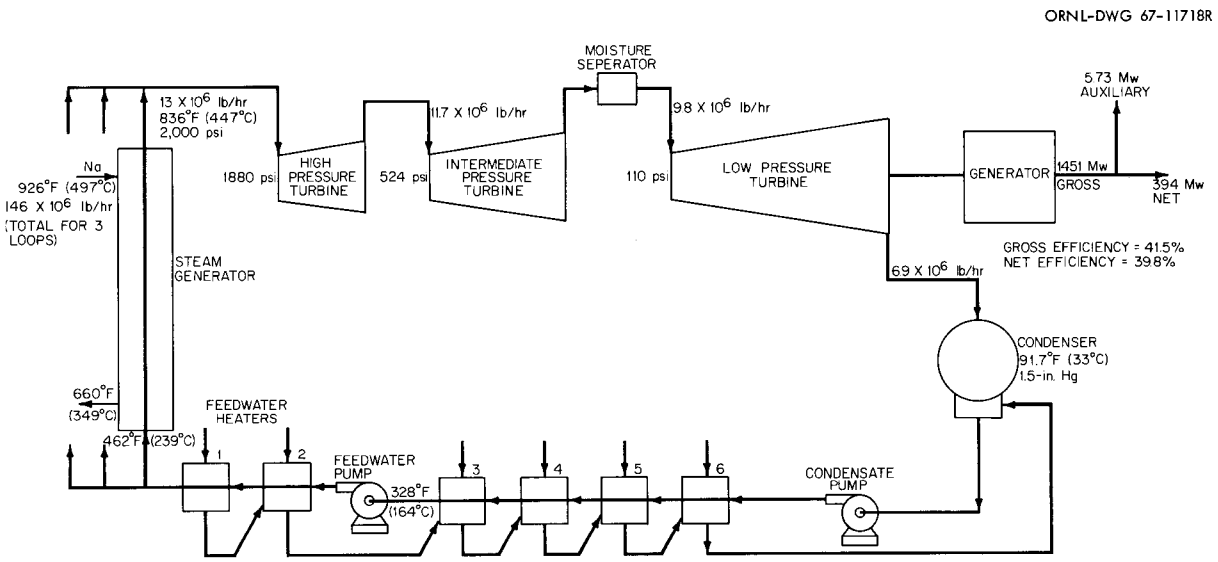

Fig. A.7. Steam Cycle for Th-^{233}U Fueled Reactor.

References

1. L. Burris, Jr., I. G. Dillon, and R. K. Steunenberg, The EBR-II Skull Reclamation Process — Part I. General Process Description and Performance, USAEC Report ANL-6818, Argonne National Laboratory, January 1964.

2. G. A. Bennett et al., Halide Slagging of U-Pu Alloys, USAEC Report ANL-6918, Argonne National Laboratory, July 1964.

3. K. F. Smith and L. R. Kelman, Irradiation of Cast Uranium-Plutonium Base Alloys, USAEC Report ANL-5677, Argonne National Laboratory, 1957.

4. J. A. Horak, J. H. Kittel and R. J. Dunworth, The Effects of Irradiation on Uranium-Plutonium-Fissium Alloys, USAEC Report ANL-6429, Argonne National Laboratory, 1962.

5. R. P. Hammond et al., A Preliminary Study of a Low-Temperature Fast Breeder Reactor for Desalting Applications, internal memorandum, Oak Ridge National Laboratory, December 1967.

Appendix B

FUEL ELEMENT REFABRICATION COST STUDY

1. Core Fuel Elements

The operations and costs considered for refabrication of the mixed-cycle fuel (Th-U-Pu) elements for both the dual-purpose and power concepts of the reference system are based upon the parameters listed in Table B.1. It was assumed in selecting the refabrication method that the fuel could be hydrided and dehydrided remotely. If further work proved this assumption to be invalid, a reprocessing stage might be required before refabrication.

Table B.1. Basis for Estimating Fuel Refabrication Cost

	Process-Heat-Production Reactor		Power-Production Reactor	
	Case I	Case II	Case III	Case IV
Reactor thermal power, Mw	3,500	10,000	3,500	10,000
Number of reactors per site	3	3	3	3
Average fuel burnup prior to refabrication, Mwd/kg	33	33	33	33
Number of fuel elements refabricated per operating day	9	26	11	30
Number of fuel channels per element	127	127	169	169
Weight of fuel channel, g	299.7	299.7	204.5	204.5
Weight of fuel element, kg	38.07	38.07	34.56	34.56
Refabrication rate per operating day, kg	342.6	989.8	380.2	1036.8
Fuel element core life, calendar days	127	127	167	167
Number of fuel elements per core	249	712	376	1085

1.1 Refabrication Facility

Since the exposed fuel is introduced to the refabrication facility after only a 15-day cooling time, a remote refabrication facility is required. It is assumed that a thickness of 5 ft of normal concrete will provide adequate shielding for operating personnel. In addition, the nature of the fuel and the refabrication process require inert-gas atmospheres in the refabrication cells.

Compensation for equipment downtime and fluctuations in processing load is accommodated by sizing the facility to operate on a single-shift five-day-per-week basis.

1.2 Refabrication Method

The refabrication process assumed is shown in Fig. B.1. When a fuel element enters the refabrication facility it is disassembled. The top and bottom portions of the assembly are salvaged for reuse, and the center section is discarded. Because they receive very little irradiation, it is assumed that the top and bottom portions of the assembly can be used for ten refabrication cycles.

The fuel is removed from the fuel container, cleaned, and weighed to provide a materials-accountability balance. The upper and lower axial blankets are put in temporary storage until they are replaced in a new fuel assembly. The axial blanket elements in the process-heat-production reactor experience four core fuel refabrication cycles before they are reprocessed. Those in the power-production reactor undergo three such cycles before they are reprocessed.

The charge to the hydriding furnaces includes the discharged fuel element plus reject material and process scrap. After hydriding and then dehydriding, the material is milled to size and classified. The portion that is acceptable is blended with makeup fuel and the remainder recycled. The blended fuel is mixed with a binder and extruded into fuel channels. The channels are then lightly sintered, sized, and inspected. Acceptable channels are assembled into elements and given a final sinter. After further inspection, the elements are cut to length and reassembled into the fuel element containers. The fuel element assembly is shown in Fig. 3.4.

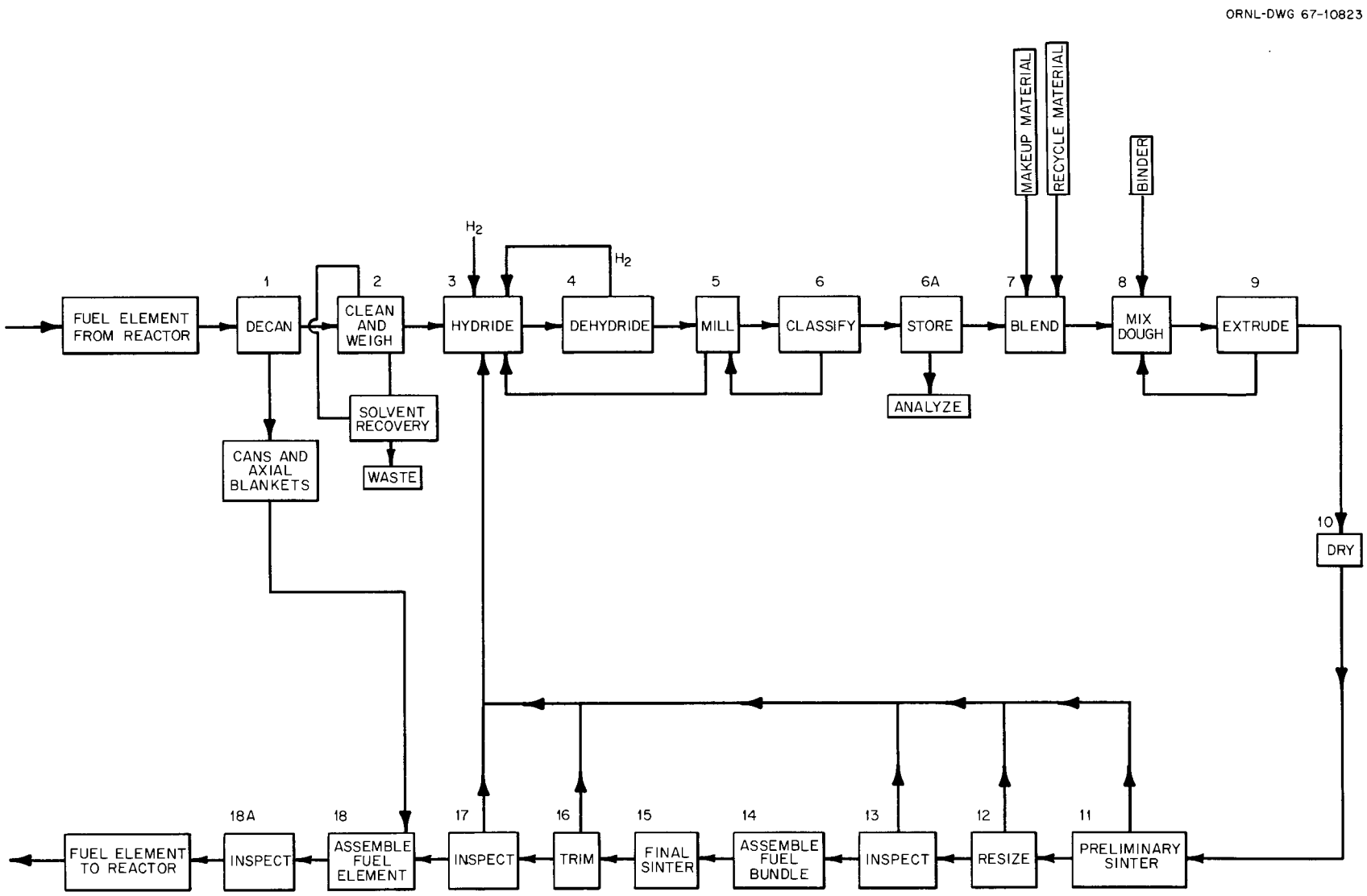

Fig. B.1. Mixed-Cycle Fuel Refabrication Process Flow Diagram.

The inspection of channels was considered to be performed primarily with gages, insofar as possible. It may be feasible to perform simultaneous inspection for hole dimensions, web thickness, and porosity, but determination of the presence of inclusions might be somewhat more difficult and less certain due to the problems involved in detecting foreign material that is fairly well bonded with the base material.

1.3 Refabrication Cost Factors

1.3.1 Equipment Cost. Estimates of the equipment and manpower requirements for refabrication are presented in Table B.2. The process step numbers in this table are the same as the process step numbers on the fabrication flowsheet in Fig. B.1. The fabrication unit that controls the equipment requirements and cost of each step is given in column 3. For example, the number of kilograms to be processed through the hydriding operation would essentially determine the size and cost of the items of equipment for this process step, and there would be little or no effect of the shape subsequently processed. For the purposes of this study, factors other than the primary controlling unit have not been considered.

Estimations of equipment capital costs were difficult because the process requires equipment that is not readily available from commercial suppliers. The estimates were also complicated by the conceptual nature of the process. The values given represent best estimates of the costs that would be incurred to purchase the pieces of equipment required to perform the specified operations. These estimated costs are the prices that would be charged by commercial equipment suppliers to provide the basic pieces of equipment. Estimates for the remaining items of equipment are based on estimates previously used for costs of fuel fabrication with similar equipment items.[1]

1.3.2 Capital Cost. In previous economic studies at ORNL of fuel element fabrication costs, certain relationships between the cost of the basic equipment and the total capital investment in a fuel fabrication facility were developed.[2] These relationships and the conversion of the equipment cost to total cost are illustrated in Table B.3. The basic equipment cost is the purhcase price from a commercial supplier for installation in a normal open-shop facility.

Table B.2. Estimated Manpower and Equipment Requirements for Powder-Metallurgy Refabrication of Th-U-Pu Fuel Elements

Step	Operation	Controlling Fabrication Unit	Operator Manpower (man-hr/day)				Equipment		Total Equipment Cost (thousands of dollars)			
			Case I	Case II	Case III	Case IV	Type	Unit Cost (thousands of dollars)	Case I	Case II	Case III	Case IV
1	Decan element	Element	24	40	24	40		20	20	40	20	40
2	Clean and weigh	Element	8	16	8	16	Ultrasonic bath and electronic scale	55	55	110	55	110
3	Hydride	Critical mass					Multiple tunnel furnaces	10	90	260	110	300
4	Dehydride	Critical mass	24	40	32	56	Multiple retorts	10	90	260	110	300
5	Mill	Critical mass					Fluid energy mills	25	225	650	275	750
6	Classify	Critical mass					Classifiers	15	135	390	165	450
7	Blend	Critical mass	16	24	16	24	Mixer	20	60	180	80	200
8	Mix	Critical mass					Mixer					
9	Extrude	Fuel channel	24	40	24	40	Extrusion press	120	120	240	120	360
10	Dry	Fuel channel					Oven	50	150	450	200	500
11	Sinter	Fuel channel	16	24	16	24	Furnace					
12	Resize	Fuel channel	16	24	16	24	Sizing mill	50	100	200	100	250
13	Preliminary inspection	Fuel channel	24	40	24	40	Gages	50	50	100	50	100
14	Assembly	Element	16	40	16	40	Fixture	50	50	100	50	100
15	Final sintering	Element					Furnace	50	100	200	100	250
16	Cut to length	Element	8	16	8	16	Cut-off saw	25	25	50	25	50
17	Final inspection	Element	24	40	24	40	Gages	50	50	100	50	100
18	Fuel element assembly and inspection	Element	16	40	16	40	Fixture	50	50	100	50	100
		Total	216	384	224	400			1370	3430	1560	3960

Table B.3. Conversion of Basic Equipment Cost to Capital Investment in the Fuel Refabrication Facility

Cost Item	Cost Multiplier Factor		Capital Cost (thousands of dollars)							
			Case I		Case II		Case III		Case IV	
	First Plant	Subsequent Plants	First Plant	Subsequent Plants	First Plant	Subsequent Plants	First Plant	Subsequent Plants	First Plant	Subsequent Plants
Basic equipment	1.0	1.0	1,370	1,370	3,430	3,430	1,560	1,560	3,960	3,960
Remote equipment	1.625	1.625	2,226.25	2,226.25	5,573.75	5,573.75	2,535.0	2,535.0	6,435.0	6,435.0
Installation	0.31	0.31	424.70	424.70	1,063.30	1,063.30	483.6	483.6	1,227.6	1,227.6
Instrumentation	0.275	0.275	376.75	376.75	943.25	943.25	429.0	429.0	1,089.0	1,089.0
Design	1.275	0.2	1,746.75	274	4,373.25	686	1,989	312	5,049	792
Laboratory	0.17	0.17	232.9	232.9	583.1	583.1	265.2	265.2	673.2	673.2
Building	2.15	2.15	2,945.5	2,945.5	7,374.5	7,374.5	3,354	3,354	8,514.0	8,514.0
Design	0.48	0.1	657.6	137	1,646.4	343	748.8	156	1,900.8	396
Contingency	1.25	1.25	1,712.5	1,712.5	4,287.5	4,287.5	1,950	1,950	4,950	4,950
Preliminary operation	2.50	1.0	3,425	1,370	8,575	3,430	3,900	1,560	9,900	3,960
Total	10.035	7.08	13,750	9,700	34,420	24,280	15,650	11,040	39,740	28,040

For the first plant of its kind (see first column under Cost Multiplier Factor in Table B.3), installation of the equipment and instrumentation were estimated to add 31 and 27.5%, respectively, to the basic equipment costs. Since the equipment would be utilized in a very specialized and unusual application, an engineering design factor of 1.275 was used to provide the desired operational performance of the equipment and to solve the interface problems when matching this equipment in a process line. Supporting laboratory equipment was estimated to be 16% of the basic equipment cost.

Since the building would be a heavily shielded facility, building costs were estimated at 215% of the basic equipment cost. The design and supervision of the building construction were estimated at 48% of the basic building cost. A contingency factor of 20% of the sum of the preceding costs was included.

A "prior-to-operation" cost factor of 33% of all preceding costs was then added in this estimate. This was based on the assumption that a substantial number of professional people, craftsmen, and skilled operators would be required in the initial shakedown operations of the facility. It was assumed that no useful product would be produced during this preliminary period. This time would be utilized in defining and solving the practical problems of getting the individual items of equipment to perform, as well as in integrating each item of equipment into the overall process scheme.

The second column under Cost Multiplier Factor in Table B.3 contains multipliers for subsequent plants constructed to the same basic design. Because the design would be essentially the same, the design factors for the remote equipment were reduced, and the preliminary operation factor was decreased to compensate for the experience gained from operation of prior similar plants. The total capital cost estimate was capitalized and depreciated over an anticipated 30-year life of the facility.

1.3.3 Manpower Requirements. The estimated operator man-hours per day are given in Table B.2. The basis adopted for estimation of operator requirements was the man-hours required per day to perform the required process operations. The operator efficiency in a remote facility was assumed to be lower than normal. These man-hours were therefore divided

by 0.8 to arrive at the manpower allocations at any specific time. Also, since approximately 10% of the worker's year would be consumed by vacation, sick leave, and personal absence, the number of operators was increased by 10% to compensate for these absences. The assigned manpower breakdown is shown in detail in Table B.4.

1.3.4 Annual Operating Cost. Table B.5 illustrates the estimated annual operating costs for this concept. The utilities are assumed to be derived from the reactor complex, and the remaining costs are based on reasonable judgment and prior studies of similar operations.

1.3.5 Cost of Expendable Materials. The major expendable items, as shown in Table B.6, are the fuel containers. The cost for the end pieces, which are exposed to little radiation, was estimated to be $150, and the cost for the center section, which is exposed to a high neutron flux was estimated to be $50. It was assumed that the center section would be disposed of at each refabrication cycle, while the top and bottom pieces would be reused ten times each. This assumption implies both a reasonable compatibility between the end pieces and their sodium environment and a method of joining the reused end pieces to a replacement center section. Both these implications warrant further study.

The costs of the remaining expendable items are very rough estimates. The values, however, are insignificant with respect to the major cost items, so no further investigation of more accurate costs is deemed necessary at this time.

1.3.6 Summary of Costs. A summary of the costs estimated for fuel refabrication for the second and subsequent plants is given in Table B.6. The capital charges are calculated at annual rates of 7 and 12%. In addition to the normal interim replacement allowance of 0.35% included in the capital charge rate, a special allowance of 0.65% was made to provide replacement of the fabricating equipment on an eight-year cycle. The operating costs were based upon the assumption that certain staff employees (i.e. doctors, nurses, etc.) were shared with the reprocessing facility and reactor complex.

Table B.4. Fuel Fabrication Facility Manpower Requirements and Annual Costs[a]

	Annual Cost			
	Case I	Case II	Case III	Case IV
Plant Manager	$ 25,000	$ 25,000	$ 25,000	$ 25,000
Secretary	7,200	7,200	7,200	7,200
Engineering Manager	10,000	10,000	10,000	10,000
Quality Control Manager	10,000	10,000	10,000	10,000
Services Manager	9,000	9,000	9,000	9,000
Secretary	6,000	6,000	6,000	6,000
Shift Foremen at $13,000/year	26,000	39,000	26,000	39,000
Area Leaders at $9,000/year	27,000	45,000	27,000	45,000
Operators at $7,000/year	231,000	336,000	238,000	350,000
Plant Engineers				
At $15,000/year	15,000	15,000	15,000	15,000
At $12,000/year	12,000	12,000	12,000	12,000
At $8,000/year	8,000	16,000	8,000	16,000
Quality Control Engineer	15,000	15,000	15,000	15,000
Nondestructive Testing Engineer	15,000	15,000	15,000	15,000
Technicians at $7,000/year	14,000	28,000	14,000	28,000
Statisticians at $8,000/year	8,000	16,000	8,000	16,000
Metallurgy Laboratory				
Supervisor	12,000	12,000	12,000	12,000
Technicians at $7,000/year	14,000	28,000	14,000	28,000
Chemistry Laboratory				
Technicians at $7,000/year	14,000	28,000	14,000	28,000
Spectrographic Laboratory				
Technicians at $7,000/year	14,000	28,000	14,000	28,000
Health Physics				
Engineer at $13,000/year	13,000	13,000	13,000	13,000
Technicians at $6,500/year	13,000	26,000	13,000	26,000
Accountability Section				
Engineer at $13,000/year	13,000	13,000	13,000	13,000
Technicians at $7,000/year	14,000	28,000	14,000	28,000
Personnel Section				
Area Supervisor at $10,000/year	2,500	5,000	2,500	5,000
Clerk at $5,000/year	2,500	5,000	2,500	5,000
Typist (pool) at $4,000/year	1,000	2,000	1,000	2,000

[a]It is assumed that an on-site reprocessing plant also services the three-reactor complex. Certain staff personnel expenses are divided between the reprocessing plant and the refabrication facility.

Table B.4 (continued)

	Annual Cost			
	Case I	Case II	Case III	Case IV
Security Section				
Area Supervisor	$ 7,000	$ 7,000	$ 7,000	$ 7,000
Guards at $5,000/year	20,000	20,000	20,000	20,000
Medical Section				
Doctor at $30,000/year	7,500	15,000	7,500	15,000
Nurses at $5,000/year	10,000	15,000	10,000	15,000
Purchasing Section				
Clerk at $5,000/year	1,250	2,500	1,250	2,500
Maintenance Section				
Foremen at $11,000/year	11,000	22,000	22,000	11,000
Welder, Pipefitter, Electrician, Instrument Mechanics, Janitors, General Repairman, Materials Handler at $8,000 av	72,000	128,000	72,000	128,000
Subtotal	$679,950	$1,001,700	$686,950	$1,015,700
Fringe benefits at 20%	135,990	200,340	137,390	203,140
Upper management overhead burden at 10%	67,995	100,170	68,695	101,570
Total Payroll Costs	$883,935	$1,302,210	$893,035	$1,320,410

2. Blanket Fuel Elements

A previous study[3] indicated that the cost for on-site refabrication of an exposed U-Pu-Fs fuel element would be $6.64/kg. The following estimate for central facility fabrication of depleted-uranium blanket fuel elements is a modification of that study.

The following assumptions were made:

1. The blanket fuel would be depleted uranium.

2. The depleted uranium would be either virgin or decontaminated material from a reprocessing plant.

3. The cross-sectional dimensions of the fuel would be limited by fabrication techniques or in-reactor handling equipment, not by reactivity considerations.

Table B.5. Fuel Refabrication Facility Estimated Annual Operating Costs

	Annual Cost			
	Case I	Case II	Case II	Case IV
Payroll	$ 883,900	$1,302,200	$ 893,000	$1,320,400
Utilities				
Electricity, 2.8 Mw at $2.00/Mwhr	40,000	108,000	40,000	108,000
Steam	20,000	54,000	20,000	54,000
Water	20,000	54,000	20,000	54,000
Telephone, TWX	20,000	40,000	20,000	40,000
	$ 100,000	$ 256,000	$ 100,000	$ 256,000
Supplies				
Maintenance, 1% of capital	97,000	242,000	110,400	280,400
Regulated clothing	20,000	35,700	20,000	35,700
Laboratory supplies	30,000	85,700	30,000	85,700
Office and miscellaneous	70,000	100,000	70,000	100,000
	$ 217,000	$ 464,200	$ 230,400	$ 501,800
Travel and consultants	30,000	30,000	30,000	30,000
Liability insurance, 1/2% of payroll	4,400	6,500	4,500	6,600
Data processing equipment rental (computer time, three remote stations, ten calculators)	20,000	40,000	20,000	40,000
Contract analytical work	50,000	140,000	50,000	140,000
Contract maintenance, 1/2% of capital	49,200	121,400	54,500	143,700
Subtotal	$1,354,500	$2,360,300	$1,382,400	$2,438,500
Contingency, 10% for estimate of conceptual process	135,000	236,000	138,000	244,000
Total	$1,489,500	$2,596,300	$1,520,400	$2,682,500

Table B.6. Summary of Core Fuel Refabrication Costs

	Cost ($/kg)							
	Case I		Case II		Case III		Case IV	
	Public Financing	Private Financing	Public Financing	Private Financing	Public Financing	Private Financing	Public Financing	Private Financing
Capital charge:[a]								
$\frac{\text{Capital investment} \times \text{Annual capital charge rate}}{\text{Throughput (kg/day)} \times 260 \text{ days/year}}$	7.62	13.07	6.60	11.32	7.73	13.41	7.28	12.48
Operating costs:								
$\frac{\text{Annual operating cost}}{\text{Throughput (kg/day)} \times 260 \text{ days/year}}$	16.72	16.72	10.09	10.09	15.38	15.38	9.95	9.95
Special equipment interim replacement allowance (eight-year cycle):[b]								
$\frac{\text{Capital investment} \times 0.65\%}{\text{Throughput (kg/day)} \times 260 \text{ days/year}}$	0.71	0.71	0.61	0.61	0.72	0.72	0.68	0.68
Expendable materials								
Fuel container	1.71	1.71	1.71	1.71	1.88	1.88	1.88	1.88
Cleaning fluids	0.01	0.01	0.01	0.01	0.01	0.01	0.01	0.01
Hydrogen	0.10	0.10	0.10	0.10	0.10	0.10	0.10	0.10
Extrusion binder	0.10	0.10	0.10	0.10	0.10	0.10	0.10	0.10
Total	26.97	32.42	19.22	23.94	25.92	31.60	20.00	25.20

[a]Annual capital charge rate:

7% for public financing
12% for private financing

[b]An additional 0.35% for interim equipment replacement is included in capital charge rate.

4. The fabrication technique would consist of melting and casting fuel slugs.

5. The fabrication plant would be a contact plant, involving neither hoods, glove boxes, nor shielding.

6. The plant would be a large central facility serving a large nuclear industry.

7. The plant would be unipurpose.

For a plant of the same capacity as that described in the previous study[3] (i.e., approximately 2000 kg per operating day) the capital investment shown in Table B.7 was assumed.

In the same manner, the manpower requirements were reviewed, and because of the reduced complexity of the operation, the annual operating costs were reduced from $2,067,000 to $1,700,000.

The expendable materials were assumed to remain the same, since the molds, crucibles, and element containers would all be required for this plant.

Table B.7. Conversion of Basic Equipment Cost to Capital Investment for a Central Blanket Fuel Element Fabrication Facility

Item	Multiplier Factor	Cost
Basic equipment	1	$1,122,000[a]
Installation	0.20	224,000
Instrumentation	0.15	168,000
Building	1.00	1,122,000
Building design	0.45	505,000
Laboratory equipment	0.10	112,000
Contingency	0.10	112,000
Preliminary operation	1.00	1,122,000
Total	3.00	~$3,400,000

[a]From Ref. 3.

The following blanket fuel element costs were obtained:

	Cost ($/kg U)
$\frac{\text{Capital investment} \times 0.22^*}{2000 \text{ kg} \times 260 \text{ days}}$	$1.27
$\frac{\text{Operating cost}}{2000 \text{ kg} \times 260 \text{ days}}$	3.26
Expendable materials	0.70
Total	$5.23

*A 22% capital charge rate was assumed for a privately financed plant.

References

1. T. N. Washburn and A. L. Lotts, FABCØST — A Computer Code for Estimating Fuel Fabrication Costs, unpublished internal document, ORNL.

2. M. W. Rosenthal, A Comparative Evaluation of Advanced Converters, USAEC Report ORNL-3686, Oak Ridge National Laboratory, January 1965.

3. Memo to T. D. Anderson, ORNL, from A. Goldman, ORNL, June 29, 1967.

Appendix C

PRELIMINARY ESTIMATES OF FUEL PREPARATION AND REPROCESSING COSTS FOR EVALUATION OF Th-U-Pu METAL-FUELED FAST BREEDER REACTOR

These estimates are based on the following throughput rates per 3500-Mw(th) reactor:

	Throughput (MT/year)
Core fuel	
Recasting	28.0
Reprocessing	9.35
Blanket fuel	
Recasting	101.0
Reprocessing	36.9

Two different bases for cost estimating were used: (1) off-site aqueous reprocessing and reconversion to metal and (2) on-site pyrochemical (salt transport) reprocessing and reconversion to metal, with the on-site plant serving three 3500-Mw(th) reactors. The reference off-site reprocessing plant was assumed to have a nominal capacity of 10 MT/day for BWR-PWR fuels or 6 MT/day for standard FBR fuel (mixed core and blanket). The reference fuel is nonstandard in that the core and blanket cannot be mixed. The reference fuel preparation (conversion) plant was assumed to service 75,000-Mw(th) capacity of reference reactors and to convert recycle enriched uranium-plutonium nitrates, virgin thorium nitrate, and depleted UF_6 to metal for return to the recasting operation.

The cost estimates for off-site conversion and aqueous reprocessing were based on current evaluations of the AEC civilian nuclear power program. They are similar to but not exactly the same as previous estimates for ORNL desalination-reactor evaluations, since they represent some updating and normalization. They are based on a reference value of 22% per year for the fixed-charge rate on capital investment.

The on-site estimates for pyrochemical reprocessing and reconversion are based on extrapolation and/or interpolation of 1966–67 Argonne National Laboratory estimates for U-Pu FBR fuels. It was assumed that the

costs for U-Pu-Th core fuel would be the same as for U-Pu core fuel. The U-Pu blanket fuel is no problem, since it is very similar to the fuel ANL assumed. As in the off-site case, the core and blanket must be processed separately. The on-site estimates are based on public ownership, with a 7+%/year fixed-charge rate; the "plus" represents a higher interim-replacement allowance than for the reactor. The ANL cost estimates used 15+%, based on private utility ownership.

1. Off-Site Fuel Preparation

The fuel preparation (conversion) cost estimates are based on those made earlier and their recent updating and normalization. For a metal-preparation plant serving a 75,000-Mw(th) industry of the reference reactor type, the throughput rates are as follows:

	Throughput (MT/year)
Core U-Pu-Th	200
Blanket U-Pu	790

For core fuel preparation the cost estimate is

Capital investment	$15,250,000
Annual operating cost	$4,370,000
Unit cost at 22% fixed-charge rate	$38.6/kg

These numbers are based on an estimate for preparation of thorium metal containing about 3% ^{233}U multiplied by a cost penalty factor of 2.5 for the reference U-Pu-Th mixture. The numbers may seem high, but they represent remote reduction of high-fissile-content gamma-active fuel to metal.

For blanket fuel preparation (conversion of depleted UF_6 to U metal), cost estimates for 790- and 2600-MT/year (10-MT/day) throughput rates are as follows:

	790-MT/Year Throughput	2600-MT/Year Throughput
Capital investment	$10,180,000	$21,700,000
Annual operating cost	$3,690,000	$8,480,000
Unit cost at 22% fixed-charge rate	$7.51/kg	$5.10/kg

Since the blanket material is not unique to the reference reactor, it is probably justifiable to change the ground rule to permit use of the 10-MT/day numbers. If so, the weighted-average core-plus-blanket preparation cost is $11.9/kg.

2. Off-Site Reprocessing

The estimated costs for a dual-purpose 10-MT/day aqueous reprocessing plant are as follows:

Capital investment	$71,000,000
Annual operating cost	$7,300,000
Annual high-level-waste charge	$9,600,000
Daily charge at 22% fixed-charge rate	$125,000

For blanket fuel, the full 10-MT/day processing rate gives a unit cost of $12.5/kg, but for core fuel, the processing rate must be much smaller. For recovery of the uranium and plutonium alone, with the thorium discarded with the fission products, a throughput rate of about 2.0 MT/day for core fuel is estimated. This gives a unit reprocessing cost for core fuel of $62.5/kg. The weighted-average core-plus-blanket processing cost is $22.6/kg.

3. On-Site Reprocessing and Reconversion

W. J. Mecham of ANL made the following estimates of on-site pyrochemical reprocessing costs for FBR uranium-plutonium metal fuels (core and blanket), including reconversion to metal, for the current AEC evaluation study:

Throughput (MT/year)	Unit Cost ($/kg)
107.6	47.1
214.2	40.8

If it is assumed that extrapolations can be made from these estimates for the reference case for core and blanket separately, since they cannot

be mixed, the following costs are obtained for three 3500-Mw(th) reactors:

	Throughput (MT/year)	Unit Cost ($/kg)
Core fuel	28.0	64
Blanket fuel	110.7	47

The core estimate probably is low and the blanket estimate high, but the weighted average of $50.3/kg may be about right. For public financing, this ANL-based estimate can be reduced by about 25% to $37.7/kg.

4. Off-Site Versus On-Site Operations

Adding the off-site preparation and reprocessing cost estimates gives a weighted-average core-plus-blanket unit cost of $34.5/kg. This is almost as high as the on-site weighted-average figure of $37.7/kg, and the off-site cost will be higher when the extra shipping and inventory costs are added. The main advantage of the on-site plant is, however, its low fixed-charge rate on capital investment. The on-site cost would increase to about $63/kg if a 22% fixed-charge rate were used. The on-site estimate is also more speculative, since it involves more extrapolation of present-day technology.

The following time periods are suggested for inventory-charge purposes to put the on-site and off-site plants on a comparable basis:

	Time (days)	
	On-Site	Off-Site
Cooling	15	30
Shipping, both ways		30
Processing	30	30

Appendix D

REFUELING TIME STUDY

A survey was made of the schemes for refueling fast breeder reactors described in the LMFBR design studies by Allis Chalmers,[1] Combustion Engineering,[2] General Electric,[3] Westinghouse,[4] and Argonne National Laboratory.[5] Information on the methods of refueling Fermi and EBR II was obtained in conversations with personnel associated with these reactors.[6,7] Table D.1 lists the pertinent results of this survey.

It may be noticed that the transfer times per assembly are similar in most cases, while the allotted times for shutdown and startup are substantially different. This variation is attributed primarily to differences in the amount of work required to prepare the reactor for fuel-handling operations; for example, shield-plug removal, hot-cell preparation, etc. When these time-consuming operations are not required, a shutdown and startup time of several hours should be sufficient.

Calculations to determine plant availability in the reference designs were based upon the following assumptions:

1. Shutdown time, 3 hr. This is in good agreement with the allotted time for shutdown of the Fermi and EBR II reactors. If the configuration of the reactor system is not altered (i.e., removal of shield plugs), a longer shutdown time is not believed necessary.

2. Fuel handling time, 20 min per core or blanket assembly. This is about the same as the other reactors are presently allowing.

3. Zero power test and startup, 5 hr. This again is in agreement with time allotted in the Fermi and EBR II systems.

4. Fuel may be transferred between the reactor vessel and the refabrication plant while the reactor is operating.

5. Two fuel transfer machines are located inside the reactor vessel and operate simultaneously during the fuel transfer period.

6. The plant is shut down once every ten full-power days.

Table D.1. Summary of Refueling Methods and Time Allowances for Several Sodium-Cooled Fast Breeder Reactors

Reactor or Designer	Refueling Method	Shutdown Time	Fuel Handling Time per Assembly (min)	Startup Time (hr)	Refueling Interval (months)	Total Time per Interval (hr)	Refueling Time per Year (hr)	Plant Down Time for Refueling (%)
Argonne 10,000-Mw VLFBR	Rotating plug	25 hr	40	39	6	192	384	4.4
Allis Chalmers	Rotating plug	24 hr	20 core 8 blanket	24	12	298	298	3.4
Combustion Engineering	Rotating plug				2 2/3	111	500	5.7
General Electric	Hot cell	7 days[a]	15		6	144	288	3.5
Westinghouse	Hot cell	30 hr	19	8	7	160	274	3.3
Fermi reactor	Transfer rotor	(b)			1/2	24	624	7.1
EBR II	Rotating plug (inside secondary system tank)	4 hr[c]	60	3–4				

[a] Includes physics tests.

[b] Shut down one day every two weeks; 5 to 10 hr for shutdown and startup; remainder for fuel transfer.

[c] Length of time required to melt freeze seal. Could be accomplished in 1 to 2 hr if seal could be melted quickly.

References

1. Allis Chalmers Manufacturing Company, Large Fast Reactor Design Study, USAEC Report ACNP 64503, January 1964.

2. Combustion Engineering, Liquid Metal Fast Breeder Reactor Design Study, USAEC Report CEND 200, January 1964.

3. General Electric Company, Liquid Metal Fast Breeder Reactor Design Study, USAEC Report GEAP 4418, January 1964.

4. Westinghouse Electric Corporation, Liquid Metal Fast Breeder Reactor Design Study, USAEC Report WCAP 3251-1, January 1964.

5. K. A. Hub et al., Feasibility Study of Nuclear Steam Supply System Using 10,000-Mw, Sodium-Cooled Breeder Reactor, USAEC Report ANL-7183, Argonne National Laboratory, September 1966.

6. J. J. Morabito, USAEC-RDT, personal communication to D. B. Lloyd, ORNL, July 1967.

7. K. Whitham, ANL, personal communication to D. B. Lloyd, ORNL, July 1967.

Appendix E

SUMMARY REACTOR DESIGN SPECIFICATIONS AND CAPITAL COST ESTIMATES

Capital cost estimates are presented in Tables E.1 and E.2 for four reactor design concepts. In Table E.1 the direct installed costs are tabulated by account. In Table E.2 indirect costs are tabulated and totalled with the direct cost estimates. The estimated split in total cost between the nuclear and turbine islands is also shown in Table E.2. For convenience in the preparation of cost estimates, the four design concepts were designated cases 1, 2, 3, and 4, corresponding to the four unclad-metal-fueled versions:

Case 1 — Th-U-Pu fuel, power production only
Case 2 — Th-U-Pu fuel, process-heat and power production
Case 3 — Th-^{233}U fuel, power production only
Case 4 — U-Pu-Fs fuel, process-heat and power production

The estimates are based on 1967 dollars at current material and labor rates. At this conceptual stage, the estimates have considerable uncertainty. While no set percentage increase was applied to equipment prices, an attempt was made to avoid underestimates in all accounts. No specific development costs were included; however, the tendency was to increase the price of equipment if there was a high degree of uncertainty in its availability.

In order to be consistent from one case to another, cost data from a variety of actual plant costs and study estimates were graphed as functions of electrical and thermal ratings and used for these estimates. For this reason there is probably more accuracy in the relative costs of the four cases than in the total cost for any case.

1. Structures and Improvements

Pricing of the reactor containment structure was related to the VLFBR design.[1] The allowable working pressure for the spherical steel shell was taken as 28 psig. A steel plate thickness of 1 1/2 in. appeared adequate for all four cases. For cases 1 through 3, the shell was 185 ft

Table E.1. Direct Capital Cost Estimates

	Costs (thousands of dollars)			
	Case 1	Case 2	Case 3	Case 4
Account				
21 – Structures and improvements				
211 Ground improvements	1,000	1,000	1,000	1,000
212 Building and structures	4,776	2,056	4,919	1,651
218 Stack	100	100	100	100
219 Reactor containment structure	12,131	12,131	12,131	13,536
Total cost, account 21	18,007	15,287	18,150	16,287
22 – Reactor plant equipment				
221 Reactor equipment				
.1 Reactor vessel	3,210	2,646	2,900	6,572
.2 Reactor controls	1,200	1,000	1,200	2,260
.3 Reactor shielding	1,004	928	1,004	1,395
.4 Reactor auxiliary cooling and heating systems	2,333	2,340	2,333	2,765
.5 Reactor plant cranes and hoists	180	180	180	195
Total cost, item 221	7,927	7,094	7,617	13,187
222 Heat transfer systems				
.1 Reactor and secondary coolant valves	516	492	516	688
.2 Reactor and secondary coolant pumps and drives	4,491	4,310	3,990	8,128
.3 Reactor and secondary coolant piping	2,560	2,441	2,560	3,412
.4 Intermediate heat exchangers	6,624	6,624	6,624	9,384
.5 Steam generators	13,800	15,155	18,116	18,143
.6 Reactor and secondary coolant receiving, supply, and treatment	4,170	4,170	4,170	4,170
Total cost, item 222	32,161	33,192	35,976	43,925
223 Nuclear fuel-handling and storage equipment	4,500	4,500	4,500	4,500
225 Radioactive waste treatment and disposal	400	400	400	400
226 Instrumentation and control				
.1 Reactor plant control system	2,000	2,000	2,000	2,000
.2 Computer	800	800	800	800
.3 Heat transfer systems	300	300	300	400
.4 Fuel handling and storage	500	500	500	500
.5 Radioactive waste systems	300	300	300	300
.6 Radiation monitoring	200	200	200	200
.7 Control and instrument piping, tubing and wiring	600	600	600	700
.8 Steam generator controls	300	600	300	800
Total cost, item 226	5,000	5,300	5,000	5,800
227 Feedwater supply and treatment				
.1 Raw and makeup water supply	300	300	300	300
.2 Purification and treatment	683	625	652	642
.3 Feedwater heaters	2,067	0	2,212	0
.4 Feedwater pumps and drives	1,143	98	1,404	70
Total cost, item 227	4,193	1,023	4,568	1,012
228 Steam, condensate, and feedwater piping	4,000	4,888	3,847	5,420
229 Other reactor plant equipment				
.1 Cranes	500	500	500	500
.2 Special tools	500	500	500	500
.3 Decontamination equipment	700	700	700	700
.4 Replacement equipment	700	700	700	700
.5 Miscellaneous	600	600	600	600
Total cost, item 229	3,000	3,000	3,000	3,000
Total cost, account 22	61,181	59,397	64,908	77,244
23 – Turbine-generator units				
231 Turbine-generators	35,134	11,937	29,991	9,660
232 Circulating water systems	2,396	0	2,273	0
233 Condensers and auxiliaries	3,809	0	3,559	0
234 Central lubricating system	60	60	60	60
235 Turbine plant boards, instruments, and controls	550	550	450	550
236 Turbine plant piping	750	450	870	450
237 Auxiliary equipment for generators	167	34	181	20
238 Other turbine plant equipment	150	150	150	150
Total cost, account 23	43,016	13,181	37,534	10,890
24 – Accessory electric equipment	4,575	3,825	4,675	4,400
25 – Miscellaneous equipment	1,225	1,203	1,225	1,203
Total direct construction cost	128,004	92,893	126,492	110,024

Table E.2. Estimates of Indirect and Total Plant Costs

	Case 1		Case 2		Case 3		Case 4	
	Cost Basis (%)[a]	Cost	Cost Basis (%)[a]	Cost	Cost Basis (%)[a]	Cost	Cost Basis (%)[a]	Cost
Indirect construction costs								
General and administrative	5.5	$ 7,040,000	5.9	$ 5,481,000	5.5	$ 6,957,000	5.7	$ 6,271,000
Miscellaneous construction	1	1,350,000	1	984,000	1	1,334,000	1	1,163,000
Architectural and engineering services	4.7	6,411,000	5.0	4,968,000	4.7	6,335,000	4.8	5,638,000
Nuclear engineering	2.6	3,731,000	3.5	3,651,000	2.6	3,669,000	3.0	3,693,000
Startup costs		1,000,000		1,000,000		1,000,000		1,000,000
Contingency	10	14,752,000	10	10,898,000	10	14,579,000	10	12,779,000
Interest during construction								
Private financing	10.8	17,525,000	10.8	12,947,000	10.8	17,320,000	10.8	15,181,000
Public financing	7.2	11,683,000	7.2	8,631,000	7.2	11,546,000	7.2	10,121,000
Total depreciable capital costs								
Private financing		179,795,000		132,822,000		177,686,000		155,749,000
Public financing		173,953,000		128,506,000		171,912,000		150,689,000
Land		360,000		360,000		360,000		360,000
Total construction cost								
Nuclear island								
Private financing		108,818,000		106,407,000		112,721,000		132,651,000
Public financing		105,289,000		102,956,000		109,064,000		128,347,000
Turbine island								
Private financing		71,337,000		26,775,000		65,325,000		23,458,000
Public financing		69,024,000		25,910,000		63,208,000		22,702,000
Total plant								
Private financing		180,155,000		133,182,000		178,046,000		156,109,000
Public financing		174,313,000		128,866,000		172,272,000		151,049,000
Gross electric power, Mw		1333		284		1451		196.5
Indirect costs as percentage of direct cost								
Private financing		40.7		43.4		40.8		41.9
Public financing		36.2		38.7		36.2		37.3

in diameter and, for case 4, 195 ft in diameter to accommodate a larger number of primary and secondary sodium loops. Reinforced-concrete inside the sphere was taken as a fixed percentage of the volume. Excavation costs and exterior reinforced concrete were also related to variations in diameter. A constant amount was added for services and penetrations. Turbine building volume and costs were determined from a set of graphs as a function of electrical power output. Data on personnel requirements and corresponding building sizes were used to graph administration building needs.

2. Reactor Plant Equipment

Reactor vessel plate thicknesses were calculated on a consistent basis for all four cases. In order to reflect the relative costs between cases, differences in vessel plate thicknesses were not rounded out. The effect of plate thickness on cost per pound was included to further show the effect of reactor inlet pressure on cost. Cases 1 and 3 included 12 control rods and mechanisms; case 2 included 10 rods; and case 4 included 60 rods with 12 cluster drives. Costs for components such as shielding, insulation, cranes and other minor items varied with the case. The penalty for more primary and secondary loops showed up repeatedly for case 4 in such items as reactor and secondary coolant valves, pumps, intermediate heat exchangers, and even instrumentation and control. Pump and intermediate heat exchanger costs were taken from graphs containing actual costs, as well as bids and study cost estimates. Performance data obtained primarily from Babcock & Wilcox were used to estimate steam-generator costs. These data appear to be more conservative than other reported information. A large penalty was imposed on the coolant treatment system relative to other estimates, since separate treatment of a contaminated primary system and a clean secondary system would be required. Stress calculations were not made for steam, condensate, and feedwater piping. Costs were obtained by assuming a 10-fps velocity for water lines and a 175-fps velocity for steam lines. Standard pipe was used except for the high-pressure steam lines. Over $2 million was added to account 22 because of the requirement for remote maintenance of contaminated

systems. This would be divided among costs for special tools and equipment for decontamination, replacement, and an equipment transfer system.

3. Turbine-Generator Units

General Electric Company pricing data were used for the turbine-generators. The case 1 turbine-generator was priced as a tandem-compound six-flow 1800-rpm unit with a 52-in. last-stage-blade length. For cases 2 and 4, noncondensing 1800-rpm units were assumed. Case 3 heat balance and cost estimates were based on two different turbine-generator configurations. In case 3 the heat balance was based on a tandem-compound six-flow, 1800-rpm unit with a 52-in. last-stage-blade length, while the cost estimate was based on a cross-compound four-flow 1800/3600-rpm unit with a 52-in. last-stage-blade length, which would have a higher exhaust loss. The change in the design basis for cost estimating was made too late to revise the heat-balance diagram.

Reference

1. K. A. Hub et al., Feasibility Study of Nuclear Steam Supply System Using 10,000-Mw, Sodium-Cooled Breeder Reactor, USAEC Report ANL-7183, Argonne National Laboratory, September 1966.

ORNL-4202
UC-80 — Reactor Technology

Internal Distribution

1. S. E. Beall
2. R. L. Beatty
3. L. L. Bennett
4. E. G. Bohlmann
5. H. I. Bowers
6. R. H. Bryan
7. C. C. Burwell
8. R. S. Carlsmith
9. R. O. Chester
10. C. W. Collins
11. G. L. Copeland
12. J. E. Cunningham
13. J. G. Delene
14. F. F. Dyer
15. J. I. Federer
16. M. H. Fontana
17. L. C. Fuller
18. E. H. Gift
19. A. E. Goldman
20. R. P. Hammond
21. W. O. Harms
22. L. B. Holland
23. J. M. Holmes
24. R. W. Horton
25. A. Houtzeel
26. G. H. Jenks
27. W. H. Jordan
28. P. R. Kasten
29. C. E. Larson (Y-12)
30. D. B. Lloyd
31. A. L. Lotts
32. M. I. Lundin
33. H. G. MacPherson
34. R. E. MacPherson
35. F. C. Maienschein
36. H. C. McCurdy
37. H. F. McDuffie
38. H. A. McLain
39. J. R. McWherter
40. J. W. Michel
41. F. W. Miles
42. W. R. Mixon
43. T. Nilsson
44. H. G. O'Brien
45. A. M. Perry
46. R. B. Pratt
47. G. L. Ragan
48. J. T. Roberts
49. M. W. Rosenthal
50. R. G. Ross
51. T. H. Row
52. A. W. Savolainen
53. J. E. Savolainen
54. A. C. Schaffhauser
55. C. E. Sessions
56. M. J. Skinner
57. G. M. Slaughter
58. R. C. Steffy
59. D. A. Sundberg
60. R. E. Thoma
61. D. R. Vondy
62. J. L. Wantland
63. G. M. Watson
64. A. M. Weinberg
65. R. P. Wichner
66. F. W. Wiffen
67. Gale Young
68. F. C. Zapp

69-71. Central Research Library
72-73. Y-12 Document Reference Section
74-322. Laboratory Records Department
323. Laboratory Records, RC

External Distribution

324. J. A. Swartout, Union Carbide Corporation, New York, N.Y.
325. Laboratory and University Division, ORO
326-545. Given distribution as shown in TID-4500 under Reactor Technology category (25 copies — CFSTI)